



TECHNISCHE UNIVERSITÄT MÜNCHEN

Fakultät für Medizin

Deutsches Herzzentrum München

The role of p22phox mediated reactive oxygen species in tumour progression: a study based on proteomics, in vitro and in vivo approaches

Ioannis Vouldis

Vollständiger Abdruck der von der Fakultät für Medizin der Technischen Universität München zur Erlangung des akademischen Grades eines

Doctor of Philosophy (Ph.D.)

genehmigten Dissertation.

Vorsitzender: Univ.-Prof. Dr. Dr. Stefan Engelhardt

Betreuerin: Univ.-Prof. Dr. Agnes Görlach

Prüfer der Dissertation:

1. Univ.-Prof. Dr. Gabriele Multhoff
2. Univ.-Prof. Dr. Manfred Schmitt

Die Dissertation wurde am 07.07.2014 bei der Fakultät für Medizin der Technischen Universität München eingereicht und durch die Fakultät für Medizin am 28.08.2014 angenommen.

Contents

Chapter 1: Introduction	1
1.1 Cancer	2
1.1.1 Cancer overview by the World Health Organization	2
1.1.2 Definition and different categories of cancer	2
1.1.3 Tumour biology and medicine	3
1.1.4 The hallmarks of cancer	5
1.2 Reactive oxygen species (ROS)	7
1.2.1 Introduction to ROS	7
1.2.2 Chemistry and biology of ROS	8
1.2.3 ROS from health to disease	9
1.2.4 The NOX Family of ROS-Generating NADPH Oxidases	10
1.2.4.1 Structure and function of the phagocytic NADPH oxidase	13
1.2.4.2 NADPH oxidases, p22phox, ROS and cancer	15
1.3 Proteomics	18
1.3.1 Introduction to Proteomics	18
1.3.2 Proteomics towards the future of medicine	19
1.3.3 Proteomics as a powerful analytical platform	20
1.3.4 Two-dimensional gel electrophoresis (2-DE) for protein expression profiling	21
Chapter 2: Aim of the study	23
2.1 Aim of the study	24
Chapter 3: Materials and methods	25
3.1 Materials	26
3.1.1 Cellular and molecular biology	26
3.1.2 Protein biochemistry and proteomics	28
3.1.3 General equipment and device	29
3.1.4 Xenograft mouse model	30
3.1.5 Software and databases	30
3.2 Methods	31
3.2.1 Cellular biology methods	31
3.2.1.1 Maintenance and storage of cells	31
3.2.1.2 Counting of cells	31
3.2.1.3 Stable and transient transfection of cells	32
3.2.1.4 Dihydroethidium (DHE) staining of cells	33

3.2.1.5	BrdU ELISA assay	33
3.2.1.6	Alamar Blue assay	34
3.2.1.7	Clonogenic assay	35
3.2.1.8	Immunofluorescence (IF) and fluorescence microscopy	35
3.2.1.9	Immunohistochemistry (IHC)	37
3.2.2	Molecular biology methods	38
3.2.2.1	DNA amplification and polymerase chain reaction (PCR)	38
3.2.2.2	Total RNA purification	40
3.2.2.3	Reverse Transcription PCR	41
3.2.2.4	Quantitative PCR	41
3.2.2.5	DNA sequencing	42
3.2.2.6	In vivo method : Xenograft model	42
3.2.3	Protein biochemistry and proteomics methods	43
3.2.3.1	Protein isolation	43
3.2.3.2	Bradford assay	44
3.2.3.3	Western blot analysis	44
3.2.3.4	Two-dimensional gel electrophoresis (2-DE)	47
3.2.3.4.1	Sample preparation for 2-DE	49
3.2.3.4.2	Rehydration of IPG strips	49
3.2.3.4.3	First dimension (IEF)	50
3.2.3.4.4	Equilibration of IPG strips	51
3.2.3.4.5	Second dimension (SDS-PAGE)	52
3.2.3.4.6	2-DE gel staining and digitalization	53
3.2.3.4.7	2-DE gel image analysis	55
3.2.3.4.8	Excision of protein spots and in-gel trypsin digestion	56
3.2.3.4.9	Mass spectrometry (MS) analysis	57
3.2.3.4.10	Bioinformatics data analysis	58
3.2.4	Statistical analysis	59
Chapter 4: Results		60
4.1	Results	61
4.1.1	Assessment of differential p22phox levels in stably transfected HepG2 cells	61
4.1.2	Evaluation of p22phox regulatory effect on ROS generation	63
4.1.3	Role of p22phox in proliferative activity of HepG2 cells	64
4.1.3.1	p22phox modulates the proliferative and metabolic activity of HepG2 cells	64
4.1.3.2	N-acetyl cysteine decreases metabolic activity in HepG2 cells	66
4.1.3.3	p22phox modulates colony formation capacity of HepG2 cells	66
4.1.4	Control of HepG2 tumour growth by p22phox in vivo	67
4.1.4.1	Silencing of p22phox reduces HepG2 tumour growth in a xenograft mouse model	67

4.1.4.2	p22phox modulates the balance between proliferation and apoptosis in HepG2 xenografts	69
4.1.5	Proteomic analysis of p22phox over-expressing HepG2 cells	70
4.1.5.1	Two dimensional gel electrophoresis (2-DE) analysis	70
4.1.5.2	Mass spectrometry (MS) analysis	72
4.1.5.3	Validation of differentially expressed proteins	72
4.1.5.4	Pathway and network analysis of differentially expressed proteins	73
4.1.6	Role of HSP90 in the p22phox proliferative response of HepG2 cells	76
4.1.7	Regulation of Cathepsin D by p22phox in HepG2 cells	79
4.1.7.1	p22phox modulates Cathepsin D expression	79
4.1.7.2	The modulation of Cathepsin D by p22phox is ROS dependent	80
4.1.7.3	p22phox regulates Cathepsin D localization and secretion	81
4.1.7.4	p22phox affects lysosomal structure in HepG2 cells	82
4.1.7.5	Evaluation of Cathepsin D effect on the proliferative activity of HepG2 cells	82
4.1.7.6	p22phox modulates HepG2 proliferation dependent on Cathepsin D	85
4.1.7.7	p22phox regulates Cathepsin D expression in HepG2 xenografts	88
Chapter 5: Discussion		90
5.1	Discussion	91
5.1.1	p22phox modulates ROS levels in HepG2 cells	91
5.1.2	p22phox modulates proliferation of HepG2 cells	92
5.1.3	Proteomic analysis of HepG2 cells over-expressing p22phox	93
5.1.4	Role of HSP90 in the p22phox regulated proliferation of HepG2 cells	96
5.1.5	Role of Cathepsin D in the p22phox regulated proliferation of HepG2 cells	97
5.1.6	Limitations of the study	101
Chapter 6: Summary		103
6.1	Summary	104
Appendix 1: Acknowledgements		105
Appendix 2: Index of figures and tables		108
Appendix 3: References		112

Chapter 1: Introduction

1.1 Cancer

1.1.1 Cancer overview by the World Health Organization

Cancer, according to the World Health Organization (WHO), is the uncontrolled growth and spread of cells that can affect almost any part of the body. The growths often invade surrounding tissue and can spread to distant sites. Cancer can affect everyone regardless of age, gender or social status and represents a tremendous burden on patients, families and societies. Also, cancer is one of the leading causes of death in the world, particularly in developing countries [1].

Facts about cancer [1]:

- There are more than 100 types of cancers. Any part of the body can be affected.
- In 2008, 7.6 million people died of cancer representing 13% of all deaths worldwide.
- About 70% of all cancer deaths occur in low- and middle-income countries.
- Worldwide, the 5 most common types of cancer that kill men are (in order of frequency): lung, stomach, liver, colorectal and oesophagus.
- Worldwide, the 5 most common types of cancer that kill women are (in order of frequency): breast, lung, stomach, colorectal and cervical.
- Tobacco use is the single largest preventable cause of cancer in the world causing 22% of cancer deaths.
- One fifth of all cancers worldwide are caused by a chronic infection, for example human papillomavirus (HPV) causes cervical cancer and hepatitis B virus (HBV) causes liver cancer.
- Cancers of major public health relevance such as breast, cervical and colorectal cancer can be cured if detected early and treated adequately.

1.1.2 Definition and different categories of cancer

Cancer is not just one disease but many diseases. As previously stated, there are more than 100 different types of cancer. Cancer refers to the disease state in which abnormal cells divide without control and are able to invade other tissues: cancer cells can spread to other parts of the body through the blood and lymph systems via a process known as metastasis. Most

cancers are named after the organ or type of cell in which they start. For example, a cancer that begins in the colon is called “colon cancer”, a cancer that begins in melanocytes of the skin is called “melanoma”[2].

The different types of cancer can be grouped into broad categories in regard to their birthplace [2-4]. According to this classification scheme, the main categories include:

- Carcinomas: cancers that begin in the skin or in tissues that line or cover internal organs.
- Sarcomas: cancers that begin in bone, cartilage, fat, muscle, blood vessels, or other connective or supportive tissue.
- Leukemias: cancers that start in blood-forming tissue such as the bone marrow and cause large numbers of abnormal blood cells to be produced and enter the blood.
- Lymphomas and myelomas: cancers that begin in the cells of the immune system.
- Central nervous system cancers: cancers that begin in the tissues of the brain and spinal cord.

Cancers can also be classified either as hereditary or sporadic [2, 5]. 5–10% of cancer cases are attributed to genetic (hereditary cancers) and 90–95% of the cases are due to environmental factors (sporadic cancers). Hereditary cancers are primarily caused by an inherited genetic defect. Less than 0.3% of the population carry a genetic mutation which has a large risk on the development of cancer. For example, certain inherited mutations in the genes BRCA1 and BRCA2 entail more than 75% risk of breast cancer and ovarian cancer [6, 7]. Sporadic cancers, as mentioned above, include the vast majority of cancers. These are not inherited genetically but they are caused by common environmental factors including tobacco use, infections, diet and obesity, radiation (both ionizing and non-ionizing), stress, lack of physical activity, and environmental pollutants.

1.1.3 Tumour biology and medicine

All cancers initiate in cells, the body's basic unit of life. There are many different types of cells which grow and divide in a controlled way to produce more cells as they are needed to keep the body healthy. When cells become old or damaged, they die and are replaced by new cells. However, sometimes this strictly regulated process goes wrong. The genetic material (DNA)

of a cell can become damaged or changed, producing mutations that affect normal cell growth and division. When this happens, cells do not die when they should and new cells form when the body does not need them. The extra cells may form a mass of tissue called “tumour”. Not all tumours are cancerous. Tumours can be benign or malignant and some cancers do not form tumours at all such as in the case of leukemias. Benign tumours are not cancerous. They can often be removed, and, in most cases, they do not come back. Cells in benign tumours do not metastasize. On the contrary, malignant tumours are cancerous. Cells in these tumours can invade nearby tissues and spread to other parts of the body via metastasis [2, 8].

Box 1: Glossary and etymology for terms of interest related to cancer [9, 10].

Cancer: the term originates from Greek “καρκίνος” meaning crab. It was first described by Hippocrates and later, Celsus translated the term to Latin “cancer” meaning also crab. In medicine, the term concerns a group of diseases which cause cells in the body to change and grow out of control.

Onco- : word-forming element originating from Greek “ὄγκος” meaning “bulk, mass”. In medicine, its use is firmly linked to cancer. Synonym word: tumour (see below).

Oncology: composite word of two parts: “onco-“ (see above) and “-logy”. The second part “-logy” originates from Greek “λόγος” meaning “study of, word, reason, account, speech, opinion”. The term as a whole concerns the branch of medicine that specializes in the research, diagnosis and treatment of cancer.

Tumour: the term is derived from Latin “tumor” meaning “swelling, condition of being swollen”. It concerns an abnormal lump or mass of tissue. In the Commonwealth the spelling "tumour" is commonly used, whereas in the U.S. it is usually spelled "tumor".

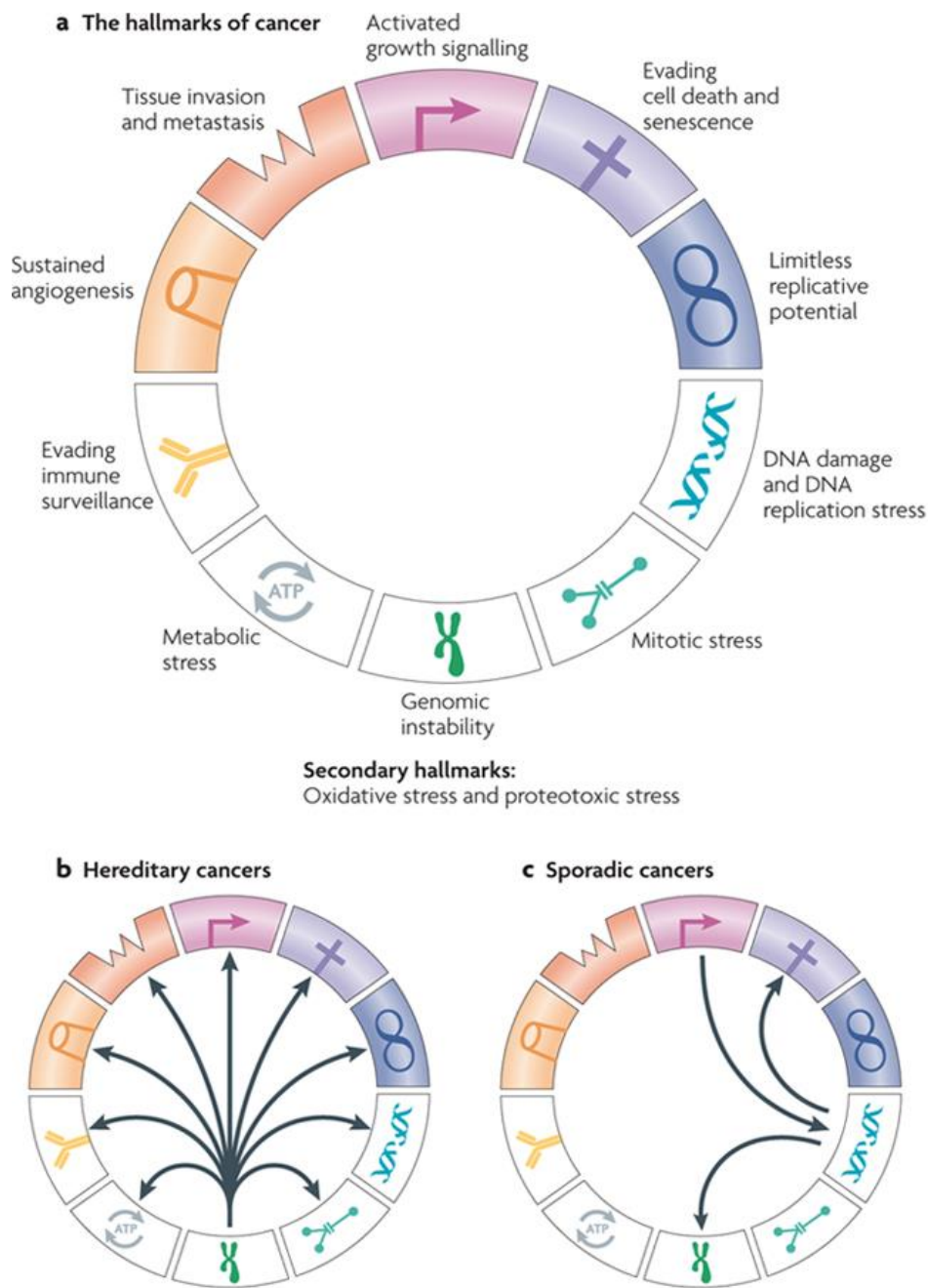
Tumourigenesis: composite word of two parts: “tumour” (see above) and “-genesis” which originates from Greek “γένεσις” meaning “origin, initiation, creation, birth”. It concerns the process of initiation and progression of cancer. Synonyms: oncogenesis, carcinogenesis.

1.1.4 The hallmarks of cancer

Hanahan and Weinberg described six major functional capabilities of cancers that they called “hallmarks of cancer” in their seminal review article indicating aberrant events that mediate cellular transformation [11].

The six major hallmarks which were initially proposed, constituted an organizing principle for rationalizing the complexities of neoplastic disease and they included: (1) sustaining proliferative signalling, (2) evading growth suppressors, (3) resisting cell death (apoptosis), (4) enabling replicative immortality, (5) inducing angiogenesis, and (6) activating invasion and metastasis. The authors suggested that most, if not all cancers have acquired the same set of functional capabilities during their development via various mechanistic strategies. They introduced also the concept that mutations leading to the hallmarks did not have to be acquired in any specific order. Finally, genomic instability was considered by them separately from the six hallmarks, in that it is not a functional capability of cancer *per se* but a property that enables the acquisition of the hallmarks [11, 12].

Negrini, Gorgoulis and Halazonetis, took their own approach in 2010 and published another review article focusing on the hallmarks of cancer [13]. They were based on the hallmarks of cancer which had been proposed in the scientific literature since the first systematic attempt of Hanahan and Weinberg, but also reported additional ones. New hallmarks included evading immune surveillance and five more related to the presence of stress in cancer, namely: DNA damage and DNA replication stress, oxidative stress, mitotic stress, proteotoxic stress and metabolic stress. These five new hallmarks are qualitatively different from the original hallmarks in that they do not describe functional capabilities of cancers but rather the state of cancer cells which is characterized by the presence of various stresses. Therefore, in the authors’ opinion, the expansion of the concept of hallmarks to include states of cancer cells warrants the inclusion of genomic instability as one of the hallmarks, too (Figure 1.a). Genomic instability is present in all stages of cancer, from precancerous lesions to advanced cancers. Moreover, they consolidated the self-sufficiency in growth signals and insensitivity to anti-growth signals into the single hallmark of activated growth signalling [13].



Nature Reviews | Molecular Cell Biology

Figure 1: Presentation of the hallmarks of cancer. a. The main hallmarks of cancer are depicted on the circle and the secondary hallmarks (oxidative stress and proteotoxic stress) are shown separately. b. The temporal order by which the hallmarks are acquired in hereditary cancers. c. The temporal order by which the hallmarks are acquired in sporadic (non-hereditary) cancers. The figure is reprinted with Nature Publishing Group's permission (www.nature.com License Number: 3266051294627) [13].

Another way that was demonstrated in the same review [13] in order to handle the numerous hallmarks was to consider that some of them are secondary to others. For example,

proteotoxic stress may be secondary to aneuploidy, which in turn is a manifestation of genomic instability, and oxidative stress may be secondary to oncogenic signaling and metabolic stress. Based on these considerations, the authors proposed that the secondary hallmarks can be presented separately from the primary hallmarks (Figure 1.a).

Finally, the question remained whether the acquisition of hallmarks occurs in any specific order, or in no specific order as originally proposed by Hanahan and Weinberg. Attempting to answer that question, the following hypotheses were given by Negrini and her co-authors. Hereditary cancers are often characterized by the presence of mutations in DNA repair genes, such as *BRCA1*, *BRCA2*, *MSH2* and *MYH*, which lead to genomic instability. Thus, in accordance with the mutator hypothesis, the presence of genomic instability in hereditary cancers probably precedes the acquisition of mutations in oncogenes and tumour suppressor genes and therefore precedes the acquisition of the other hallmarks (Figure 1.b) By contrast, in sporadic cancers, the high throughput sequencing studies suggest that caretaker genes might not be frequently inactivated early in cancer development. Instead, the first hallmark to be acquired in sporadic cancers might be activated by growth signaling, owing to mutations in oncogenes or antioncogenes (Figure 1.c). The DNA replication stress that is associated with oncogene activation could then lead to genomic instability and the selection for *TP53* mutations, which results in cells evading cell death and senescence.

1.2 Reactive oxygen species (ROS)

1.2.1 Introduction to ROS

Oxidative stress as one of the new hallmarks of cancer is considered as increased load of reactive oxygen species (ROS) which overwhelms the body's antioxidant capacity. All types of ROS, including superoxide anions and hydrogen peroxide, have unpaired valence electrons or unstable bonds [14, 15]. When ROS were first introduced into biomedical concepts it was thought that they caused exclusively toxic effects and were associated with pathologies [16]. At high concentrations, ROS react readily with proteins, lipids, carbohydrates, and nucleic acids, often inducing irreversible functional alterations or even complete destruction. However, this approach of considering only the toxic effects of ROS action was amended when

mounting evidence has been provided that ROS are able to act in lower concentrations as signalling molecules. This action of ROS takes place through covalent modifications of target molecules (redox signalling) thereby inducing distinct changes at the cellular (regulation of growth, apoptosis and other signaling) and systems level (contribution to complex functions such as blood pressure, cognitive and immune function) which are crucial in both physiological and pathophysiological processes.

Furthermore, ROS in human body were once thought to originate almost entirely from mitochondrial metabolism. Indeed, in the case of normal mitochondrial function, the final oxygen electron receptor is reduced to water and it is possible, particularly under pathological conditions, that electrons leak out of the system prematurely and create ROS. However, it has been indicated extensively in the scientific literature that cellular enzymes referred to as NADPH oxidases (NOX) are a major source of ROS in humans, too [17-20]. Nevertheless, there is not yet a complete understanding how ROS signaling may function within cells, tissues and organs [16, 21].

1.2.2 Chemistry and biology of ROS

Taking a close look on the chemistry and biology of reactive oxygen species (ROS), these are defined as oxygen-derived small molecules, including oxygen radicals such as superoxide ($O_2^{\bullet-}$), hydroxyl ($\bullet OH$), peroxy (RO_2^{\bullet}), and alkoxy ($RO\bullet$) and certain non-radicals that are either oxidizing agents and/or are easily converted into radicals, such as hypochlorous acid (HOCl), ozone (O_3), singlet oxygen (1O_2), and hydrogen peroxide (H_2O_2) [22, 23]. ROS generation is generally a cascade of reactions (Figure 2) that starts with the production of superoxide. Two molecules of superoxide can react to generate hydrogen peroxide (H_2O_2) in a reaction known as dismutation, which is accelerated by the enzyme superoxide dismutase (SOD) [24]. In the presence of iron, superoxide and H_2O_2 react to generate hydroxyl radicals. In inflamed areas, ROS include hypochlorous acid (HOCl), formed in neutrophils from H_2O_2 and chloride by the phagocyte enzyme myeloperoxidase (MPO). Singlet oxygen might be formed from oxygen in areas of inflammation through the action of Phox and MPO-catalysed oxidation of halide ions and ozone can be generated from singlet oxygen by antibody molecules. The last reaction is

likely to be important in inflamed areas in which antibodies that bound to microorganisms are exposed to ROS produced by phagocytes [22].

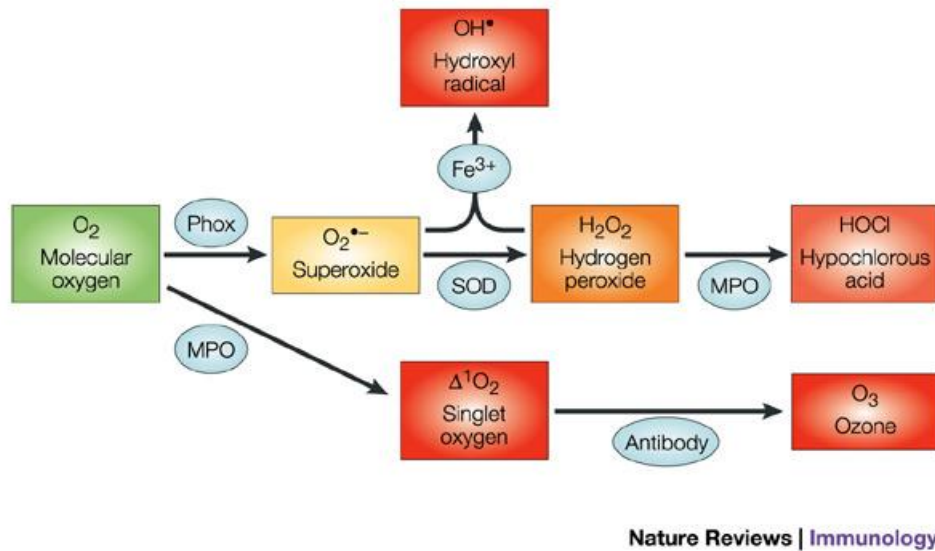


Figure 2: Cascade of reactions involving ROS generation. The colour coding indicates the reactivity of individual molecules (green: relatively unreactive, yellow: limited reactivity, orange: moderate reactivity, red: high reactivity and non-specificity). The figure is reprinted with Nature Publishing Group's permission (www.nature.com License Number: 3266041429501) [22].

1.2.3 ROS from health to disease

Regarding the role of ROS in health, it is well established nowadays that they are involved at low regulated levels in many vital physiological processes and functions. Examples include modulation of nutrient sensors and aging as well as immune, thyroid and cognitive function. ROS participate in various signaling cascades, such as response to growth factor stimulation and control of inflammatory responses. Furthermore, they participate in the regulation of many cellular processes including differentiation, proliferation, growth, apoptosis, cytoskeletal regulation, migration, and contraction [14, 25].

Concerning disease, ROS contribute to a wide range of pathologies and many of them are leading causes of death. Cancer, cardiovascular diseases, neurological diseases, sensory impairment and psychiatric diseases, all show robust evidence of ROS involvement (Table 1) [14, 24, 26, 27].

Table 1: Selected ROS mediated diseases [14].

Disease family & example	Potential mechanisms of ROS involvement
Cancer e.g. renal cell carcinoma	a. Hypoxia inducible factor (HIF-1a) expression induces vascular endothelial growth factor (VEGF), a mediator of angiogenesis, tumour growth and metastasis. NADPH-oxidase-4 (NOX4) activity is required for HIF-1a expression. b. Fumarate hydratase deficiency may induce hypoxia-inducible transcription factor stabilisation by glucose-dependent generation of ROS. c. Obligate glycolytic switch is critical to HIF stabilisation via ROS generation. d. Cells exhibit upregulation of p22phox, NOX4, and NOX-mediated ROS generation. e. Tumour cell growth is suppressed by diphenyleneiodonium (DPI), a chemical inhibitor of NADPH oxidases.
Cardiovascular e.g. hypertension	a. Superoxide reacts with .NO, forming peroxynitrite (ONOO ⁻), causing a reduction in .NO bioavailability and endothelium-dependent vasodilation. b. NOX4 is strongly expressed in media of small pulmonary arteries and is causally involved in development of pulmonary hypertension. c. NOX-derived ROS are a hypertensive signaling element. d. Decreased systolic blood pressure response to angiotensin II and to bone morphogenetic protein-4 in p47phox-deficient mice. e. Decreases in blood pressure in NOX1-deficient mice.

1.2.4 The NOX Family of ROS-Generating NADPH Oxidases

The NADPH oxidases were originally identified as a key component of human innate host defence and were thought to be specific to phagocytic cells [28]. In these cells, this enzyme complex is activated to produce superoxide anion and other secondarily derived ROS which promote the destruction of invading micro-organisms (see detailed description of activation in the following paragraph). However, the presence of NADPH oxidases in non-phagocytic tissues and cells is now well-established, too. Actually, NADPH oxidases participate in very important cellular processes besides the host defence, including signal transduction, cell proliferation and apoptosis [29-31]. These enzymes are essentially present in every organ system in the body and contribute to a multitude of physiological events (Figure 3 and Table 2) [32].

The primary catalytic function of the NADPH oxidase family of enzymes is the generation of reactive oxygen species (ROS). This property sets them apart from all other ROS-generating enzymes that produce radical species, either as a by-product of their normal catalytic activity or as a result of aberrant functioning in disease. Members of the NADPH oxidase family

catalyze the reduction of molecular oxygen to generate superoxide and/or hydrogen peroxide (as previously described) in various intracellular compartments.

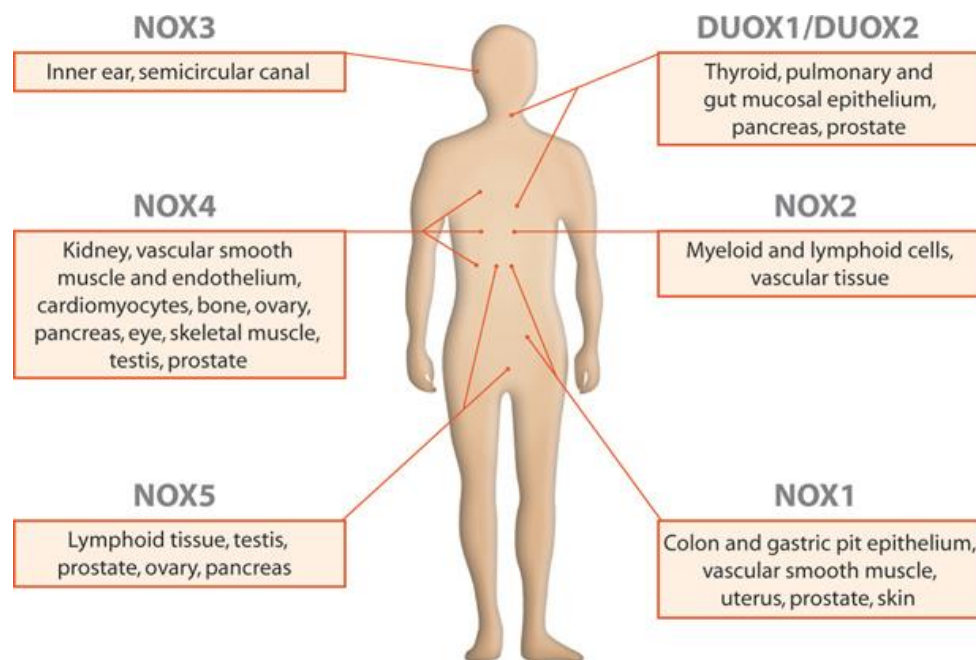


Figure 3: Locations of NOX proteins in the human body. Tissues reported to express NOX homologues throughout the human body are displayed. Figure is reprinted with permission granted from its source: M. Quinn, M.C. Ammons and F. Deleo. The expanding role of NADPH oxidases in health and disease: no longer just agents of death and destruction. *Clinical Science* (2006) 111, (1-20) © Portland Press Limited [32].

Table 2: Tissue expression of the NOX proteins [32].

Oxidase protein	Tissue expression
NOX1	Vascular smooth muscle, gastric pit and colon epithelium.
NOX2 (gp91phox)	Phagocytes, lymphocytes, vascular smooth muscle, fibroblasts, endothelium, skeletal muscle, neurons, lung, carotid body and kidney.
NOX3	Fetal tissue and inner ear.
NOX4	Fetal tissue, kidney, pancreas, placenta, ovary, testis, skeletal muscle, carotid body, melanocytes, osteoclasts, eye and lung.
NOX5	Fetal tissue, lymphocytes, spleen, testis ovary, placenta, pancreas, stomach, mammary glands and cerebrum.
p22phox	Phagocytes, lymphocytes, testis, placenta, ovary, kidney, liver, lung, spleen, pancreas, skeletal muscle, neurons, eye, vascular smooth muscle, fibroblasts, endothelium, carotid body, melanocytes and osteoclasts.
p47phox	Phagocytes, lymphocytes, testis, placenta, ovary, kidney, liver, lung, spleen, pancreas, skeletal muscle, neurons, eye, vascular smooth muscle, fibroblasts, endothelium and carotid body.
p67phox	Phagocytes, lymphocytes, testis, placenta, ovary, kidney, liver, lung, spleen, pancreas, skeletal muscle, neurons, eye, vascular smooth muscle, fibroblasts, endothelium and carotid body.
DUOX1	Thyroid, salivary glands, colon, rectum, bronchi and cerebellum.
DUOX2	Thyroid, salivary glands, colon, rectum, bronchi, pancreas and prostate.
NOXO1	Colon, liver, small intestine, gastric mucosal cells, cochlea, liver, pancreas, thymus and testis.
NOXA1	Colon, uterus, salivary glands, small intestine, stomach, lung, thyroid, liver, kidney, pancreas, spleen, prostate, testis and ovary.

Seven isoforms of NADPH oxidase have been described in mammals. In general, these isoforms vary in their composition, tissue localisation, mechanisms of activation, and roles in pathologies. In more detail, each of these isoforms comprises a core catalytic subunit (the so-called NADPH oxidase (NOX) and dual oxidase (DUOX) subunits) and up to five regulatory subunits. These regulatory subunits have important role in the maturation and expression of the NOX and DUOX subunits in biological membranes (DUOX activator 1 (DUOXA1) and DUOXA2), in enzyme activation (p67phox and NOX activator 1 (NOXA1)), and in spatial organization of the various components of the enzyme complex (p47phox, NOX organizer 1 (NOXO1) and p40phox). Some NADPH oxidase isoforms also rely on a small GTPase (RAC1 or RAC2) for their activation. As illustrated (Figure 4), each NADPH oxidase isoform may be defined by the nature of its core catalytic subunit (NOX1–NOX5, DUOX1 or DUOX2) as well as its suite of regulatory subunits. Studying further the role of all NADPH oxidase isoforms and their regulatory subunits is justified without doubt considering that the ROS generated by these enzymes have crucial roles in various physiological and pathophysiological functions in human body [33, 34].

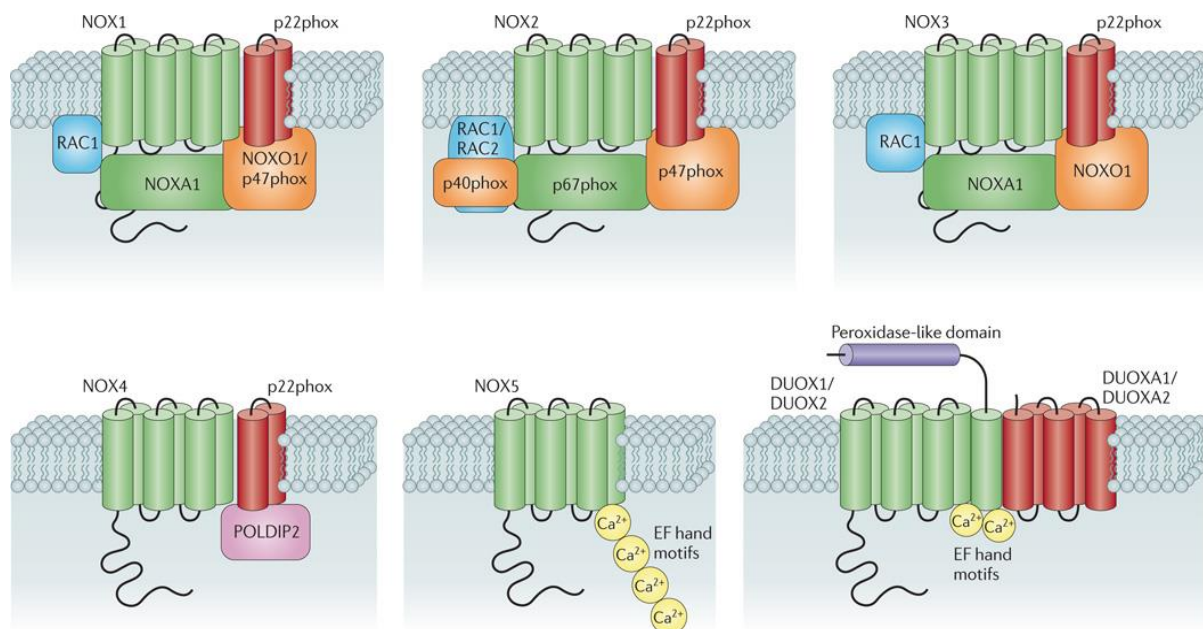


Figure 4: Subunit composition of the seven mammalian NADPH oxidase isoforms. The catalytic core subunits of the enzymes and the cytosolic activators are shown in green. NOX and DUOX maturation and stabilization partners such as p22phox are shown in red. Cytosolic organizers are shown in orange. Small GTPases (RAC1, RAC2) are shown in blue. Also, polymerase δ -interacting protein 2 (POLDIP2) is shown in pink. EF hand motifs (yellow circles) are also shown, which bind to Ca^{2+} . Last, the figure also illustrates the putative amino-terminal transmembrane domain and extracellular peroxidase-like region (shown in purple) on DUOX1 and DUOX2. The figure is reprinted with Nature Publishing Group's permission (www.nature.com License Number: 3266050237615) [33].

1.2.4.1 Structure and function of the phagocytic NADPH oxidase

As previously mentioned, the structure and function of the NADPH oxidases were primarily described in neutrophils [28]. In that regard, the structure and activation of the phagocytic NADPH oxidase is well described as a prototype in the scientific literature (Figure 5).

The complex formed by NOX2 (gp91phox) and p22phox has been biochemically isolated and is referred to as flavocytochrome b558 (the catalytic core of the NADPH oxidases) which is essential for electron transfer from NADPH to molecular oxygen [30, 35, 36]. Other important components are the cytosolic subunits p40phox, p47phox, p67phox and the small GTP-binding protein Rac. The NADPH oxidase is inactive in unstimulated phagocytes, but becomes activated after exposure of cells to microorganisms or inflammatory mediators as a result of assembly of cytosolic subunits with flavocytochrome b558. Cell activation by microorganisms or inflammatory mediators initiates at least three molecular triggers (protein phosphorylation, lipid metabolism and guanine nucleotide exchange on RAC) with the flavocytochrome. This complex regulation protects against accidental activation of the oxidase. Neutrophils can transition from undetectable to high levels of ROS production within 30 seconds of cell activation. Therefore, the regulatory features of the Phox seem to be ideally suited to control the high levels of ROS production seen in phagocyte-mediated host defense [22].

An outline of the distinct stages during the activation of the phagocytic NADPH oxidase can be given as follows: (1) dormant in resting neutrophils, p47phox becomes phosphorylated after stimulation with pathogens like bacterial lipopolysaccharides [30, 37], (2) this phosphorylation leads to a change in their conformation and to subsequent translocation and association with the flavocytochrome b558 at the membrane, (3) in addition, loading of Rac with GTP and interaction of active Rac with p47phox and p67phox triggers the translocation of Rac to the flavocytochrome b558 at the flavocytochrome b558 in the right direction for electron transfer [38, 39], (4) finally, the activated oxidase releases large amounts of superoxide in the well characterized respiratory burst.

The significance of the events described above can be easily understood in the example of chronic granulomatous disease (CGD) caused by mutations in any of the genes encoding NOX2 (gp91phox), p22phox, p47phox or p67phox. The phagocytes of patients suffering from CGD are unable to produce $O_2^{\cdot-}$, and these patients are therefore highly susceptible to bacterial and fungal infections [40]. The important membrane-bound component of the flavocytochrome b558, p22phox, is a protein with a molecular weight of 22-kDa. As mentioned, p22phox forms

together with NOX2 the catalytical core of the phagocytic NADPH oxidase [41, 42]. Moreover, upon stimulation, p22phox binds to gp91phox to assemble the active oxidase [30]. Importantly, the expression of p22phox is ubiquitous, underlying the essential function of this component for the assembly and activation of NADPH oxidases. Interestingly, several polymorphisms in the p22phox gene have been identified [43]. Also, increased levels of p22phox have been detected in various cancers, atherosclerosis, hypertension, diabetes and other disorders and have been associated with elevated ROS levels in these disorders [44-48].

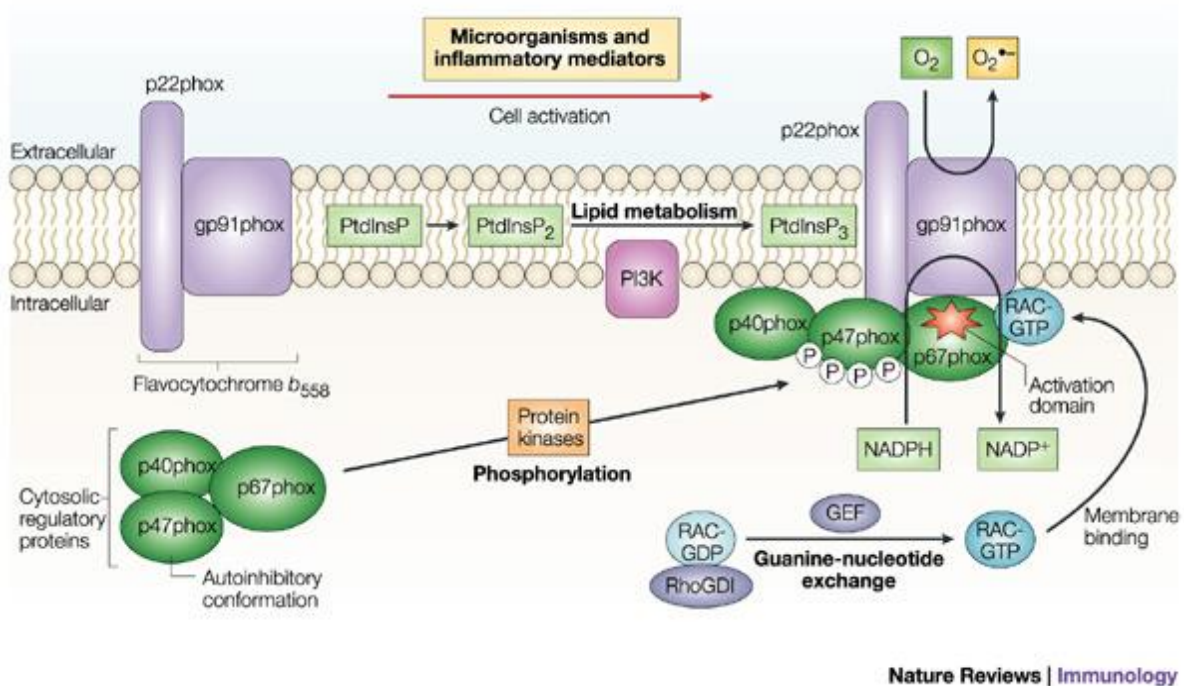


Figure 5: Schematic overview of the structure and activation of the phagocytic NADPH oxidase. In resting phagocytic cells, NOX2 (gp91phox) forms with p22phox a membrane bound flavocytochrome b558 and the cytosolic factors p40phox, p47phox and p67phox forms a cytosolic complex. In activated phagocytic cells, the cytosolic complex translocates to the membrane upon phosphorylation of p47phox. Activation of Rac leads to the full activation of the NADPH oxidase. The figure is reprinted with Nature Publishing Group's permission (www.nature.com License Number: 3266041429501) [30].

Box 2: Glossary for terms of interest related to reactive oxygen species [22, 33].

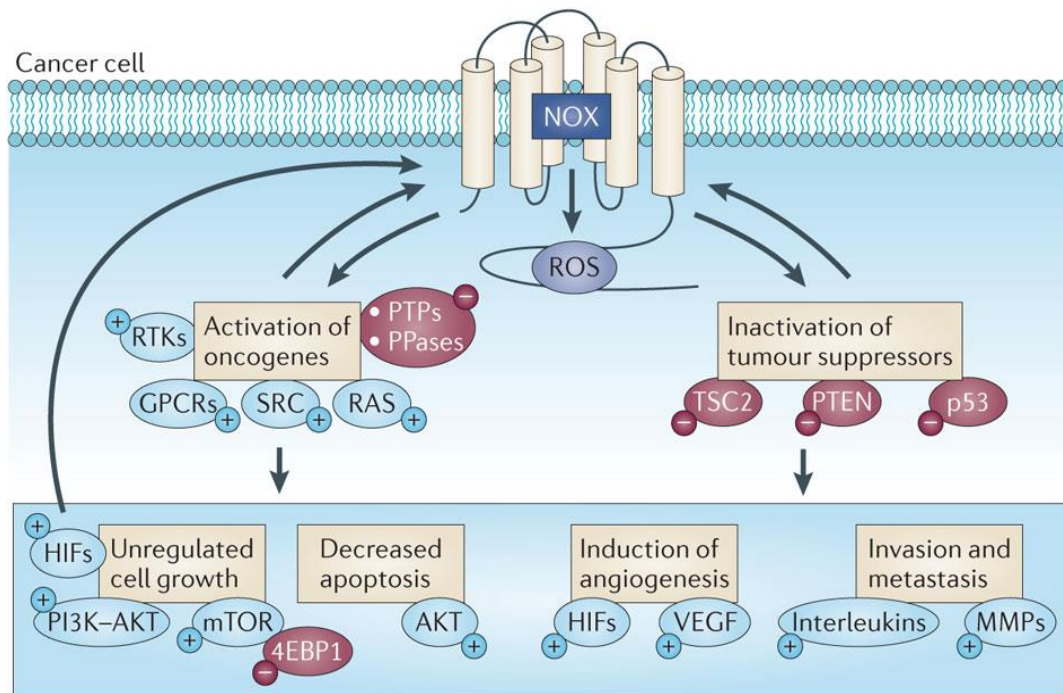
Oxidative stress: reflects the imbalance between the production of reactive oxygen species and the ability of cells to neutralize their reactive intermediates.

Redox signalling: the concept that electron-transfer processes play a key messenger role in biological systems.

Respiratory burst: the large increase in oxygen consumption and reactive oxygen species generation that accompanies exposure of neutrophils to microorganisms and/or inflammatory mediators.

1.2.4.2 NADPH oxidases, p22phox, ROS and cancer

In cancer cells, high levels of superoxide and hydrogen peroxide have been described [49]. Initial studies demonstrating the expression of NADPH oxidase subunits in differentiated HL60 promyelocytic leukemia cells and in HepG2 cells [50, 51] pointed towards a potential role of NADPH oxidases in tumour biology. Studies demonstrating that diphenyleneiodonium (DPI) which inhibits flavin-containing enzymes including NADPH oxidases, but also that the mitochondrial electron transfer chain [52] could decrease ROS production and proliferation in cancer cells, were first hints that NADPH oxidases could play a role in tumour cells [53]. Now, several sources of ROS in cells and tissues have been identified. However, the mitochondrial electron transfer chain and NADPH oxidases of the NOX family are the two major sources implicated in cancer. ROS derived from these two major sources are not mutually exclusive, and corresponding studies suggest that crosstalk exists between these major producers [20]. NADPH oxidases are dedicated ROS generating enzymes that broadly and specifically regulate redox-sensitive signalling pathways which are involved in cancer development and progression. They act through the activation of oncogenes and the inactivation of tumour suppressor proteins [54]. Notably, the regulatory protein subunit p22phox of NADPH oxidases, necessary for complex formation with four out of the five homologues of the family of NADPH oxidases, appears to have an essential role in ROS production and subsequent signaling pathways involved in a broad range of pathophysiological conditions including cancer [55-57]. Cellular transformation is a multistep process that requires an as yet undetermined sequence of genetic alterations and changes in intracellular signalling. As previously mentioned, scientific reviews focusing on the “hallmarks of cancer” indicated various aberrant events that mediate cellular transformation. However, an underlying event very poorly discussed is the role of oxidative stress in these processes. The role of oxidative stress in cellular transformation was first described in 1981 by Oberley and colleagues. This seminal paper described the insulin stimulated generation of intracellular hydrogen peroxide as a second messenger that induces cellular proliferation. Additionally, it was suggested that increased superoxide production leads to cellular immortality. This work became known as “the free radical theory of cancer” [58]. Similar to the importance of free radicals, was the discovery of enzymes that are involved in scavenging these radicals, which are referred to as antioxidants [59].

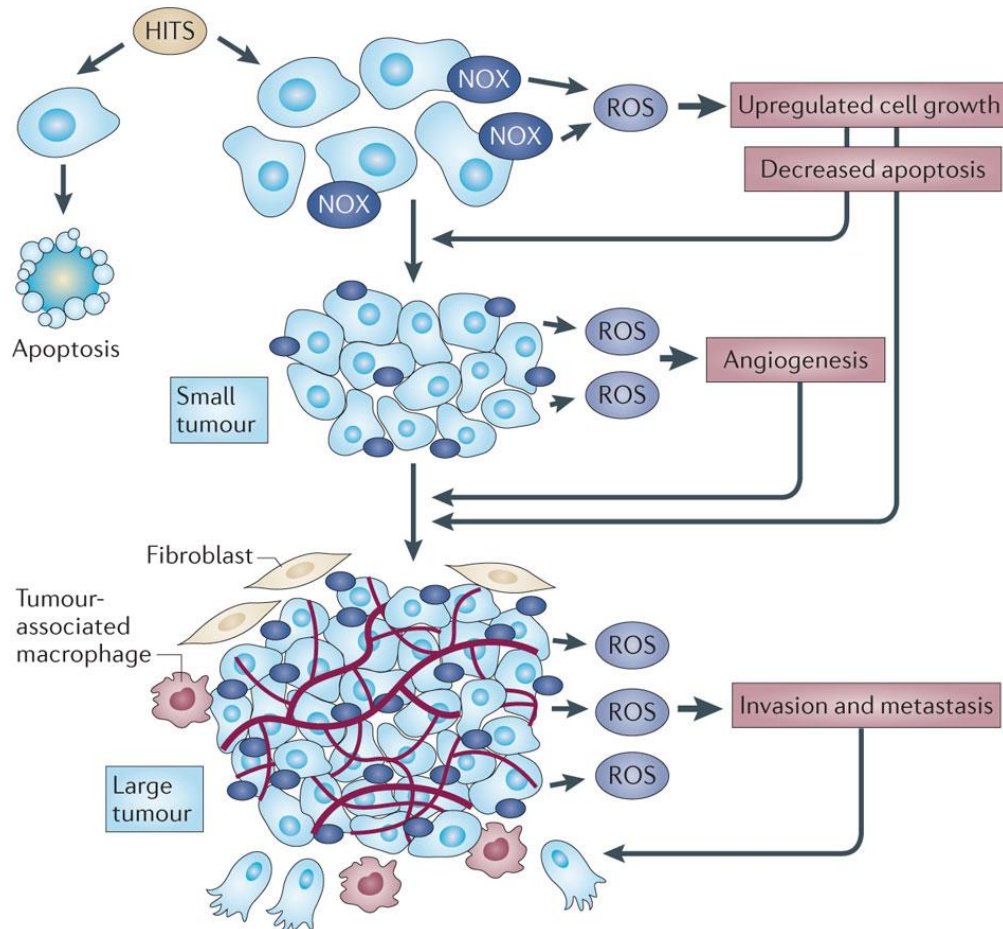


Nature Reviews | Cancer

Figure 6: Integration of NOX oxidase-derived ROS with the hallmarks of cancer. The figure shows the potential signalling pathways that are activated (+) or inactivated (-) by NADPH oxidase (NOX) oxidases and how they relate to some of the suggested hallmarks of cancer cells, such as deregulated cell growth and angiogenesis. The figure is reprinted with Nature Publishing Group's permission (www.nature.com License Number: 3203081425218) [54].

The biological roles of NADPH oxidases in cancer have been mostly deduced from knowledge gained during examination of the physiological and pathophysiological roles of NADPH oxidases in diabetic kidney disease, cardiovascular disease, Alzheimer's disease, fibrosis and atherosclerosis. Although primarily based on *in vitro* data, authors Block and Gorin highlight in their recent review article in 2012 [54] the roles of the NOX complexes in cellular transformation and maintenance of the malignant phenotype (Figure 6). Due to the “*in vitro* only data” limitation, the reviewed studies fail to address the biological complexity that exists in tumours, such as intra-tumour heterogeneity, micro-environmental changes and the systemic influence of factors, including growth factor levels, inflammation and nutrition [54]. Nevertheless, the authors formed the following hypothesis regarding the function of NOX-derived ROS in the progression of carcinogenesis (Figure 7): “In the changing environments of tumour initiation and development, some cells will gain function while others that have intact apoptotic pathways will undergo necrosis or apoptosis. Owing to the pleiotropic nature of NOX-derived ROS, tumour cells that upregulate NOX oxidases and NOX-derived ROS will progress and those that do not, will necrose, apoptose or exhibit a biochemically benign

phenotype. As the tumour progresses, NOX-derived ROS will maintain activated growth pathways, evade cell death and initiate angiogenesis and metastasis” [54, 60].



Nature Reviews | Cancer

Figure 7: A hypothesis for the function of NOX-derived ROS in the progression of carcinogenesis. Multiple genetic and epigenetic alterations (HITS) are required for cellular transformation. Cells that do not activate NOX-derived ROS will undergo apoptosis or necrosis. The cells that upregulate NADPH oxidase (NOX) oxidases and NOX-derived reactive oxygen species (ROS) will progress towards the development of a clinically relevant tumour. In tumours of approximately 1–2 mm in diameter, NOX oxidases sense hypoxia and can help to mediate activation of the angiogenic switch while maintaining unregulated cell growth and evasion of cell death. As the tumour continues to grow, a complex tumour environment, including stromal cells, endothelial cells and tumour-associated macrophages (TAMs), secrete various metastatic agonists. NOX oxidases are responsive to the extracellular fluid surrounding the tumour environment and facilitate invasion and metastasis. The figure is reprinted with Nature Publishing Group’s permission (www.nature.com License Number: 3203081425218) [54].

Therefore, further investigation on the particular role of NADPH oxidases and the underlying signaling cascades in cancer are of great interest. Of particular interest is the membrane bound subunit p22phox, since it is important for the function of the vast majority of NOXes in

order to perform their ROS generating activity, as it forms a mutually stabilizing complex with NOX homologues (NOX1, NOX2, NOX3, NOX4) and allows the recruitment of cytosolic subunits to NOX1, NOX2 and NOX3 to form an active complex. Better understanding of redox-linked signaling systems that are influenced by p22phox dependent ROS generation can give us valuable information about the role of NADPH oxidases in the aetiology of cancer and justifies the investigation on how modulation of expression of p22phox might affect cancer pathophysiology [27, 54, 61].

1.3 Proteomics

1.3.1 Introduction to Proteomics

The term “proteomics” concerns a large-scale comprehensive study of a specific proteome, including information on protein abundances, their variations and modifications, along with their interacting partners and networks, in order to understand cellular processes. The term “proteome” which was coined by Marc Wilkins in 1994 refers to the entire complement of proteins, including the modifications made to a particular set of proteins, produced by an organism or a cellular system. This varies with time and distinct environment, such as stresses, that a cell or organism experiences [62].

Proteomics has evolved substantially from genomics, which involves sequencing and mapping of the genomes of a wide variety of organisms, including humans [63]. Therefore, a brief comparison between genomics and proteomics can facilitate the understanding of the two different fields which are firmly linked.

There is one genome for each organism. Also, genomics allows for the high throughput sequencing of DNA. This process is complex and focuses on the information of one target molecule, DNA. In contrast, proteomics focuses on the identification, localization, and functional analysis of the protein make-up of the cell. The proteins which are present in a cell, together with their function, subcellular location, and structure, change dramatically with the organism, and the conditions faced by their “host” cells including age, checkpoint in the cell cycle, and external or internal signaling events [64]. Thus, there are many proteomes for each organism and consequently, the quantity and complexity of the data derived from the

sequencing and mapping of the human proteome are estimated to be at least three times greater than that involved in the human genome project [65].

1.3.2 Proteomics towards the future of medicine

Proteomics is particularly important in medicine because most diseases are manifested at the level of protein activity. Also, proteomics can have direct and critical “bedside” applications having a leading role on individualised healthcare treatments and shaping the “personalized medicine” of tomorrow. We can foresee a future in which the physician will use different proteomic analyses at many points of disease management. Appropriate use of proteomics can directly affect clinical practice owing to its effects on all of the following crucial elements of patient care and management (Figure 8): early detection of the disease using proteomic patterns of body-fluid samples, diagnosis based on proteomic signatures as a complement to histopathology, individualized selection of therapeutic combinations that best target the entire disease-specific protein network of a patient, real-time assessment of therapeutic efficacy and toxicity, and rational redirection of therapy on the basis of changes in the diseased protein network that are associated with drug resistance [66-71].

Consequently, proteomics seeks to correlate directly the involvement of specific proteins, protein complexes and their modification status in a given disease state. Therefore, such knowledge can provide a fast track to commercialization and speed up the identification of new drug targets that can be used to diagnose and treat diseases.

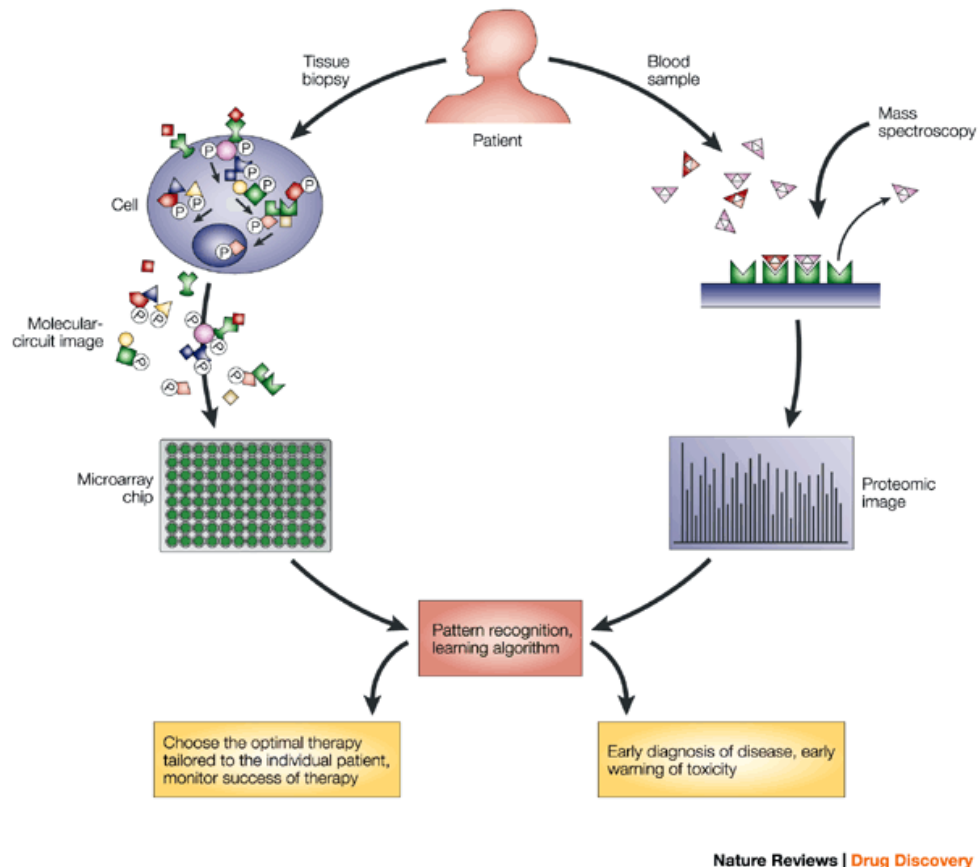


Figure 8: Proteomic technology applied to cancer-patient management. Proteomic pattern analysis of serum has the potential to detect early-stage disease, toxicity or recurrence. Once the disease has been diagnosed and biopsied, protein microarrays offer a means to profile the individual signal pathways that are deranged in the tumour cells of the patient. In this manner, the combinatorial therapy can be tailored to, and monitored in, the individual patient. The figure is reprinted with Nature Publishing Group's permission (www.nature.com License Number: 3266050460762) [71].

1.3.3 Proteomics as a powerful analytical platform

Acquiring, analyzing, and interpreting vast data sets derived from proteomics studies, require a series of well-integrated, high-throughput technologies to lead the researcher from experimental design to biological insight. Despite the hurdles, after many years of evolution, proteomics technologies have indeed managed to significantly affect the life sciences and are an integral part of biological research endeavors.

At present, the field of proteomics spans diverse research topics, ranging from protein expression profiling to analyzing signaling pathways to developing protein biomarker assay systems. It is important to note that within each area, distinct scientific questions are being asked and, therefore, distinct proteomic approaches may have to be applied. These

approaches vary widely in their versatility, technical maturity, difficulty and cost (Figure 9) [72, 73].

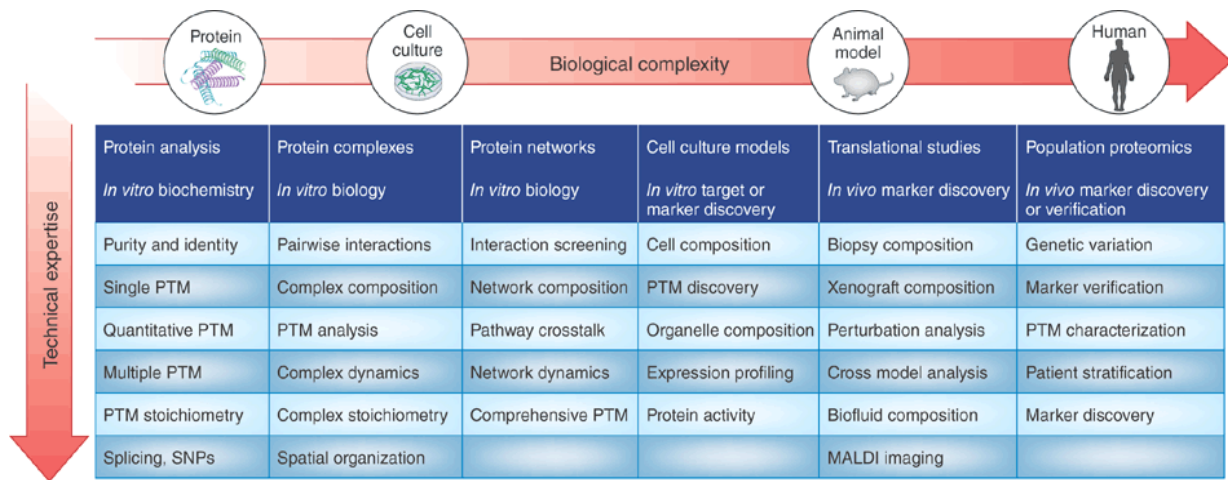


Figure 9: Applications of proteomic technologies. For the purpose of organizing the field of proteomics, it is instructive to compare and contrast the many conceivable applications on the basis of the complexity of the biological context versus the technical difficulty of implementing the appropriate technology. The figure is reprinted with Nature Publishing Group’s permission (www.nature.com License Number: 3266050726593) [72].

1.3.4 Two-dimensional gel electrophoresis (2-DE) for protein expression profiling

Two-dimensional gel electrophoresis, abbreviated as 2-DE, is a well established technique in the constantly evolving field of proteomics [74-77]. It is utilized for protein expression profiling based on high resolution analysis of complex protein mixtures. It is a robust tool for protein separation prior to protein identification allowing the analysis of protein mixtures which are derived either from cells, tissues or body liquids by taking advantage of two major properties of protein molecules. Proteins are separated according to their electric charge by isoelectric focusing (IEF) in the so called “first dimension” and subsequently, they are further separated according to their molecular weight by sodium dodecyl sulfate-polyacrylamide gel electrophoresis (SDS-PAGE) in the so called “second dimension”. Thus, based on this bi-dimensional separation of proteins in a complex mixture, 2-DE as a technique can result in the separation of hundreds of different proteins using a single gel [78, 79]. Information, such as the isoelectric point (pI), the apparent molecular mass (Mr), and the amount of each protein, can be obtained, too. The protein “spot patterns” generated by the 2-DE based methodology can be therefore compared to identify the levels of proteins that differ under unique cellular

conditions. Besides this great advantage, 2-DE analysis is compatible also with the identification of the protein species of interest by employing an appropriate mass spectrometry (MS) analysis of the target sample [77, 79, 80].

Since the introduction of the 2-DE method by O'Farrell in 1975 [81], a large number of applications have been recognised in a wide range of fields, including analysis of the proteome for the detection of disease biomarkers (in diverse areas such as oncology, endocrinology, cardiovascular and central nervous system diseases), drug discovery and protein purity checks. Examples of major limitations comprise the difficulty of resolving proteins at extreme acidic or basic pH areas, the reproducibility issues linked to inter-gel variability and the masking of less abundant proteins by highly abundant ones. However, significant developments in mass spectrometry and image analysis software as well as easy access to rapidly growing databases of protein sequences have contributed to the tremendous growth in the popularity of 2-DE. Thus, despite some inherent limitations, 2-DE based proteomic analysis has proven to be a powerful tool in biomedical research [82] .

Chapter 2: Aim of the study

2.1 Aim of the study

Although evidence has been provided that the NADPH oxidase subunit p22phox is implicated in diverse malignancies via ROS signalling, the exact mechanism still remains elusive.

The overall aim of the present thesis is to enhance the understanding of the functional role of p22phox mediated reactive oxygen species (ROS) in tumour progression by utilizing proteomics, *in silico*, *in vitro* and *in vivo* tools. The cancer cellular model systems of choice are stably transfected hepatoblastoma (HepG2) cells with (a) enhanced p22phox levels and (b) reduced p22phox levels.

The detailed experimental objectives which have been set in order to support the aim of the thesis include:

- Evaluation of the role of p22phox in tumour growth.
- Analysis of the p22phox regulated proteome by a proteomics based methodology.
- Functional analysis of p22phox regulated proteins in tumour proliferation.
- Evaluation of a link between p22phox and Cathepsin D as a known tumour progressing factor.

Chapter 3: Materials and methods

3.1 Materials

3.1.1 Cellular and molecular biology

Table 3: Mammalian cell lines.

Mammalian cell lines	Source
Human hepatoblastoma (HepG2)* (ATCC HB-8065)	ATCC, Manassas, USA
HepG2-pcDNA3.1- (HepG2-CtrK2 & HepG2-CtrK5)	available in house
HepG2-pcDNA3.1-p22phox (HepG2-p22K1 & HepG2-p22K3)	available in house
HepG2-pSTRIKE-None (HepG2-shCtr)	available in house
HepG2-pSTRIKE-p22phox (HepG2-shp22phox)	available in house

*HepG2 nomenclature is corresponding to both “hepatoblastoma” and “hepatocellular carcinoma” terms in the available literature [83].

Table 4: Cell culture media and reagents.

Cell culture media and reagents	Company
Dulbecco’s modified eagle’s medium (DMEM)	Biochrom, Berlin, Germany
Hank’s balanced salt solution (HBSS)	Biochrom, Berlin, Germany
Fetal Calf Serum (FCS)	Pan Biotech, Aidenbach, Germany
Phosphate buffered saline (PBS)	Biochrom, Berlin, Germany
Trypsin-EDTA	Biochrom, Berlin, Germany
Penicillin / Streptomycin	Biochrom, Berlin, Germany
Geneticin	Biochrom, Berlin, Germany

Table 5: siRNA targets.

siRNA targets	
Control: 5’-GAC UAC UGG UCG UUG AAG U dTdT-3’	Eurogentech, Cologne, Germany
Cathepsin D: 5’-CTG GAT CCA CCA CAA GTA CAA-3’	Qiagen, Hilden, Germany

Table 6: Primers used in qPCR*.

Primers used in qPCR	Company
Cathepsin D (forward): 5’-CAT TGT GGA CAC AGG CAC TTC-3’	Metabion, Martinsried, Germany
Cathepsin D (reverse): 5’-GAC ACC TTG AGG GTG TAG TCC-3’	Metabion, Martinsried, Germany
p22phox (forward): 5’-CAC AGC TGG GCG CTT CA-3	Metabion, Martinsried, Germany
p22phox (reverse): 5’-TCC AGC AGG CAC ACA AAC AC-3	Metabion, Martinsried, Germany
β-Actin (forward): 5’-CCA ACC GCG AGA AGA TGA-3	Metabion, Martinsried, Germany
β-Actin (reverse): 5’-CCA GAG GCG TAC AGG GAT AG-3	Metabion, Martinsried, Germany

*qPCR: see methods section.

Table 7: Kits.

Kits	Company
Qiagen RNeasy Mini	Qiagen, Hilden, Germany
QIAquick PCR purification	Qiagen, Hilden, Germany
BrdU ELISA* cell proliferation assay	Roche, Basel, Switzerland
High capacity cDNA Reverse Transcription	Applied Biosystems, Darmstadt, Germany
Perfecta SYBR Green FastMix	Quanta Biosciences, Gaithersburg, USA
Vectastain Elite ABC PK-6100	Vector Laboratories, Burlingame, USA
DAB Substrate SK-4100	Vector Laboratories, Burlingame, USA

*BrdU ELISA: see methods section.

Table 8: Primary antibodies used in IF*/IHC.**

Primary antibodies used in IF/IHC	Company
p22phox	Eurogentech, Cologne, Germany
Cathepsin D	BD Biosciences, Heidelberg, Germany
Ki-67	Abcam, Cambridge, UK
Cleaved Caspase-3	Cell Signalling, Frankfurt a.M., Germany

*IF: immunofluorescence: see methods section. **IHC: immunohistochemistry: see methods section.

Table 9: Secondary antibodies used in IF/IHC.

Secondary antibodies as used in IF/IHC	Company
Mouse IgG Alexa Fluor 488	Invitrogen, Darmstadt, Germany
Mouse IgG Alexa Fluor 594	Invitrogen, Darmstadt, Germany
Rabbit IgG Alexa Fluor 488	Invitrogen, Darmstadt, Germany
Rabbit IgG Alexa Fluor 594	Invitrogen, Darmstadt, Germany
Biotinylated anti-Rabbit IgG(H+L) BA-1000	Vector Laboratories, Burlingame, USA
Biotinylated anti-Mouse IgG(H+L) BA-9200	Vector Laboratories, Burlingame, USA

Table 10: Staining probes used in fluorescence microscopy.

Fluorescence staining probes	Company
Hoechst 33342 for nucleic acid staining	Invitrogen, Darmstadt, Germany
Lysotracker Deep Red for cellular acidic organelles staining	Invitrogen, Darmstadt, Germany

Table 11: Equipment used in cellular and molecular biology methods.

Equipment	Company
Laminar airflow cabinet (Hera Safe)	Heraeus, Hanau, Germany
Incubator (Hera Cell)	Heraeus, Hanau, Germany
Microscope (HAL 100)	Zeiss, Oberkochen, Germany
Fluorescence microscope (IX 50)	Olympus, Hamburg, Germany
Thermocycler RT-PCR (GeneAmp 9700)	Life Technologies, Darmstadt, Germany
Thermocycler qPCR (Rotor-Gene 6000)	Corbett Research, Hilden, Germany
Spectrophotometer (Nanodrop 2000C)	Thermo Scientific, Dreieich, Germany
Plate reader (Tecan Safire)	Tecan, Männedorf, Switzerland
Cell counting chamber (Neubauer)	Menzel-Glaeser, Brunswick, Germany
Microwave oven	Siemens, Munich, Germany

Table 12: Reagents used in cellular and molecular biology methods.

Reagents	Company
Ascorbic acid (Vitamin C)	Sigma Aldrich, Taufkirchen, Germany
N-acetyl cysteine (NAC)	Sigma Aldrich, Taufkirchen, Germany
Bovine serum albumin (BSA)	Appllichem, Darmstadt, Germany
Dihydroethidium (DHE)	Invitrogen, Darmstadt, Germany
Dichloro-dihydro-fluorescein (DCF)	Invitrogen, Darmstadt, Germany
Alamar Blue	Invitrogen, Darmstadt, Germany
Citric acid	Carl Roth, Karlsruhe, Germany
Dimethyl-sulfoxide (DMSO)	Carl Roth, Karlsruhe, Germany
Ethyl-diamine-tera-acetic acid (EDTA)	Carl Roth, Karlsruhe, Germany
Luminol	Sigma Aldrich, Taufkirchen, Germany
Thrombin	Haemochrom Diagnostica, Essen, Germany
Lipofectamine 2000	Invitrogen, Darmstadt, Germany
Pepstatin A	Calbiochem, Darmstadt, Germany
NVP-AUY922	Novartis, Basel, Switzerland

3.1.2 Protein biochemistry and proteomics

Table 13: Primary antibodies used in Western blot* analysis.

Primary antibodies used in Western blot analysis	Company
p22phox	Active Bioscience, Hamburg, Germany
Cathepsin D	BD Biosciences, Heidelberg, Germany
Glutaredoxin-3	Sigma Aldrich, Taufkirchen, Germany
Lamin B1	Cell Signalling, Frankfurt a.M., Germany
Heat shock protein 90 a/b	Enzo Life Sciences, Loerrach, Germany
Heat shock cognate protein 70	Cell Signalling, Frankfurt a.M., Germany
Heat shock protein 70	Enzo Life Sciences, Loerrach, Germany
Heat shock protein 27	Enzo Life Sciences, Loerrach, Germany
MAPRE1	Sigma Aldrich, Taufkirchen, Germany
p53	Cell Signalling, Frankfurt a.M., Germany
phosphorylated-Akt	Cell Signalling, Frankfurt a.M., Germany
Cleaved Caspase 3	Cell Signalling, Frankfurt a.M., Germany
PARP	Cell Signalling, Frankfurt a.M., Germany
β-Actin	Santa Cruz, Heidelberg, Germany

*Western blot: see methods section.

Table 14: Secondary antibodies used in Western blot analysis.

Secondary antibodies used in Western blot analysis	Company
Goat anti-Rabbit HRP conjugated (1/10.000 5% milk in TBST)	Calbiochem, Darmstadt, Germany
Goat anti-Mouse HRP conjugated (1/10.000 5% milk in TBST)	Calbiochem, Darmstadt, Germany
Rabbit anti-Goat HRP conjugated (1/10.000 5% milk in TBST)	Calbiochem, Darmstadt, Germany

Table 15: Equipment used in 2-DE* and Western blot analyses.

Equipment in 2-DE and Western blot analyses	Company
Power supply unit (Power PAC 3000)	Bio-Rad, Munich, Germany
Isoelectrofocusing unit (Ettan IPGphor3)	GE Healthcare, Munich, Germany
Electrophoresis unit (Ettan DALTsix)	GE Healthcare, Munich, Germany
Gel caster (DALTsix)	GE Healthcare, Munich, Germany
Gel scanner (Typhoon TRIO)	Amersham Biosciences, Munich, Germany
Dust free cabinet (Captair flow)	Erlab, Rowley, USA
Western blot method equipment	Bio-Rad, Munich, Germany

*2-DE: two dimensional gel electrophoresis: see methods section.

Table 16: Chemical solvents and reagents.

Chemical solvents and reagents	Company
Ethanol	CLN, Freising, Germany
Methanol	CLN, Freising, Germany
Isopropanol	CLN, Freising, Germany
Acetic acid	CLN, Freising, Germany
Acetone	Fluka, Taufkirchen, Germany
Acetonitrile	Fluka, Taufkirchen, Germany

Table 17: Reagents used in 2-DE and Western blot analyses.

Reagents used in 2-DE and Western blot analyses	Company
Rotiphorese Gel30 (30% acrylamide with 0,8% bis-acrylamide)	Carl Roth, Karlsruhe, Germany
Urea	GE Healthcare, Munich, Germany
Thiourea	GE Healthcare, Munich, Germany
Sodium dodecyl sulphate (SDS)	GE Healthcare, Munich, Germany
Dithiothreitol (DTT)	GE Healthcare, Munich, Germany
Iodoacetamide (IAA)	GE Healthcare, Munich, Germany
Ammonium persulphate (APS)	GE Healthcare, Munich, Germany
Trifluoroacetic acid (TFA)	Fluka, Taufkirchen, Germany
Spermine	Fluka, Taufkirchen, Germany
Low melting agarose	Fluka, Taufkirchen, Germany
Protein ladder	Fermentas, Schwerte, Germany
Glycine	GE Healthcare, Munich, Germany
Glycerol	GE Healthcare, Munich, Germany
Tris-base	GE Healthcare, Munich, Germany
De streak reagent	GE Healthcare, Munich, Germany
Silver nitrate	Sigma Aldrich, Taufkirchen, Germany
Formaldehyde	Carl Roth, Karlsruhe, Germany
Glutardialdehyde	Carl Roth, Karlsruhe, Germany
Sodium chloride	Carl Roth, Karlsruhe, Germany
Sodium carbonate	Carl Roth, Karlsruhe, Germany
Sodium acetate	Carl Roth, Karlsruhe, Germany
Sodium thiosulphate	Carl Roth, Karlsruhe, Germany
Ruthenium(II) tris(bathophentroline disulfonate (RuBPS)	RubiLAB, Burgdorf, Switzerland
PlusOne acrylamide 40% solution for 2-DE	GE Healthcare, Munich, Germany
PlusOne N,N'-Methylene-bisacrylamide 2% solution for 2-DE	GE Healthcare, Munich, Germany
Immobiline dry strips (pH: 4-7, 24 cm & 6-11, 18 cm)	GE Healthcare, Munich, Germany
N,N,N',N'-tetramethylethylenediamine (TEMED)	GE Healthcare, Munich, Germany
Cholamidopropyl-dimethylammonio-1-propane-sulfonate	GE Healthcare, Munich, Germany
Ponceau S (PonS)	Carl Roth, Karlsruhe, Germany
Roti –Quant	Carl Roth, Karlsruhe, Germany
Tween 20	Sigma Aldrich, Taufkirchen, Germany
Skim milk powder	Merck, Darmstadt, Germany

3.1.3 General equipment and device

Table 18: General equipment and device.

Equipment/device	Company
Micropipettes (P2, P10, P20, P200, P1000)	Gilson, Middleton, USA
Analytical balance (BP301S, BP4100S)	Sartorius, Goettingen, Germany
Autoclave (KSG 25-2-3)	KSG , Olching, Germany
Centrifuge (Biofuge Pico, Stratos, Fresco)	Heraeus, Hanau, Germany
Centrifuge (Varifuge 3.0R)	Heraeus, Hanau, Germany
Heating block	Eppendorf, Hamburg, Germany
Heating plate	Leica, Wetzlar, Germany
Millipore water supply (Milli-Q Synthesis)	Millipore, Frankfurt a.M., Germany
pH Meter (pH 540 GLP)	WTW, Weilheim, Germany
Vacuum pump	KNF Neuberger, Trenton, USA
Vortex (Genie-2)	Heidolph, Schwabach, Germany
Magnetic stirrer and heater (M3001)	Heidolph, Schwabach, Germany
Shaker (Polymax 1040)	Heidolph, Schwabach, Germany
Rotator	Froebel Labortechnik, Lindau, Germany
Thermo-mixer (Comfort)	Eppendorf, Hamburg, Germany
Speed Vacuum (Centrivac)	Kendro lab equipment, Dreieich, Germany

3.1.4 Xenograft mouse model

Table 19: Animals used in the xenograft model.

Animals	Provider
Rag2 ^{-/-} γC ^{-/-} male immunodeficient mice	CIEA, Kawasaki, Japan

3.1.5 Software and databases

Table 20: Software.

Software	Company
MS Office 2007 (word, excel, powerpoint)	Microsoft, Redmond, USA
Adobe Photoshop CS3 (image editing)	Adobe Systems, San Jose, USA
Progenesis SameSpots (2-DE image analysis)	TotalLab, Newcastle upon Tyne, UK
IPA (pathway & network analysis)	Ingenuity Systems, Redwood City, USA
GraphPad Prism (statistics software)	GraphPad Software, Inc, La Jolla, USA
EndNote X7 (bibliography software)	Thomson Reuters, New York City, USA

Table 21: Databases.

Databases	Source
PubMed (http://www.ncbi.nlm.nih.gov/pubmed)	NIH, Bethesda, USA
BLAST (http://blast.ncbi.nlm.nih.gov/Blast.cgi)	NIH, Bethesda, USA
UniProtKB / Swiss-Prot (http://www.uniprot.org/uniprot/)	UniProt Consortium, Switzerland, UK, USA

3.2 Methods

3.2.1 Cellular biology methods

3.2.1.1 Maintenance and storage of cells

Cell culture refers to the removal of cells from an animal or a plant and their subsequent growth in a favorable artificial environment. The cells may be removed from the tissue directly and disaggregated by enzymatic or mechanical means before cultivation, or they may be derived from a cell line or cell strain that has already been established [84].

In this study, hepatoblastoma (HepG2) cells were maintained in culture by providing DMEM 4.5 g/l glucose medium supplemented with 10% FCS, 100 U/ml penicillin and 100 U/ml streptomycin. During each passage of all adherent cells which were in use, pre-existing medium was first aspirated, cells were then washed with PBS and trypsin was finally added for 2 min in order to detach the cells. Then, fresh medium was added to neutralize the trypsin and the detached cells were transferred into a fresh T75 flask kept in a humidified incubator at 5% CO₂ until the next passage. Regular controls were also taken place under the microscope in order to assess the viability and sterility of cells in use. In particular, regarding the HepG2 cells, since they tend to form clusters when they grow, in addition to the above, a 10 ml syringe with a fixed 20 G needle was used in order to dissolve the cell clusters into single cells during each passage [85, 86]. Cells were stored in liquid nitrogen tank according to the following steps. Confluent cells were detached by trypsinisation and centrifuged at 1000 rpm for 5 min. Cells were then resuspended in culture medium containing 10% DMSO and transferred to cryo-vials. To allow gradual freezing, cryo-vials were then placed in a cold isopropanol freezing box and kept for at least 24 h at -70°C in order to acclimate to extreme cold. Finally, cells were transferred to and stored in liquid nitrogen tank (-196°C) [87].

3.2.1.2 Counting of cells

In biomedical research, a key step in many experimental workflows involves the counting of cells. Researchers often need to count cells prior to cell culture or before studying downstream processes and using analytical techniques that require an accurate and consistent number of input cells [84]. Knowing the number of input cells is important for

standardizing experiments and for measuring assay impact. Examples of processes that require accurate and consistent numbers of input cells include transfection, cell proliferation or viability studies, and quantitative PCR. In practise, a clean cover-slip was placed on the Neubauer chamber firmly (Newton rings appearance) and 10 μl of cell suspension was distributed between the cover-slip and the chamber. Cells were then counted in the 4 grid areas of the chamber using a 10x objective under the microscope. Finally, the number of cells contained in 1 ml of cell suspension was estimated.

3.2.1.3 Stable and transient transfection of cells

The process of introducing nucleic acids into eukaryotic cells by non-viral methods is defined as transfection [88]. Cell transfection can be classified into two main types, namely stable and transient transfection. In stable transfection integration of foreign genes into genomic DNA of host cells takes place whereas in transient transfection the foreign genes do not integrate into the genome of host cells. Using various chemical, lipid or physical methods, this gene transfer technology is a powerful tool to study gene function and protein expression in the context of a cell [89-93].

In this study, stably transfected HepG2 clones with differential levels of p22phox were used which were generated in our lab by Dr. Michael Weitnauer (former colleague at the German Heart Center Munich) using Fugene HD (Roche, Penzberg, Germany). These cells were cultivated and maintained in standard DMEM medium supplemented with geneticin.

Regarding the transient transfection of HepG2 cells in the present study, the following methodology was performed. For 6 cm dishes 5 μg of plasmid DNA and Lipofectamine 2000™ (Invitrogen, Karlsruhe, Germany) were used. A day before the transfection, 1×10^6 cells were cultivated in culture dishes (6 cm) in appropriate volume of 4 ml growth medium so that they were 70% confluent at the time of transfection. The plasmid DNA was incubated with 500 μl culture medium (without FCS and antibiotics) for 5 min. At the same time, 25 μl of the Lipofectamine 2000™ with 500 μl of the culture media (without FCS and antibiotics) were incubated for 5 min. After the incubation, both solutions, diluted DNA and diluted Lipofectamin 2000™ were combined, mixed gently and incubated for 20 min at room temperature in order to allow the DNA-Lipofectamine 2000™ complexes to be formed. In the meantime, the cells were washed 3 times with cell culture medium (without FCS and

antibiotics), and covered with 3 ml of the same medium. The DNA-Lipofectamine 2000™ complexes were added to the plate, mixed gently by rocking the plate back and forth, and the cells were incubated at 37°C in a CO₂ incubator. After 3 hours of incubation, the medium was replaced with 4 ml fresh medium (containing FCS and antibiotics), and the cells were incubated for 48 hours. The expression of the recombinant proteins was confirmed by Western blot analysis.

3.2.1.4 Dihydroethidium (DHE) staining of cells

Levels of ROS were visualized by the fluoroprobe dihydroethidium (DHE), which is also called hydroethidine. DHE passively diffuses into the cells exhibiting blue fluorescence. After oxidation, predominantly with O₂^{-•}, DHE is oxidized to ethidium, giving a more polar compound that intercalates within DNA and stains the nucleus in fluorescent red (Figure 10). To evaluate the levels of ROS, HepG2 cells were grown in 96-well plates to 80% confluence for 16 h. Cells were then washed with HBSS and incubated in the dark with DHE (50 μM) for 10 min at 37°C. Cells were washed with HBSS again to remove excess dye. Then DHE fluorescence was analyzed using 480 nm excitation and 640 nm emission wavelength [94, 95].

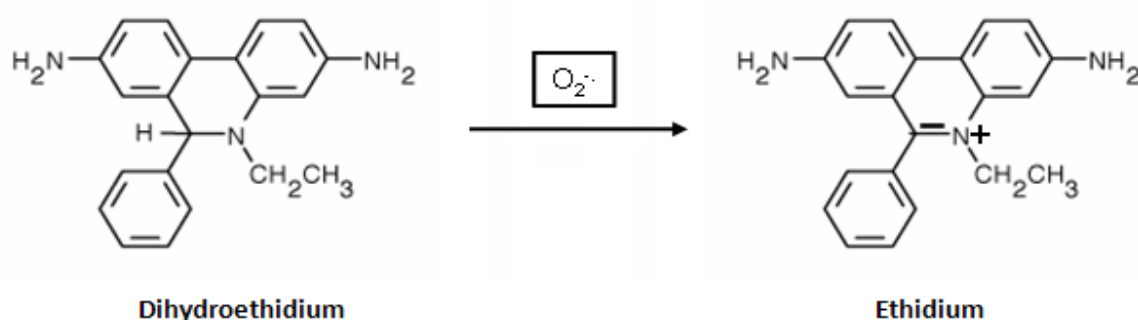


Figure 10: Principle of the DHE assay for the measurement of ROS. After oxidation with O₂^{-•}, dihydroethidium (DHE) is converted to the polar compound ethidium that intercalates into the DNA.

3.2.1.5 BrdU ELISA assay

Cellular proliferation requires DNA replication. Therefore, monitoring of DNA synthesis is an indirect marker of the rate of proliferation in response to different stimuli. To assess proliferative activity of EC we used 5-bromo-2′deoxyuridine (BrdU) labelling. BrdU is an

analogue of the DNA nucleoside thymidine, and is incorporated in newly synthesized DNA of proliferating cells. The incorporated BrdU is detected by an immunoassay, using a peroxidase-conjugated antibody that specifically recognizes BrdU bound to denaturated DNA. The bound antibody is detected by a peroxidase-catalysed colorimetric reaction, using tetramethylbenzidine (TMB) as a substrate [96-98].

Cells were seeded in 96 well plates to achieve 50% of confluency. In order to assess proliferation, 24 h after seeding, cells were incubated with BrdU (10 μ M) for 16 h. During this labelling period, BrdU is incorporated in place of thymidine into the DNA of cycling cells. After removing the labelling medium, the cells were fixed for 30 min, and the DNA is denaturated in one step by adding FixDenat. After removing FixDenat, the anti-BrdU-POD antibody is added for 1 h. The antibody binds to the BrdU incorporated into the newly synthesized cellular DNA. The immune complexes were then detected by the reaction incurred by adding the colorimetric substrate TMB. When the blue colour developed as a result of the reaction, the reaction was terminated by using 1 M H₂SO₄. Finally, the reaction product was quantified by measuring the absorbance in an ELISA reader (Tecan Safire) at 450 nm with a reference wavelength at 690nm.

3.2.1.6 Alamar Blue assay

The Alamar Blue assay is designed to measure quantitatively the proliferation of various human and animal cell lines, bacteria and fungi. It incorporates a fluorometric /colorimetric growth indicator based on detection of metabolic activity. Specifically, the system incorporates an oxidation-reduction (redox) indicator that both fluoresces and changes colour in response to chemical reduction of growth medium resulting from cell growth. As cells being tested grow, innate metabolic activity results in a chemical reduction of Alamar Blue. Continued growth maintains a reduced environment while inhibition of growth maintains an oxidized environment in the cytosol. Reduction related to growth causes the redox indicator to change from oxidized Resazurin (non-fluorescent, blue) form to reduced Resorufin (fluorescent, red) form (Figure 11) [99, 100]. In practise, cells were seeded in 96-well plates and 24 h after seeding, 10 μ l of Alamar Blue reagent were added to each well. Data were subsequently collected monitoring fluorescence at 555nm excitation wavelength and 585nm emission wavelength on a plate reader.

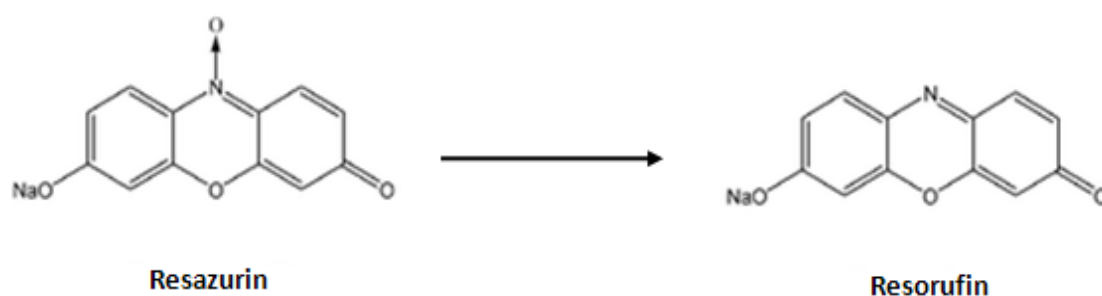


Figure 11: Principle of the Alamar Blue metabolic activity assay. Alamar Blue works as a cell viability and proliferation indicator through the conversion of resazurin to resorufin. Resazurin, a non-fluorescent indicator dye, is converted to highly red fluorescent resorufin via reduction reactions of metabolically active cells. The amount of fluorescence produced is proportional to the number of living cells.

3.2.1.7 Clonogenic assay

Clonogenic assay or colony formation assay is an *in vitro* cell survival assay based on the ability of a single cell to grow into a colony. The colony is defined to consist of at least 50 cells. The assay essentially tests every cell in the population for its ability to undergo "unlimited" division. Clonogenic assay is the method of choice to determine cell reproductive death after treatment with ionizing radiation, but can also be used to determine the effectiveness of other cytotoxic agents. Only a fraction of seeded cells retains the capacity to produce colonies [101, 102]. Before or after treatment, HepG2 cells were seeded out in 6-well plates in appropriate dilution (1.500 cells in 2 ml Medium) to form colonies in 1–4 weeks. Colonies were stained with crystal violet (0.5% w/v), digitalized as images after scanning the plates and counted.

3.2.1.8 Immunofluorescence (IF) and fluorescence microscopy

The immunofluorescence (IF) method detects and provides information about specific target antigens. These antigens can be visualized after treatment with corresponding primary antibodies and subsequent treatment with secondary antibodies conjugated with a fluorescent label. In that way, antigen signals can be viewed eventually under a fluorescent microscope [103]. Fluorescent molecules absorb only at specific wavelengths and therefore a fluorescence microscope must have a light source able to produce various wavelengths for excitation. Having a xenon arc lamp or mercury-vapour lamp that generates white light, which

is a mixture of all visible wavelengths, usually solves this problem. A special optical filter called an excitation filter removes any other wavelength of light other than the wavelength used to excite the fluorescent molecule. The next element in the optical pathway is called a dichroic mirror, which is a special mirror that is able to reflect certain wavelengths of light and let other wavelengths pass through. When the filtered wavelength exits the excitation filter it gets reflected onto the sample containing the fluorescent molecules. This leads to the absorption of photons and the emission of photons of a shorter wavelength. Because the emitted photons have a shorter wavelength than the absorbed photons the design of the dichroic mirror permits them to pass through the dichroic mirror onto the ocular or detector of the microscope (Figure 12) [104-106].

In experimental practise, cells were seeded onto a 8 well μ -slide with cover (60.000 cells per well). They were washed twice with PBS (5 min each time) and then fixed with cold methanol/acetone solution (-20°C) for 10 minutes. The MA solution was then aspirated and the plates left to dry at room temperature for 5 min. After, blocking solution (5% BSA in PBS) was added to each well for 1 hour at room temperature. Selected primary antibodies were diluted in 1% BSA in PBS and 100 μl of diluted primary antibody was added to each well. Incubation was carried out in a humidified chamber overnight at 4°C . In the following day, all wells were washed 3 times with PBS for 5 min each. Subsequently, secondary antibody diluted at appropriate ratios in 1% BSA in PBS and incubation was carried out for 1 h at room temperature in the dark. The wells were then washed 3 times with PBS twice for 5 minutes and monitored under the fluorescence microscope. Finally, the cells were fixed by using fluorescent mounting medium and corresponding pictures were taken.

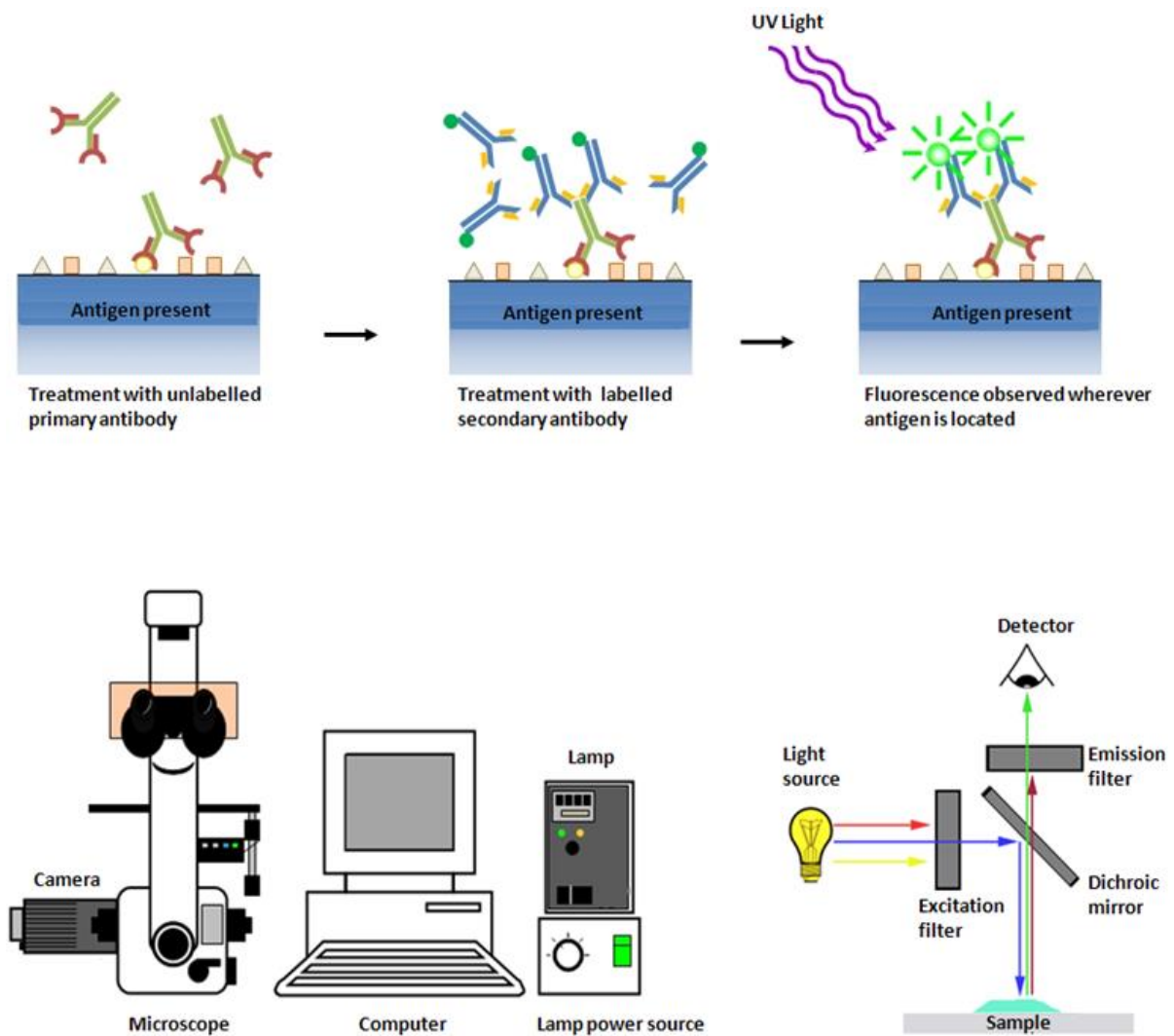


Figure 12: Schematic overview of the immunofluorescence assay and fluorescence microscope. Up: Conceptual diagram displaying the key steps involved in performing an experiment based on indirect immunofluorescence. Down: The major components of a fluorescent microscope (left part) and illustration of the mode of function (right part).

3.2.1.9 Immunohistochemistry (IHC)

Immunohistochemistry (IHC) combines anatomical, immunological and biochemical techniques to identify discrete tissue components by the interaction of target antigens with specific antibodies tagged with a visible label. IHC makes it possible to visualize the distribution and localization of specific cellular components within cells and in the proper tissue context. While there are multiple approaches and permutations in IHC methodology, all of the steps involved are separated into two groups: sample preparation and labeling. IHC has a broad

range of applications such as biological research, disease diagnosis and drug development [107, 108].

In the present study, IHC was performed in order to visualize targeted proteins in the cells of formalin-fixed paraffin embedded xenograft tissue sections. According to the protocol used, the samples were deparaffinised and rehydrated by subsequent treatment with 2x 100% xylol, 2x 100% ethanol, 2x 96% ethanol, 2x 70% ethanol and 2x deionised water. Antigens were recovered by using a Microwave (600 W) for 15 minutes in 0.01M citrate buffer pH 6.0. After cooling down at room temperature for 20 min, slides were washed two times in cold deionised water. To block endogenous peroxidase activity, the samples were then treated with 3% H₂O₂ in deionised water for 15 minutes and afterwards washed 2 times with deionised water and 2 times with PBS. Blocking was performed using 5% goat serum in PBS for 1 hour at room temperature. Slides were then incubated with primary antibodies diluted in blocking solution over night at 4 °C. Primary antibodies included: anti-cleaved Caspase 3 (1/100), anti-Ki67 (1/2500) and anti-Cathepsin D (1/100). The following day, the samples were washed 3 times with PBS and incubated with anti-rabbit or anti-mouse in goat biotinylated secondary antibody diluted in blocking solution (1/300) for 1 hour at room temperature. The samples were then washed for 3 times in PBS and incubated for 30 min at room temperature with pre-formed avidin-biotin peroxidase complex (incubated prior to usage for 30 minutes at 4°C, Vector Laboratories, CA). Following 3 times washing in deionised water, staining was developed using DAB for 2-10 minutes at room temperature. After successful staining, samples were washed in deionised water, counterstained with Mayer's Hämalaun solution, washed with tap water, dehydrated in 2x 70% ethanol, 2x 96% ethanol, 2x 100% ethanol and 2x 100% xylol. Slides were covered with pertex and analysed by light microscopy. The IHC experiments were performed with the help of Kalliope-Nina Diakopoulos (Department of Gastroenterology, University Hospital "Klinikum rechts der Isar", Munich, Technical University of Munich).

3.2.2 Molecular biology methods

3.2.2.1 DNA amplification and polymerase chain reaction (PCR)

While an organism's entire genome is present in each cell of that organism, each gene or target region of interest typically represents only a small portion of the total DNA present in

the cell. In order to study the sequences of individual genes or specific regions of interest, it is often necessary to obtain a large quantity of DNA for study. Rather than isolating a single copy of the target DNA from a large number of cells, it is possible to generate multiple copies of a target from a single molecule of DNA or mRNA. In vitro amplification relies on methods like the polymerase chain reaction (PCR).

PCR is a method to rapidly amplify sequences of DNA. During a typical PCR, template DNA (containing the region of interest) is mixed with deoxynucleotides (dNTPs), a DNA polymerase and primers. Primers are short segments of complementary DNA that base-pair with the template DNA of the region of interest, therefore defining the start and end of the amplified region, and serve as recruitment sites for the polymerase. PCR involves a series of temperature cycles that, although once conducted by moving tubes through various water baths, is now controlled automatically by the use of thermal cyclers or thermocyclers. Thermocyclers provide tight control over both the reaction temperature and the duration of each temperature step, ensuring efficient amplification. During a typical PCR, cycles of denaturation, annealing and extension are repeated to achieve exponential amplification of the target sequence. Denaturation consists of heating the samples up typically between 94-98°C to cause denaturation of the template DNA, disrupting the hydrogen bonds and base stacking interactions that hold the DNA strands together. Once the strands are separated, the temperature is decreased to the annealing temperature (TA) (typically between 48-72°C) to allow the primers to base pair (or anneal) to complementary regions of the template. During the extension step (typically 68-72°C) the polymerase extends the primer to form a nascent DNA strand. This process is repeated multiple times (typically 25-35 cycles), and because each new strand can also serve as a template for the primers, the region of interest is amplified exponentially. The final step of the PCR is generally a longer, single temperature step (often 5-10 min at 68-72°C) that allows the completion of any partial copies and the clearance of all replication machinery from the nascent DNA (Figure 13) [109-111].

Once the PCR is complete, the thermocycler is set to 4°-10°C to maintain product integrity until the time that tubes can be removed from the machine. In this study, quantitative PCR was used to detect the expression of different genes by using cDNA obtained from a reverse transcription of isolated RNA (reverse transcription PCR) [109, 112].

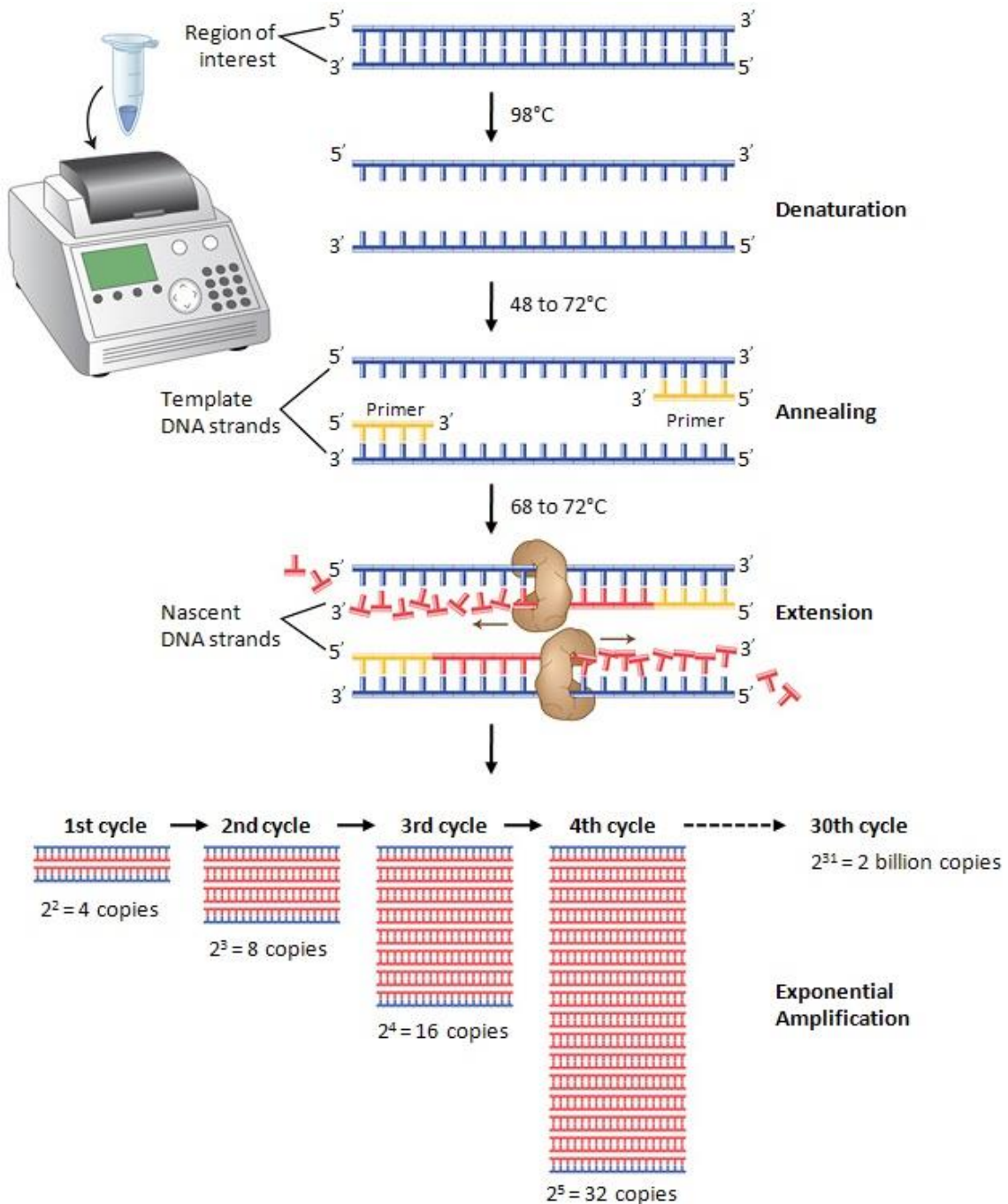


Figure 13: Schematic overview of the polymerase chain reaction (PCR). Different stages of the PCR technique which are used to amplify small samples of DNA are highlighted.

3.2.2.2 Total RNA purification

Total RNA from the cultured tumour cells was purified using the Qiagen RNeasy Mini Kit (Qiagen) in accordance to the manufacturer's manual. Briefly, cells were plated initially in 6 cm dishes. At the end of the experiment, cells were washed with cold PBS and plates were frozen on liquid nitrogen. Thereafter, cells were lysed in 600 µl RLT lysis buffer and RNA was

eventually purified and eluted in RNase free water. The determination of the concentration in purified RNA samples took place using the Nanodrop spectrophotometer 2000C (Thermo Scientific) [113, 114].

3.2.2.3 Reverse Transcription PCR

Reverse transcription PCR (RT-PCR) involves the use of a RNA-dependent DNA polymerase (reverse transcriptase) in order to produce a library of complementary DNA (cDNA) from messenger RNA (mRNA) extracted from cultured cells or tissue (Table 22). The technique is based on RNA denaturation and hybridisation to short non-gene specific DNA sequences (random hexamers). The cDNA thus produced can be used to clone genes or to analyze the mRNA expression of a specific gene by PCR or quantitative PCR [112].

Table 22: Composition of RT-PCR master mix solutions.

RT-PCR master mix solutions	Amount*
<u>including RT enzyme</u>	
10x RT buffer	14 µl
dNTP	5,6 µl
RT random primers	14 µl
Rnase free H ₂ O	29 µl
RT enzyme Multi-Scrip	7 µl
<u>not including RT enzyme (negative control)</u>	
10x RT buffer	14 µl
dNTP	5,6 µl
RT random primers	14 µl
Rnase free H ₂ O	36.4 µl

*Values are displayed for 8 samples and 10µl of master mix solution was added to each sample respectively.

3.2.2.4 Quantitative PCR

The quantitative PCR (qPCR) or else real time PCR is a variation of the PCR in which the amplification of the PCR products is monitored during the amplification process. In this study, qPCR was employed in order to evaluate the relative gene regulation by assessing the mRNA levels of target samples subjected to the analysis. Therefore, following the RNA isolation and the reverse transcription leading to cDNA synthesis, qPCR was used for amplification of the target genes with PerfeCTa[®] SYBR[®] Green FastMix[®] (Quanta BioSciences). qPCR was

performed in a Rotor-Gene 6000 Real-Time PCR System (Corbett Life Science) using gene-specific primers. The samples were loaded in triplicate for each primer pair, and the result of each sample was normalized to β -Actin mRNA. Quantification was done using the Relative Expression Software Tool - Multiple Condition Solver (REST-MCS) [115, 116]. A negative control without cDNA template was used in each assay to assess the overall specificity [117, 118].

3.2.2.5 DNA sequencing

Automated fluorescent sequencing utilizes a variation of the Sanger chain-termination protocol [119]. In this study, gene products after performing qPCR needed to be sequenced in order to verify that suitable primers were selected and the corresponding target genes have been amplified on a precise way. In practise, gene products were processed using the QIAquick PCR purification kit and were sent for DNA sequencing (LGC Genomics GmbH). Sequence was aligned to the predicted PCR product sequence using the Basic Local Alignment Search Tool (BLAST) verifying the PCR product.

3.2.2.6 In vivo method : Xenograft model

Animal models are used extensively in basic cancer research as well as in pharmaceutical research in predicting efficacy and finding toxicities for cancer chemotherapeutic agents before entering the clinic [120, 121]. This has resulted in the development of many different animal models of malignant disease. One very important group of these models concerns grafts of tumour material (syngeneic or xenogeneic) into immunocompetent or immunodeficient animals, respectively. In particular, the “xenograft models” concern heterotransplantation of human cancer cells or tumour biopsies into immunodeficient rodents. The term “xenograft” is derived from the Greek “xeno”, meaning foreign, and graft (Figure 14) [13].

In this study, xenograft mouse model experiments were carried out in collaboration with Dr. Guenther Richter (Laboratory for Functional Genomics and Transplantation Biology, Research Center of Paediatric Oncology at the University Hospital Klinikum rechts der Isar, Technical

University of Munich). Male immunodeficient mice ($Rag2^{-/-}\gamma_c^{-/-}$) 10-14 weeks old were available in the collaborating lab. In total, they were used five control (corresponding to HepG2 shCtr cells) and five treatment mice (corresponding to HepG2 shp22phox cells). On day one, $3,0 \times 10^6$ cells diluted in 200 μ l PBS, were injected subcutaneously into the groin using a 26-gauge needle attached to a 1ml syringe. Tumour size was determined as described in [122]. Mice bearing a tumour > 10 mm in diameter were considered as positive and sacrificed. The immunodeficient $Rag2^{-/-}\gamma_c^{-/-}$ mice on a BALB/c background were obtained from the Central Institute for Experimental Animals (Kawasaki, Japan) and maintained in the animal facility under pathogen-free conditions in accordance with the institutional guidelines and approval by local authorities.

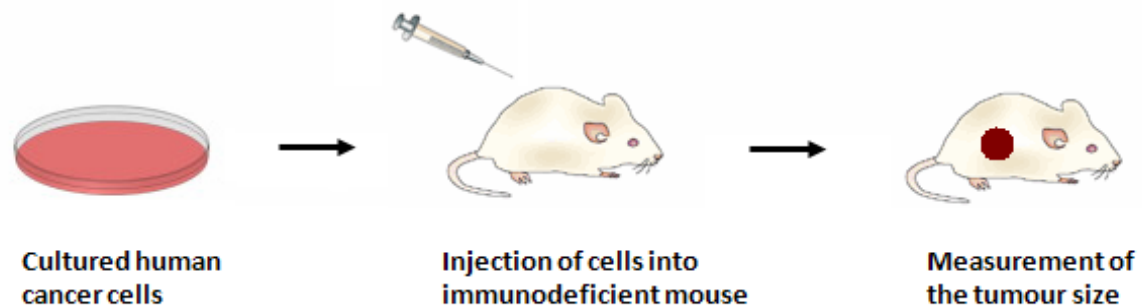


Figure 14: Diagram depicting major experimental stages in a xenograft mouse model.

3.2.3 Protein biochemistry and proteomics methods

3.2.3.1 Protein isolation

Proteins can be extracted from cultured cells using different experimental protocols and corresponding buffer solutions [123]. In this study, cells prior adding lysis buffer, were washed with phosphate buffered saline (PBS) and then, they were frozen on liquid nitrogen. After, frozen cells were lysed and scraped in 1.5x Laemmli buffer (Table 23) and total protein concentration was quantified. Alternatively, cells were scraped directly in 1.5x Laemmli loading buffer without freezing them in liquid nitrogen and directly used for further experiments as cell lysates [123-125].

Table 23: Composition of laemmli lysis buffer.

Laemmli lysis buffer	Amount*
Tris (pH 6.8 / 187 mM)	9.375 ml
SDS (6% w/v)	15 ml
Glycerol (30%)	15 ml
Bromophenol blue (0.06% w/v)	300 μ l
DTT (15 mM)	2.325 g
EDTA (60 mM)	0.5 ml
Milli-Q H ₂ O	4.325 ml

*It was prepared as 3x concentrated solution and values displayed correspond to the total amount of ~50 ml.

3.2.3.2 Bradford assay

Total protein quantification was done performing quantification after [126] using the Roti-Quant (Carl Roth GmbH, Karlsruhe, Germany) containing Coomassie Brilliant Blue Dye-G250. This dye appears in three different states which absorb at varying wavelengths (cationic 470nm, neutral 650nm, anionic 595nm). By binding the dye with a protein, it changes from a cationic to an anionic state and thus, it changes its absorption level to 595nm. This absorption change is proportional to the protein concentration over a wide range, and it was first utilized in concentration analysis by Bradford [126]. Coomassie Brilliant Blue-G250 binds primarily to basic amino acids [127]. This accounts for the difference in the level of absorption of varying proteins. Therefore, while performing the analysis, it was used a BSA protein standard for quantification (0, 5, 10, 20, 30, 40, 50, 60 μ g/ml). Protein cell lysates were diluted 1:400 and 80 μ l of protein standards and samples were added to the wells of a 96 well plate. The Roti-Quant solution was diluted 1:5 and 200 μ l was added to the samples and standards. Absorbance of the proteins was analyzed using a plate reader (Tecan) and protein concentration was calculated performing a standard curve from the standard and linear regression analysis.

3.2.3.3 Western blot analysis

Western blot (also called immunoblotting) is used to detect protein levels and is a core technique in biomedical research laboratories. After protein extraction, the proteins are loaded onto a denaturing polyacrylamide gel where they are separated according to their molecular weight. They are then blotted onto a membrane which is hybridized with an

antibody (primary antibody) specific for the protein of interest (antigen). The membrane is then incubated with another antibody which recognizes the primary antibody (secondary antibody). The secondary antibody is tagged with horseradish phosphatase so the protein levels can be visualized by exposure of photographic film to the chemiluminescence given off by the secondary antibody (Figure 15) [128].

In this study, before performing the electrophoresis, samples were mixed with 3X Laemmli loading buffer and boiled at 95°C for 5 min. Proteins (50 µg) were separated by 8-12% SDS-PAGE (Table 24) in running buffer in a Mini-Protean 3 System (Biorad) and transferred to nitrocellulose Protran membranes (Schleicher & Schuell) using the Mini Trans-blot System (Biorad) in ice cold transfer buffer (Table 25). After transfer, membranes were rinsed in water and incubated in Ponceau S solution for several min. The membranes were then washed in water to reduce background staining and the membranes were scanned for documentation and loading control. For reversing the Ponceau S staining, membranes were washed with TBS-T (Table 26) and then blocked for 60 minutes in TBS-T containing 5% non-dry milk or 5% BSA and eventually they were incubated overnight at 4°C with primary specific antibodies. On the following day, after incubation with the primary antibodies, the membranes were washed initially 3 times for 10 minutes with TBS-T and were further incubated with a horseradish peroxidase-conjugated secondary antibody for 1 h. After that, the membranes were washed again 3 times for 10 minutes with TBS-T and finally protein bands were visualized by performing luminol-enhanced chemiluminescence (Table 27). Blots were analyzed and quantified using ImageJ software (NIH, USA).

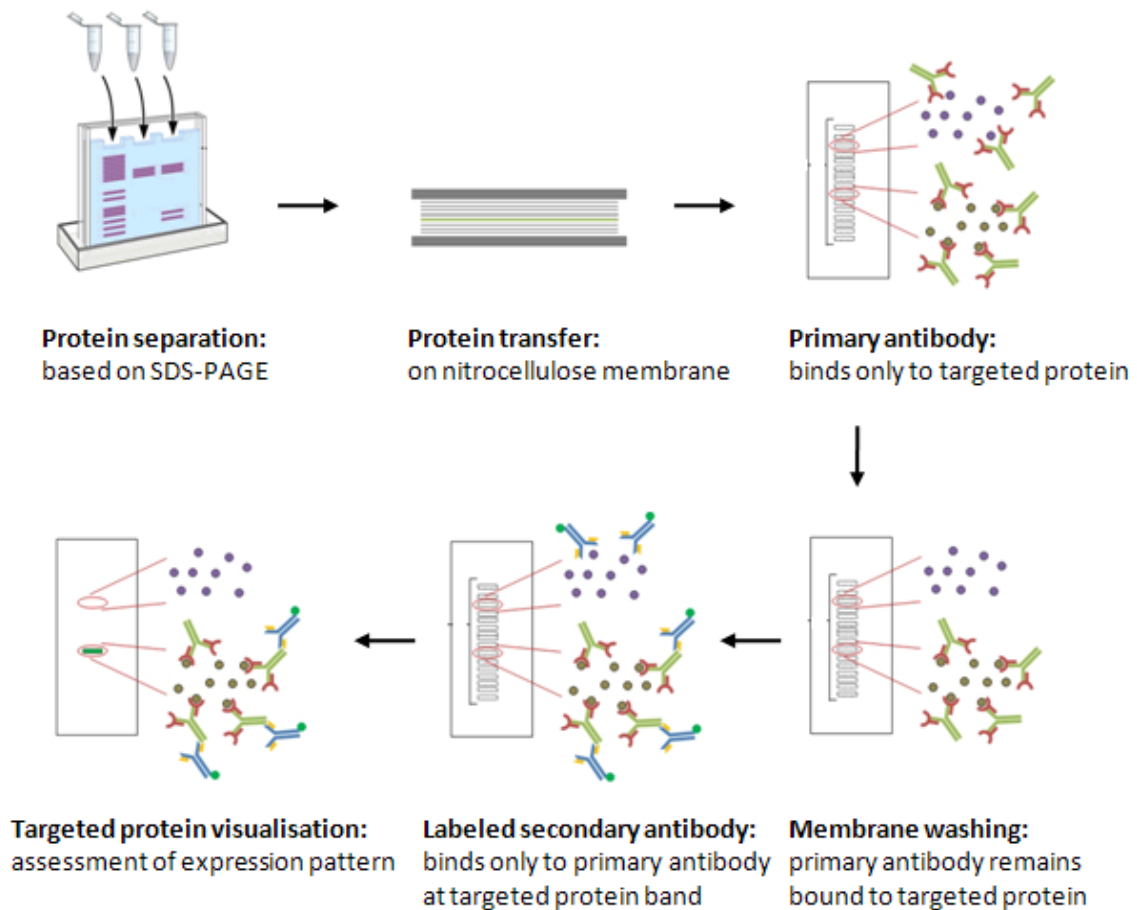


Figure 15: Schematic overview of the western blot analysis. The key experimental steps are illustrated of the western blot analysis which is used for the detection and evaluation of the expression levels of targeted proteins.

In case that reprobing of membranes was needed, the following steps were carried out. Membranes were washed 2 times for 30 minutes in TBS-T, blocked for 2 h in TBS-T containing 5% non-dry milk and then incubated with the appropriate primary antibody. Finally incubation with the secondary antibody and visualization of the protein bands were done as previously described.

Table 24: Preparation of stacking and running gels used in Western blot method.

Running and stacking gels		Amount*		
Gel percentage	5%	8%	10%	12%
Milli-Q H ₂ O	2.14 ml	3.4 ml	2.8 ml	2.1 ml
30% Acrylamide	0.488 ml	2.7 ml	3.3 ml	4 ml
1M Tris-HCl **	0.375 ml	3.7 ml	3.7 ml	3.7 ml
10% SDS	30 µl	100 µl	100 µl	100 µl

*Values represent volumes needed for preparation of 1 gel. For the polymerization of 8, 10 or 12% running gels 80 µl APS and 10 µl of TEMED were added. For the polymerization, of 5% stacking gels 15 µl APS and 3 µl of TEMED were added.

**1M Tris-HCl pH 6.8 (ml) was used for stacking gels and 1M tris-HCl pH 8.8 (ml) was used for running gels.

Table 25: Composition of running and transfer buffers.

Running and transfer buffers	Amount*
Tris (25 mM)	150 g
Glycine (200 mM)	720 g
Milli-Q H ₂ O	-up to 5 l

*Both were prepared as 10x solutions and were SDS 0.5% w/v was added in the running buffer and methanol 20% v/v was added in the transfer buffer. Both buffers were diluted in milli-Q H₂O to 1x working solutions.

Table 26: Composition of TBS-T buffer.

TBS-T buffer	Amount*
Tris (pH 7.5 / 0.5 mM)	303 g
Sodium Chloride (NaCl) (1,5 M)	438.5 g
Fuming hydrochloric acid (HCl) (0.3% v/v)	150 ml
Milli-Q H ₂ O	-up to 5 l

*TBS-T was prepared as 10x solution, pH was adjusted to 7.5 and for the working solution was diluted in milli-Q H₂O to 1x TBS-T adding as well 5 ml of Tween (0.3% v/v).

Table 27: Composition of enhanced chemi-luminescent (ECL) reagents type 1 and 2.

ECL reagents	Amount
<u>ECL type 1</u>	
Tris (pH 8.8 / 100 mM)	5 ml
Luminol (2.5 mM)	500 µl
Coumaric acid (0.4 mM)	220 µl
Milli-Q H ₂ O	- up to 50 ml
<u>ECL type 2</u>	
Tris (pH 8.8 / 100 mM)	5 ml
H ₂ O ₂ (0,15% v/v)	25 µl
Milli-Q H ₂ O	- up to 50 ml

Note: before use, ECL1 and ECL2 were mixed in a 1:1 ratio.

3.2.3.4 Two-dimensional gel electrophoresis (2-DE)

In the post-genomic era, proteins are undoubtedly considered key molecules in biomedical research which is directed towards translational and personalized medicine. The need of proteome maps is apparent but as previously mentioned (see introduction) the dynamic range of protein expression and modification makes the identification of the entire proteome a far more complex challenge than the sequencing of the genome. Two-dimensional gel electrophoresis (2-DE) is one of the preferred methods to resolve proteins extracted from cells, tissues, or other biological samples. Combined with high-throughput mass spectrometry (MS) techniques, the 2-DE gels allow the simultaneous analysis of hundreds of protein species. However, it should be highlighted that protein expression profiling per se, provides no data regarding their functional state unless additional experimental steps are included [77, 79, 80, 129].

In the present study a 2-DE proteomics methodology was employed (Figure 16). The 2-DE method is a very widely used method that consists of various experimental steps of different degrees of complexity. Moreover, different types of compatible mass spectrometry techniques, software for 2-DE image analysis and bioinformatics tools for pathway and network analysis are available. A list of the principal 2-DE experimental steps as they were performed in this thesis (Figure 16) can be outlined in the following order: (1) sample preparation, (2) generation of the 2-DE gel maps: first dimension (IEF) and second dimension (SDS-PAGE), (3) image analysis of 2-DE gels, (4) protein spot excision and in-gel trypsin digestion, (5) mass spectroscopy (MS) analysis, (6) database search and protein identification, and (7) bioinformatics data analysis.

The experiments of 2-DE analysis were performed in collaboration with Dr. Cristina-Maria Valcu (former colleague at the German Heart Center Munich) and the experiments of MS analysis were performed in collaboration with Dr. Karl-Heinz Gührs (Fritz Lipmann Institute, Jena, Germany).

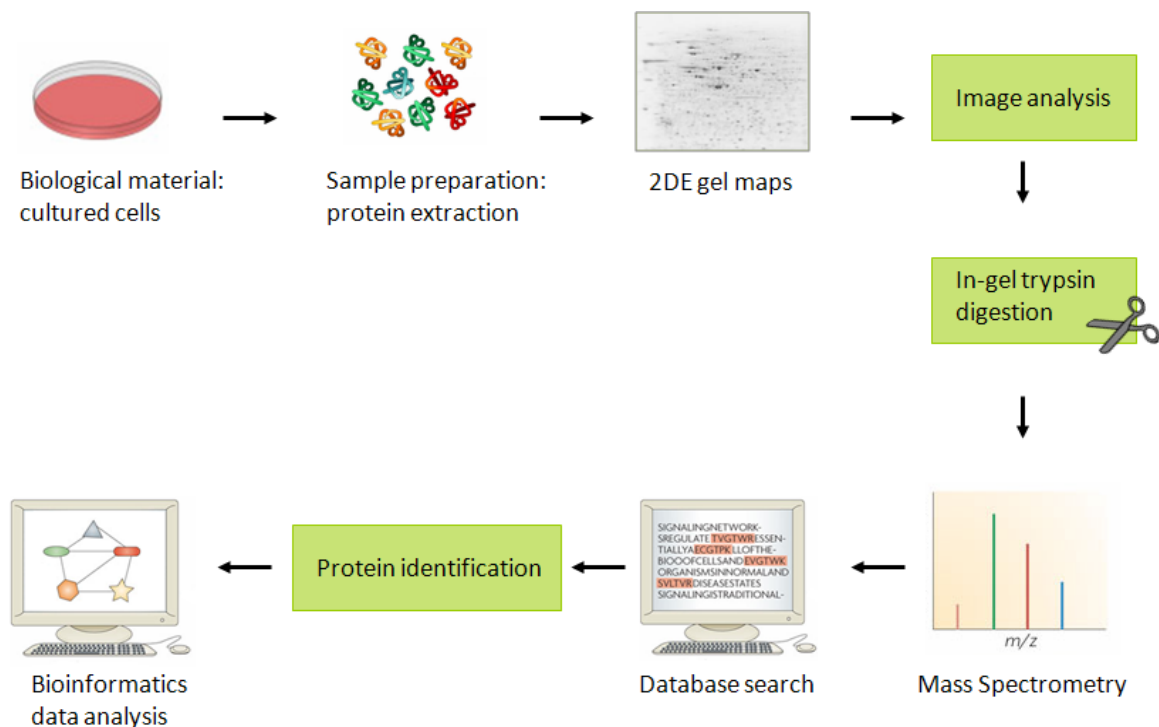


Figure 16: Schematic overview of the proteomic analysis employed in the present study. All key experimental key steps are displayed.

3.2.3.4.1 Sample preparation for 2-DE

Stable cell lines were grown to 80% confluence in 150 mm Petri dishes. Sample preparation and protein extraction were optimized using non-transformed HepG2 cells. Following the optimized protocols, two independent biological replicates each with two technical replicates were prepared for both control and over-expressing p22phox cells. Cells were washed three times with Tris-Sucrose buffer solution containing protease and phosphatase inhibitors (Table 28) and detached with a cell-scraper in the same buffer. Cells were pelleted, then resuspended in 1 ml lysis buffer (Table 29) and disrupted by tip sonication on ice (5 x 30 second cycles 90% of time at 70% power). After 1 h incubation on ice, the protein extract was centrifuged for 30 min at 40000 x g and 4°C and proteins were quantified using the Bradford assay.

Table 28: Composition of the tris-sucrose wash buffer.

Tris-sucrose buffer	Amount*
Sucrose (250 mM)	17.1 g
Tris base (10 mM/ pH 7.4)	242.28 mg
Milli-Q H ₂ O	- up to 180 ml
<u>Protease inhibitors</u>	
PMSF	34.8 mg
NaF	8.4 mg
Na ₃ VO ₄	7.4 mg

*Values are displayed for the total amount of 200 ml.

Table 29: Composition of the lysis buffer used in 2-DE.

Lysis buffer	Amount*
Urea (7 M)	4.205 g
Thiourea (2 M)	1.522 g
CHAPS (4% w/v)	400 mg
DTT (100 mM)	154.3 mg
Spermine (25 mM)	50.6 mg
Pharmalyte 3-10 (0.5% v/v)	125 µl

*Values are displayed for the total amount of 10 ml.

3.2.3.4.2 Rehydration of IPG strips

For rehydration, commercially available dry immobilized pH gradient (IPG) strips were immersed overnight in a rehydration buffer solution (Table 30). The process included pipetting first of the rehydration buffer into the ceramic strip holders. Then, the protective plastic layer of the IPG gel was removed and the IPG gel was placed onto the strip holder with the gel-

coated surface facing down, so that the gel surface would come in contact with the rehydration buffer. To prevent uneven rehydration, trapped air bubbles were smoothed carefully using a clean forceps and the strips were left over night for the rehydration process.

Table 30: Composition of the rehydration buffer solution.

Rehydration buffer	Amount*
Urea (7 M)	4.205 g
Thiourea (2 M)	1.522 g
CHAPS (2% w/v)	200 mg
HED (100 mM)	120 μ l
Pharmalyte3-10 (0,5% v/v)	125 μ l
Bromophenol blue (0.002% w/v)	20 μ l
Milli-Q H ₂ O	-up to 10 ml

*Values are displayed for acidic IPG strips (pH 4-7, 24 cm) and 450 μ l of rehydration solution were used per IPG strip.

3.2.3.4.3 First dimension (IEF)

Protein samples were mixed with rehydration buffer solution under a dust free cabinet using all precautions (laboratory coat, gloves, hut) avoiding keratin contaminations. Samples were then cup loaded (500 μ g protein/strip) on immobilized pH gradient (IPG) strips (pH4-7, 24 cm) and Isoelectric Focusing (IEF) was performed on an Ettan IPHphor 3 Cup Loading Manifold for 64 kVhr (Table 29).

To ensure that the rehydrated IPG strip gels would not dry out during the focusing process they were overlaid with Immobiline DryStrip Cover Fluid. Finally, after closing the IPGphor cover, the suitable program (temperature set at 20°C and current limited to 50 μ A per IPG strip) with desired running conditions was selected (Table 31) from the device (Ettan IPHphor 3 Cup Loading Manifold) and the isoelectric focusing run started.

After IEF process, IPG strips were removed from the Manifold and the residual cover fluid was carefully drained from the IPG strips. Afterwards, the IPG strips could be either used immediately for the second dimension or, they could be preserved at very low temperature (-70°C) for several weeks until the second dimension would be scheduled. In order to remove residual proteins after each IEF run, strip holders were cleaned with a neutral pH detergent using a toothbrush and extensively rinsed with deionised water.

Table 31: IEF running conditions.

Step	Mode	Volt	kVHours
1	gradient	300	0.6
2	gradient	600	1.2
3	gradient	1000	2
4	gradient	8000	13.5
5	step & hold	8000	46.7
total			64

Note: Values are displayed for acidic IPG strips (pH 4-7, 24 cm).

3.2.3.4.4 Equilibration of IPG strips

Strips were equilibrated prior to the second dimension in two steps for 15 min each under gentle shaking at room temperature. The first equilibration step involved reduction of the disulphide bonds as it is required for the separation of proteins during the second dimension. Gel strips were placed in an equilibration buffer solution (Table 30) containing 2% w/v dithiothreitol (DTT). After 15 min, the equilibration buffer was discarded. The second equilibration step involved alkylation of the free thiol groups of cysteines so reoxidation could be prevented. Gel strips were placed again in an equilibration buffer solution as the first step but containing 4% w/v iodoacetamide (IAA) instead of DTT (Table 32). Finally, equilibrated strips were sealed on top of 10% PAA gels with 0.5% low melting agarose solution. The second dimension was run over night in an Ettan Dalt6 chamber.

Table 32: Composition of the equilibration buffer.

Equilibration buffer	Amount
Tris-HCl (1.5M/pH 8.8)	16.67 ml
Urea (6 M)	180.18 g
Glycerol (87% w/v)	172.4 g
Milli-Q H ₂ O	-up to 460 ml
SDS (10% w/v)	50g
Bromophenol blue (1% w/v)	500 µl
Milli-Q H ₂ O	-up to 500 ml

Note: Before use, it was added 20 mg DTT / ml (2% w/v) (1st step) and 40 mg IAA / ml (4% w/v) (2nd step).

3.2.3.4.5 Second dimension (SDS-PAGE)

Gels were casted in a DALTsix Gel Caster by pouring quickly and carefully the well mixed solution (Table 33). Uniform gels (10%) were prepared. Immediately after pouring, each glass plate cassette was overlaid with 1 ml of a layer of 0.1% SDS solution to minimize gel exposure and to create a flat gel surface. After allowing a minimum of 3 h for polymerization, SDS-solution overlay was removed and the gel surface was rinsed with deionized water. Finally the gels were wrapped in dust free tissues rinsed with running buffer solution and were preserved overnight at 10-20°C until their use on the following day [79].

Table 33: Composition of the 2-DE gels.

2-DE gels	10% gel
Acrylamide 40%	115.23 ml
Bis- Acrylamide 2%	61 ml
At this point: addition of 2,2 g amberlite, stirring for 1 h and filtration through 0,45 µm membrane	
Tris-HCl-SDS (1,5M/pH:8,6)	115 ml
MilliQ H ₂ O	151.85 ml
Glycerol 99.5%	23 g
TEMED	230 µl
APS 10%	1.84 µl

Note: Values are displayed for the corresponding number of 6 gels per 2-DE run.

Equilibrated IPG strips were positioned with tweezers between the plates on the second-dimension gel surface with the plastic backing against longer glass plate. With a thin spatula, the IPG strip was gently pushed down to achieve complete contact with the top surface of the stacking gel ensuring no trapping of air bubbles. IPG strips and the molecular weight standards positioned on the edges of gels were overlaid with about 1.5 ml of agarose sealing solution (prepared by heating it up for 10 min in 100 °C and cooling it to 40-50°C). After allowing agarose to solidify for 2-3 min, gel cassette was inserted in the electrophoresis unit. In the main chamber of the electrophoresis unit were poured 3 l of diluted anode (lower) buffer whereas 500 ml diluted cathode (upper) buffer were poured into the upper buffer chamber. Diluted anode and cathode buffers were prepared according to the Table 34.

Table 34: Composition of the 2-DE anode and cathode buffers.

Components	Amount
<u>Anode buffer</u>	
Tris base (25 mM)	14.54 g
Glycine (192 mM)	69.18 g
SDS (0.1% w/v)	4.8 g
Milli-Q H ₂ O	- up to total of 4.8 l
<u>Cathode buffer</u>	
Tris base (50 mM)	8.48 g
Glycine (384 mM)	40.36 g
SDS (0.2% w/v)	2.8 g
Milli-Q H ₂ O	- up to total of 1.4 l

The second dimension electrophoresis run (gels 10%) was performed according to the SDS - PAGE running conditions displayed on Table 35. The run was terminated each time depending on the migration of the bromophenol blue dye towards the lower part of the gels.

Table 35: SDS-PAGE running conditions.

Step	mA	Volt	Watt	Hours
1	30	150	12	2
2	48	150	12	2
3	60	150	12	8
4	98	150	12	overnight*

Note: Values displayed for acidic IPG strips (pH 4-7, 24 cm). Exact duration of the step 4 depends on the position of bromophenol blue front.

3.2.3.4.6 2-DE gel staining and digitalization

Staining of 2-DE gels using Ruthenium (II) tris (bathophenanthroline disulfonate) fluorescent stain (RuBPS) was performed for comparative analysis in protein expression of control vs. treatments 2-DE gels. The experimental steps were carried out according to the Table 36 [130]. Stained 2-DE gels were digitalized using a Typhoon Trio+ scanner at 100 μ m resolution under 610 nM emission, 532 nm laser, 600 V PTM. Careful handling of the gels was needed in order to avoid damage or contamination of them during their transfer into the scanner.

Silver staining was selected to visualize protein spots prior their excision after performing quantitative 2-DE runs. It was performed according to the protocol which is presented in the Table 37 [131].

Table 36: Protocol used in the RuBPS staining of 2-DE gels.

Step	Solution	Amount	Time
<u>Fixing and staining</u>	Ethanol	480 ml	1 h
	Acetic acid	120 ml	
	RuBPS	60 ml	
	Milli-Q H ₂ O	-up to 1200 ml	
<u>De-staining of gels</u>	Ethanol	480 ml	24-48 h
	Acetic acid	120 ml	
	Milli-Q H ₂ O	-up to 1200 ml	
<u>Washing of gels</u>	Milli-Q H ₂ O	1200 ml	40 min

Note: Values are displayed for 6 gels used per 2-DE run.

Table 37: Protocol used in the silver staining of 2-DE gels.

Step	Solution	Amount	Time
<u>Fixing</u>	Ethanol	400 ml	1h
	Acetic acid	100 ml	
	Milli-Q H ₂ O	-up to 1 l	
<u>Sensitizing</u>	Ethanol	300 ml	45 min
	Sodium acetate	78 g	
	Sodium thiosulphate	2 g	
	Glutardialdehyde	20 ml	
	Milli-Q H ₂ O	-up to 1 l	
<u>Fixing</u>	Ethanol	300 ml	90 min
	Acetic acid	50 ml	
	Milli-Q H ₂ O	-up to 1 l	
<u>Washing</u>	Milli-Q H ₂ O	1 l	6x10 min
<u>Silver reaction</u>	Silver nitrate	1 g	30 min
	Formaldehyde	500 µl	
	Milli-Q H ₂ O	-up to 1 l	
<u>Washing</u>	Milli-Q H ₂ O	1 l	2x20 sec
<u>Developing</u>	Sodium carbonate	90 g	10-30 min
	Formaldehyde	0.75 ml	
	Milli-Q H ₂ O	-up to 3 l	
<u>Stopping</u>	Glycine	30 g	30 min
	Milli-Q H ₂ O	-up to 3 l	
<u>Washing</u>	Milli-Q H ₂ O	3l	8-10 min
<u>Shrinking</u>	Glycerin	250 g	8-10 min
	Ethanol	600 ml	
	Milli-Q H ₂ O	-up to 2 l	

Note: Values are displayed for 6 gels used per 2-DE run.

3.2.3.4.7 2-DE gel image analysis

2-DE gels after being digitalized into images, were analyzed using Progenesis SameSpots software (Figure 17). Relevant spot parameters were exported and stored in an MS Access database. Statistical analysis was performed on normalized spot volumes with R [132, 133].

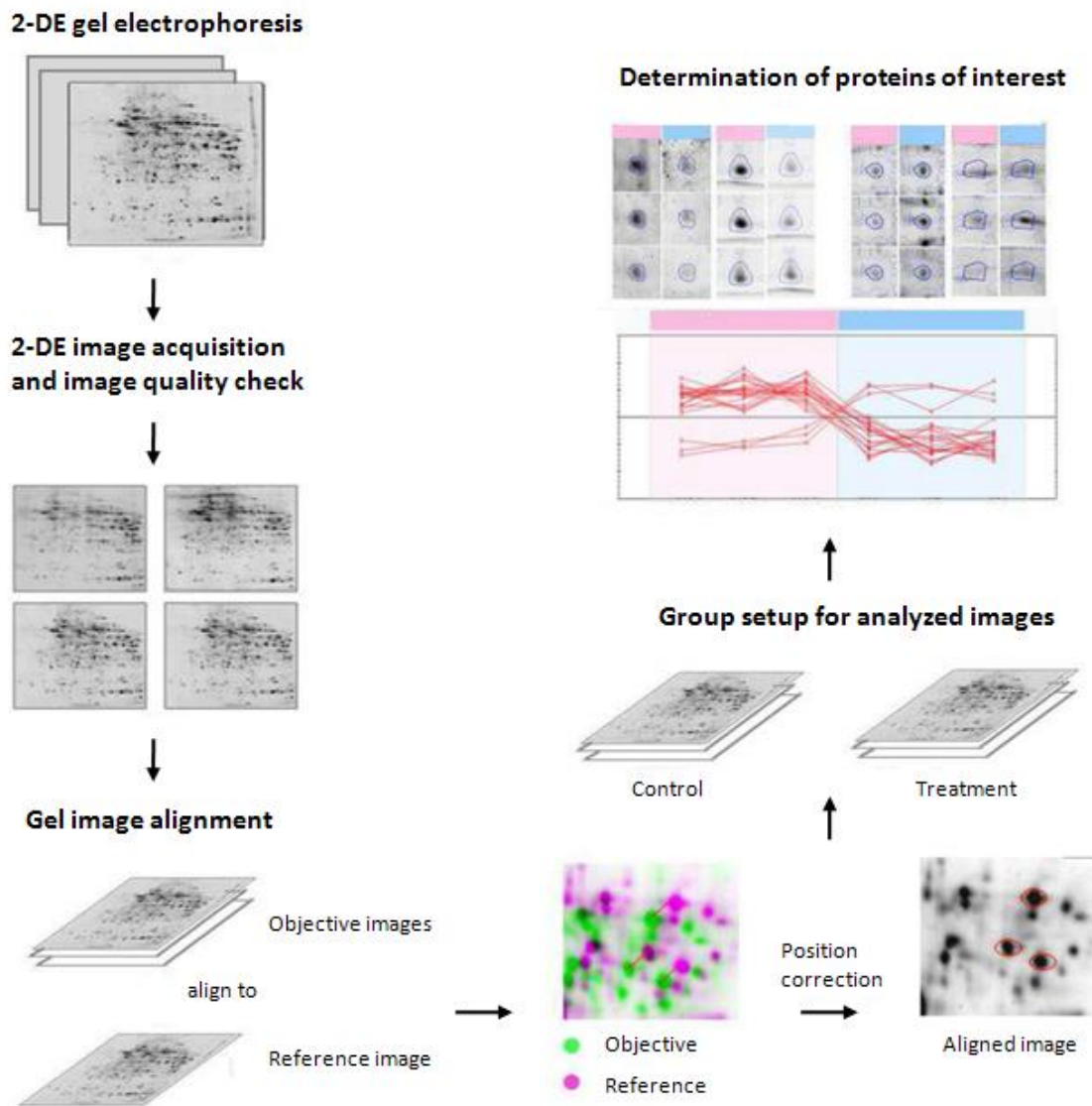


Figure 17: Schematic overview of the 2-DE image analysis. Key steps are illustrated while performing 2-DE image analysis using Progenesis SameSpots software for the determination of differentially expressed proteins [134].

Proteins were selected as differentially expressed between control and p22phox over-expressing cells based on two criteria [135]: (1) statistically significant differences based on a Welch t test for unequal variances (p values of a lower than 0.05 after applying a Benjamini-Hochberg correction applied for controlling the false discovery rate [136] and (2) a fold regulation that exceeded the intrinsic levels of spot variation modeled for each spot based on the spot volume variability measured in the control samples. In a linear model including spot normalized volume and area, molecular weight and pI as predictors (the latter two as second order polynomials), spot volume variability was found to be predicted by the normalized volume and pI. The equation of this dependence was further used to predict for each spot the intrinsic level of variance above each any difference can be considered differential expression. The protein spots had to simultaneously fulfill the two above mentioned criteria in order to be considered differentially expressed between the two cell lines.

3.2.3.4.8 Excision of protein spots and in-gel trypsin digestion

The protein spots of interest were excised manually using feather scalp. The excision of the areas in the gels was done as close to the spot as possible to minimize the amount of background gel using an illuminating base for more precise observation of their location. The excised spots were transferred to 1,5 ml eppendorf tubes in 100 μ l milli-Q H₂O. The eppendorf tubes were prior washed with 0.1% TFA / 50% ACN and rinsed twice with milli-Q H₂O. Also, in order to avoid contamination from keratin, special precautions were taken using gloves, lab coat, lab hat and a dust free hood.

Each excised spot was washed with 150 μ l of washing buffer (2.5mM ammonium bicarbonate (NH₄HCO₃), 50% acetonitrile). The tubes were sealed with an adhesive film and stored at 4°C. Subsequently, the excised proteins spots were further processed for the Mass Spectrometry (MS) analysis. This phase included: de-staining, dehydration (Table 38), reduction, alkylation and dehydration (Table 39), followed by rehydration and finally in-gel trypsin digestion.

Table 38: Protocol used in the de-staining and dehydration of excised protein spots.

Step	Solution	Amount	Time
<u>De-staining</u>	KFe(CN) ₆ / Na ₂ S ₂ O ₃ (1:1)	50 µl	until total de-staining
<u>Washing</u>	Milli-Q H ₂ O	50 µl	3x 10 sec
	NH ₄ HCO ₃ (200 mM)	50 µl	2x 15 min
	NH ₄ HCO ₃ / ACN (1:1)	50 µl	2x 3 min
<u>Dehydration</u>	ACN	10 µl	10 min

Note: All steps were performed at room temperature and in the end, all spots were dried at speed vac for 30 min and stored at -20°C. Values are displayed for each spot stored in a 1,5 ml eppendorf tube.

Table 39: Protocol used in the reduction and alkylation of excised protein spots.

Step	Solution	Amount	Time
<u>Reduction</u>	DTT (10 mM)	10 µl	30 min
<u>Alkylation</u>	IAA (55 mM)	10 µl	45 min
<u>Washing</u>	NH ₄ HCO ₃ (100 mM)	200 µl	15 min
<u>Dehydration</u>	ACN	10 µl	10 min
<u>Re-swelling</u>	NH ₄ HCO ₃ (100 mM)	10 µl	10 min
<u>De-hydration</u>	ACN	10 µl	10 min

Note: The reduction step was performed at 56°C. The alkylation step took place in dark at room temperature. Shaking of tubes using a thermoblock-shaker was applied in all steps. Finally all spots were dried at speed vac for 10 min and stored at -20°C. Values are displayed for each spot stored in a 1,5 ml eppendorf tube.

3.2.3.4.9 Mass spectrometry (MS) analysis

Preparative gels were loaded with 500 µg protein and stained with MS compatible silver staining. Differentially expressed protein spots were excised from the 2DE gels and they were subsequently reduced and alkylated before their submission to MS analysis [135, 137]. Reduced and alkylated gel pieces were washed two times with 100 µl 25 mM ammonium bicarbonate followed by 100 µl 75 % acetonitrile. The contained proteins were then digested with trypsin. The shrunk gel pieces were rehydrated with 30 µl 2.5 ng/µl trypsin dissolved in 1 mM HCl. After re-swelling of the gel pieces the excess supernatant was removed and 30 µl of digest buffer (25 mM ammonium bicarbonate, 8 % acetonitrile) were added. After overnight digestion the supernatant was removed. The gel pieces were first extracted with 50 µl of 0.1 % trifluoroacetic acid in 33 % acetonitrile and then with 100 µl of 75 % acetonitrile. After complete evaporation of the solvent in a vacuum concentrator the samples were

reconstituted with 20 µl of 5 % acetonitrile in 0.1 % formic acid. Samples were analyzed by nano-HPLC (Easy nanoLC, Proxeon) using a 100 µm x 2 cm trapping column and a 75 µm x 10 cm C18 separation column (5 µm particles, NanoSeparations). A gradient from 5 % to 38 % acetonitrile in 0.1 % formic acid was applied over 90 minutes. The efflux of the HPLC was sprayed into the sample inlet of a LTQ Orbitrap XL ETD mass spectrometer operated in the data dependent measuring scheme. A full scan at 60000 resolution was followed by measurement of up to three CID spectra in the ion trap (Top3). The evaluation of the spectra was performed by ProteomeDiscoverer and the spectra were searched by Mascot against the SwissProt database. Carbamidomethylation was set as a fixed modification and oxidation of methionine and phosphorylation of serine and threonine were allowed as variable modifications. Positive identifications required at least three peptides with Mascot ion scores of at least 20 each or two spectra with scores higher than 40. Scaffold (Proteome Software, Portland, USA) was also used to verify the identifications and showed 0.0 % peptide FDR and 0.0 % of protein FDR. Spots with multiple hits were resolved by comparing spectral counts and spectral abundance factors [138].

3.2.3.4.10 Bioinformatics data analysis

Bioinformatics software tools have become extremely popular in proteomics based studies as they offer direct high throughput links in forms of pathway analysis, network generation and functional analysis of target protein molecules to existing scientific knowledge derived from a broad range of information sources and databases.

In this study, a bioinformatics data analysis using the Ingenuity Pathway Analysis (IPA) software was performed (Ingenuity Systems <http://www.ingenuity.com>) generating a network built up of the MS identified and validated differentially expressed proteins in combination with interacting molecules as added by the software. Furthermore, information about pathways and diseases correlated functionally to this network was also obtained. In more detail about the network generation, the data set containing the UniProt database protein identifiers and corresponding fold regulation values was uploaded into the application. Each identifier was mapped to its corresponding object in Ingenuity's Knowledge Base. Other interacting molecules were then identified with a significantly differential

regulation of their expression according to the Fisher's exact test. These molecules, called network eligible molecules, were overlaid onto a global molecular network developed from information contained in Ingenuity's Knowledge Base. Networks of network eligible molecules were then algorithmically generated based on their connectivity.

Regarding the functional analysis of the generated network, biological functions and/or diseases were identified that were most significant to the molecules of the network based again on the Ingenuity's Knowledge Base. Again, Fisher's exact test was used to calculate a p-value determining the probability that each biological function and/or disease assigned to that network is due to chance alone. The IPA analysis was performed with the help of Dr. Guillaume Médard (Proteomics and Bioanalytics laboratory, Freising, Technical University of Munich).

3.2.4 Statistical analysis

Statistical analysis for the 2-DE analysis experiments was performed using the software environment R 2.14.0. For all the other experiments, the results were statistically processed and graphically represented using the GraphPad Prism software (La Jolla, USA). Values presented are means \pm standard deviation (STD) or standard error of the mean (SEM) as indicated. All experiments were performed at least 3 times ($n > 3$). To calculate significance, Student-Newman-Keuls t-test was performed. P-value < 0.05 was considered statistically significant.

Chapter 4: Results

4.1 Results

4.1.1 Assessment of differential p22phox levels in stably transfected HepG2 cells

The role of the NADPH oxidase subunit p22phox in tumour progression was the focal point of the present study. Thus, expression levels of p22phox were evaluated and validated in a cancer cellular model system which included (a) hepatoblastoma (HepG2) cells stably transfected with a plasmid for human p22phox (available as two control and two over-expressing p22phox clones already present in the lab) and (b) stably transfected HepG2 cells with a plasmid encoding for a shRNA against p22phox (available as one control and one silenced clone already present in the lab). In both cases, the protein and mRNA expression levels of p22phox as well as its intracellular localization were analysed by Western blot (Figure 18), quantitative PCR (Figure 19) and immunofluorescence (Figure 20) accordingly.

The protein expression levels of p22phox were higher in p22phox over-expressing and lower in p22phox silenced HepG2 cells versus the control clones, respectively (Figure 18). The mRNA expression levels of p22phox, similarly to protein levels, were higher and lower versus the control clones in the over-expressing and silenced p22phox HepG2 cells, respectively (Figure 19).

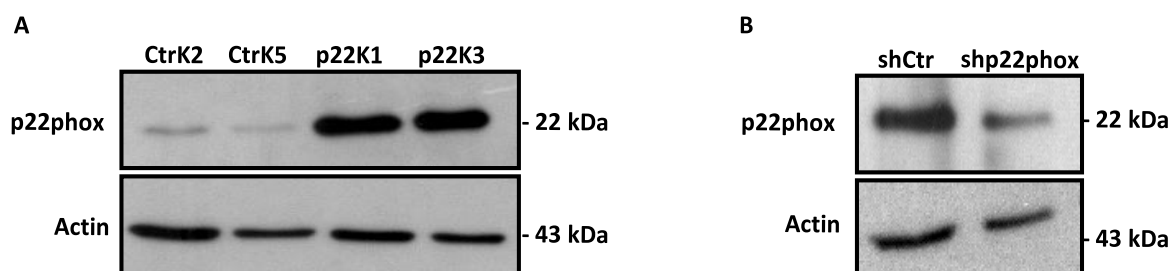


Figure 18: Western blot analysis of p22phox modified HepG2 cells. HepG2 cells were stably transfected with (A) empty control vector (CtrK2 and CtrK5) or p22phox plasmid (p22K1 and p22K3) and (B) vector encoding for control shRNA (shCtr) or short hairpin RNA against p22phox (shp22phox). Western blotting was performed with human p22phox monoclonal antibody. Actin was used as loading control. The displayed blots are representative for at least three independent experiments.

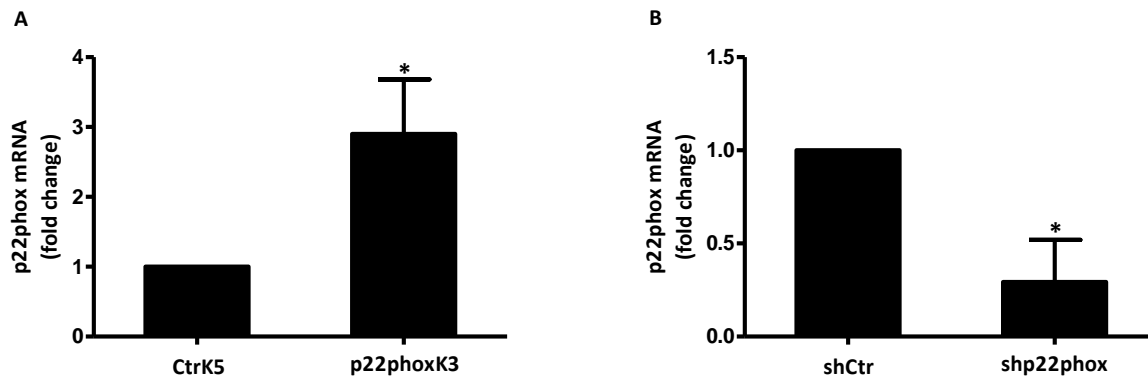


Figure 19: Quantitative PCR analysis of p22phox modified HepG2 cells. RNA of stably transfected HepG2 cells with (A) empty control vector (CtrlK5) or p22phox plasmid (p22phoxK3) and (B) vector encoding for control shRNA (shCtr) or short hairpin RNA against p22phox (shp22phox), was isolated. After cDNA synthesis, qPCR for p22phox mRNA was performed. Data are presented as relative change to control clones (CtrlK5 or shCtr) after normalization to beta actin (n=3, *p<0.05, p22phoxK3 vs. CtrlK5 or shp22phox vs. shCtr, SEM).

In addition, immunofluorescence (IF) staining of p22phox confirmed higher and lower levels of p22phox in over-expressing and silenced p22phox cells, respectively, when compared to their corresponding controls (Figure 20).

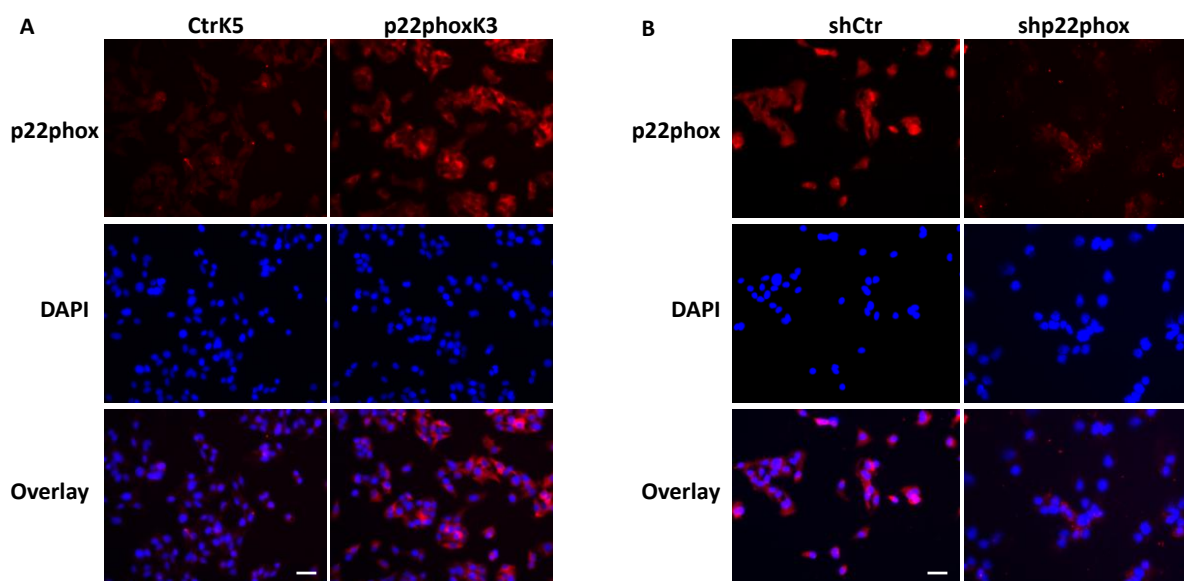


Figure 20: Immunofluorescence analysis of p22phox modified HepG2 cells. Stably transfected HepG2 cells with (A) empty control vector (CtrlK5) or p22phox plasmid (p22phoxK3) and (B) vector encoding for control shRNA (shCtr) or short hairpin RNA against p22phox (shp22phox) were stained with an antibody against p22phox (red colour) and nuclei were counterstained with DAPI (blue colour). Overlay pictures of p22phox and nuclei (DAPI) staining are displayed. Fluorescence images were taken at a 20x magnification of representative areas with equal cellular distribution, size bar= 12µm.

4.1.2 Evaluation of p22phox regulatory effect on ROS generation

To evaluate the functional impact of p22phox levels on the generation of ROS, dihydroethidium (DHE) fluorescence was performed to determine ROS levels. Compared to the respective control clones, ROS levels were elevated in cells from a p22phox over-expressing clone but decreased in cells from a shp22phox expressing clone confirming the functional importance of p22phox for the generation of ROS. In addition, fluorescence images of cells stained with DHE were taken showing an equal increase or decrease of ROS generation in p22phox over-expressing or depleted HepG2 cells, respectively (Figure 21).

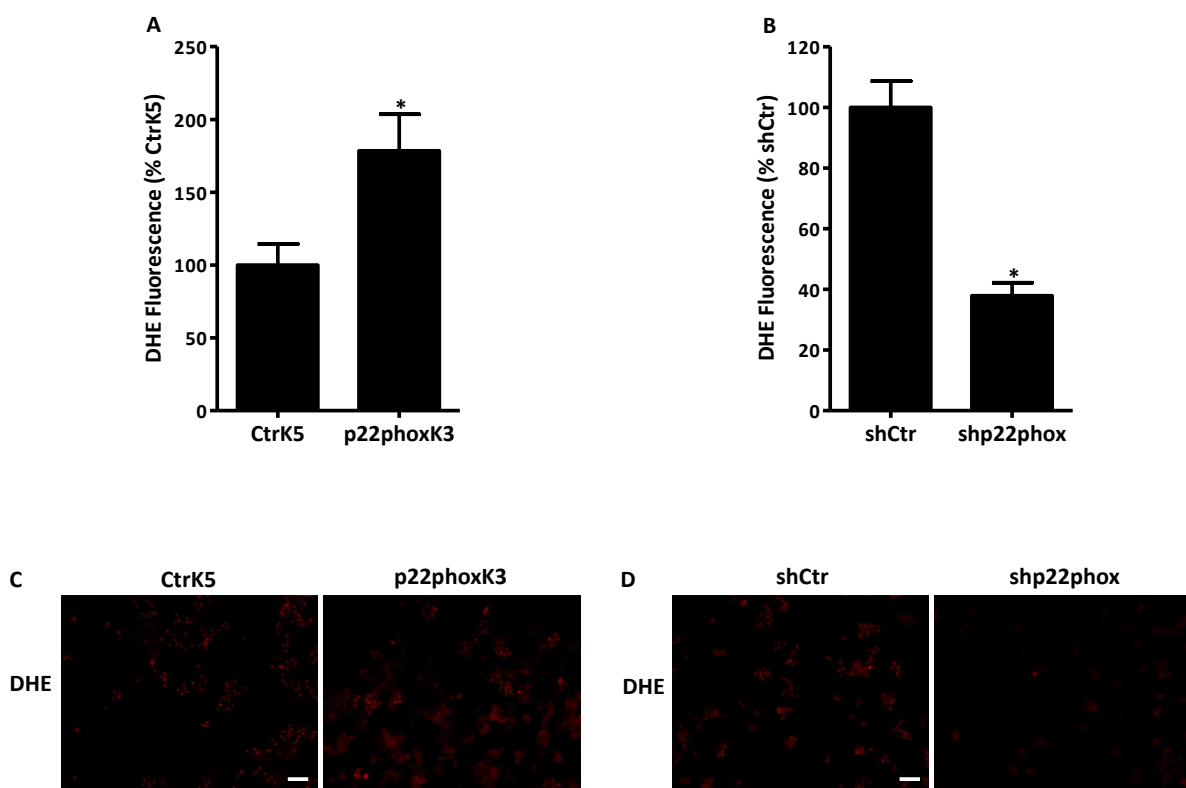


Figure 21: p22phox modulates ROS generation in HepG2 cells. HepG2 cells stably transfected with (A)(C) empty control vector (CtrK5) or p22phox plasmid (p22phoxK3) and (B)(D) a vector encoding for control shRNA (shCtr) or short hairpin RNA against p22phox (shp22phox) were used to evaluate ROS generation. (A)(B) Cells were seeded in a micro-plate and ROS generation was assessed using DHE fluorescence measured in a plate reader. Data are presented as relative change to control set to 100% (n=3, *p<0.05, p22phoxK3 vs. CtrK5 or shp22phox vs. shCtr, SEM). (C)(D) Cells were seeded in 8 well μ -slide with cover and incubated with 50 μ M DHE for 10 minutes in the dark. Fluorescence was assessed using a fluorescence microscope at 20x magnification (size bar= 12 μ m). Images are representative for at least 3 independent experiments.

4.1.3 Role of p22phox in proliferative activity of HepG2 cells

4.1.3.1 p22phox modulates the proliferative and metabolic activity of HepG2 cells

ROS and NADPH oxidases have been implicated in the regulation of tumour progression [139-141]. Therefore, the contribution of p22phox to the proliferative response of HepG2 cells was determined using 5-bromo-2'-deoxyuridine (BrdU) incorporation assay.

Results showed that the proliferative activity of HepG2 cells was significantly increased in stably transfected HepG2 cells over-expressing p22phox compared to control cells (Figure 22). In contrast, the proliferation of HepG2 cells with stable knock down of p22phox was decreased compared to control cells (Figure 22).

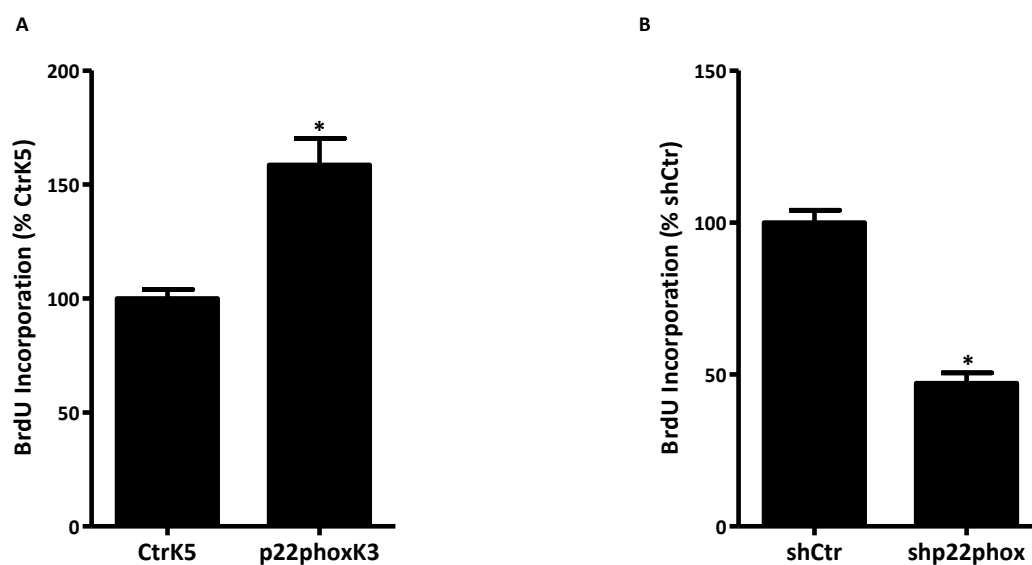


Figure 22: p22phox modulates proliferation of HepG2 cells. Stably transfected HepG2 cells with (A) empty control vector (CtrK5) or p22phox plasmid (p22phoxK3) and (B) vector encoding for control shRNA (shCtr) or short hairpin RNA against p22phox (shp22phox), were seeded in 96-well plates. Proliferative activity was assessed using 5-bromo-2'-deoxyuridine (BrdU) incorporation. Data are presented as relative change to control set to 100% (n=3, *p<0.05, p22phoxK3 vs. CtrK5 or shp22phox vs. shCtr, SEM).

Additionally, immunofluorescence (IF) assays stained for Ki-67 as a proliferation marker were performed. Ki-67 staining was increased in cells from a p22phox over-expressing clone compared to control cells and it was decreased in cells derived from a clone with decreased p22phox levels compared to control cells (Figure 23). These results underline the importance of p22phox for the proliferation of HepG2 cells.

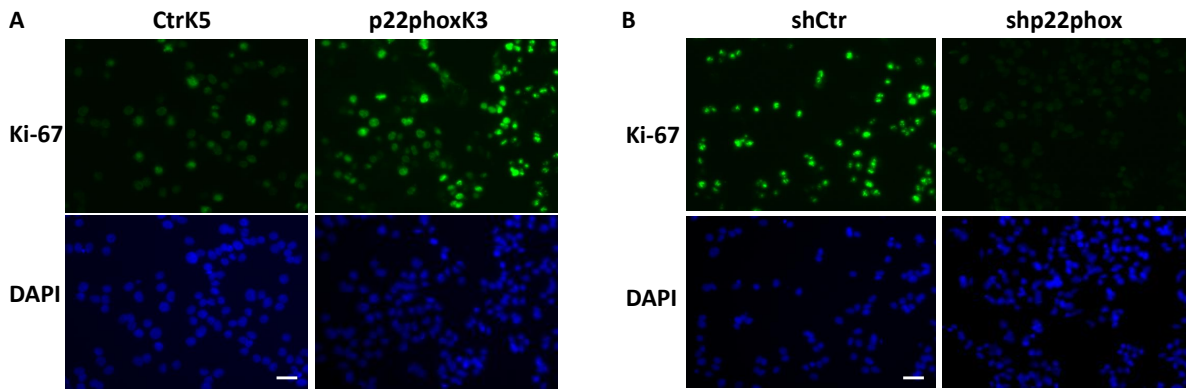


Figure 23: Expression of proliferation marker Ki-67 in p22phox modified HepG2 cells. Stably transfected HepG2 cells with (A) empty control vector (CtrK5) or p22phox plasmid (p22phoxK3) and (B) vector encoding for control shRNA (shCtr) or short hairpin RNA against p22phox (shp22phox) were stained with an antibody against Ki-67 (green colour). Nuclei were counterstained with DAPI (blue colour). Fluorescence images were taken at a 20x magnification (size bar= 12 μ m).

Furthermore, as proliferation of cells is strongly coupled to the metabolic activity of the cells, Alamar Blue assay was performed. HepG2 cells over-expressing p22phox showed enhanced metabolic activity compared to controls. In contrast, HepG2 cells depleted of p22phox showed decreased metabolic activity compared to controls (Figure 24).

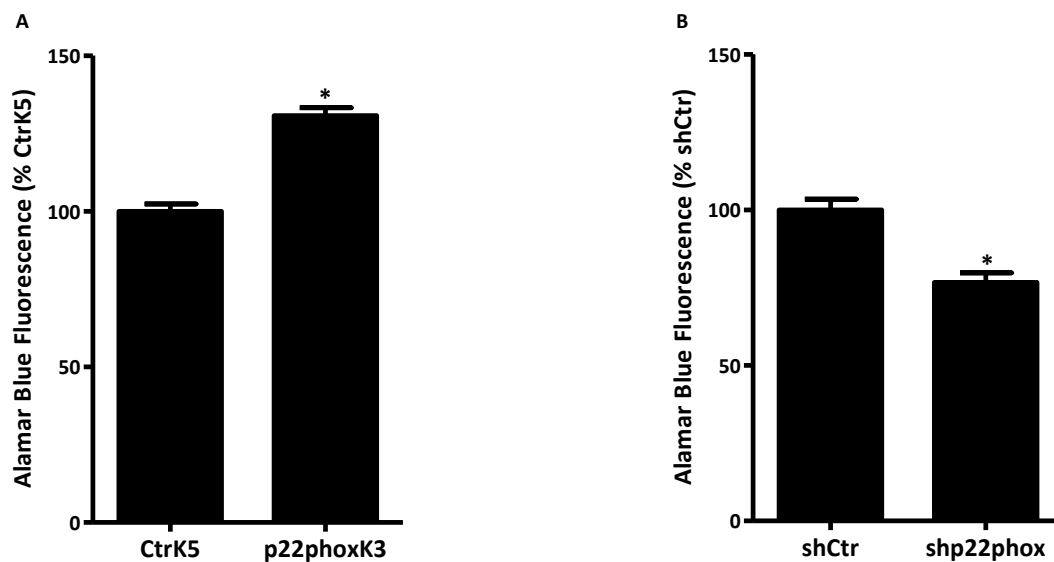


Figure 24: p22phox modulates the metabolic activity of HepG2 cells. Stably transfected HepG2 cells with (A) empty control vector (CtrK5) or p22phox plasmid (p22phoxK3) and (B) vector encoding for control shRNA (shCtr) or short hairpin RNA against p22phox (shp22phox), were seeded in 96-well plates. Metabolic activity was assessed by using Alamar Blue fluorescence measured in a plate reader. Data are presented as relative change to control set to 100% (n=3, *p<0.05, p22phoxK3 vs. CtrK5 or shp22phox vs. shCtr, SEM).

4.1.3.2 N-acetyl cysteine decreases metabolic activity in HepG2 cells

To verify that p22phox modulated metabolic activity is dependent on ROS, p22phox over-expressing and control HepG2 cells were treated with the antioxidant N-acetyl-cysteine (NAC) and metabolic activity was thereafter evaluated utilizing Alamar Blue assay.

Although NAC also reduced Alamar Blue activity of control cells, the p22phox-induced increase in Alamar Blue activity was completely reduced to control levels indicating that p22phox-induced Alamar Blue activity is mediated by ROS (Figure 25).

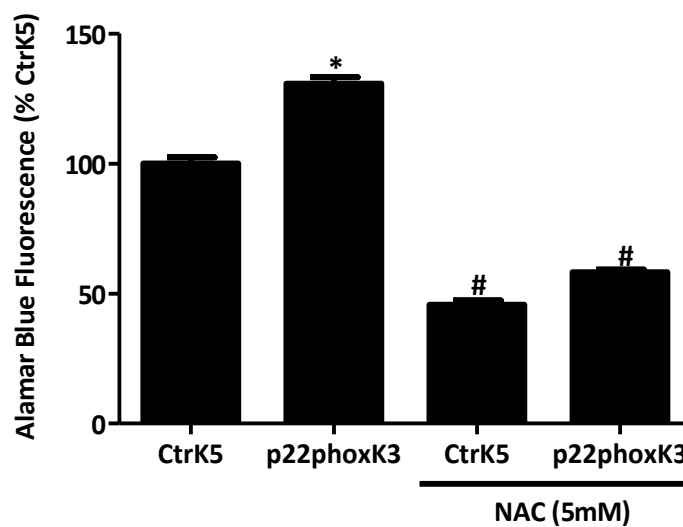


Figure 25: p22phox mediated metabolic activity is ROS dependent. Stably transfected HepG2 control cells (CtrK5) and p22phox over-expressing cells (p22phoxK3) were seeded in 96 wells. After 18h cells were pre-treated with N-acetyl-cysteine (NAC, 5mM) for 24 h before metabolic activity was determined by Alamar Blue fluorescence. Data are presented as relative changes to untreated CtrK5 clone set to 100% (n=3, *p<0.05: over-expressing p22phox vs. control, #p<0.05: NAC treatment vs. control).

4.1.3.3 p22phox modulates colony formation capacity of HepG2 cells

As tumour progression is not only characterized by the proliferative activity of tumour cells but also by the ability of these cells to survive, clonogenic assays were performed for both p22phox over-expressing and p22phox depleted HepG2 cells. It was observed that when p22phox was enhanced, colony formation was induced in a significant way whereas in case of depletion of p22phox, colony formation was almost abolished (Figure 26).

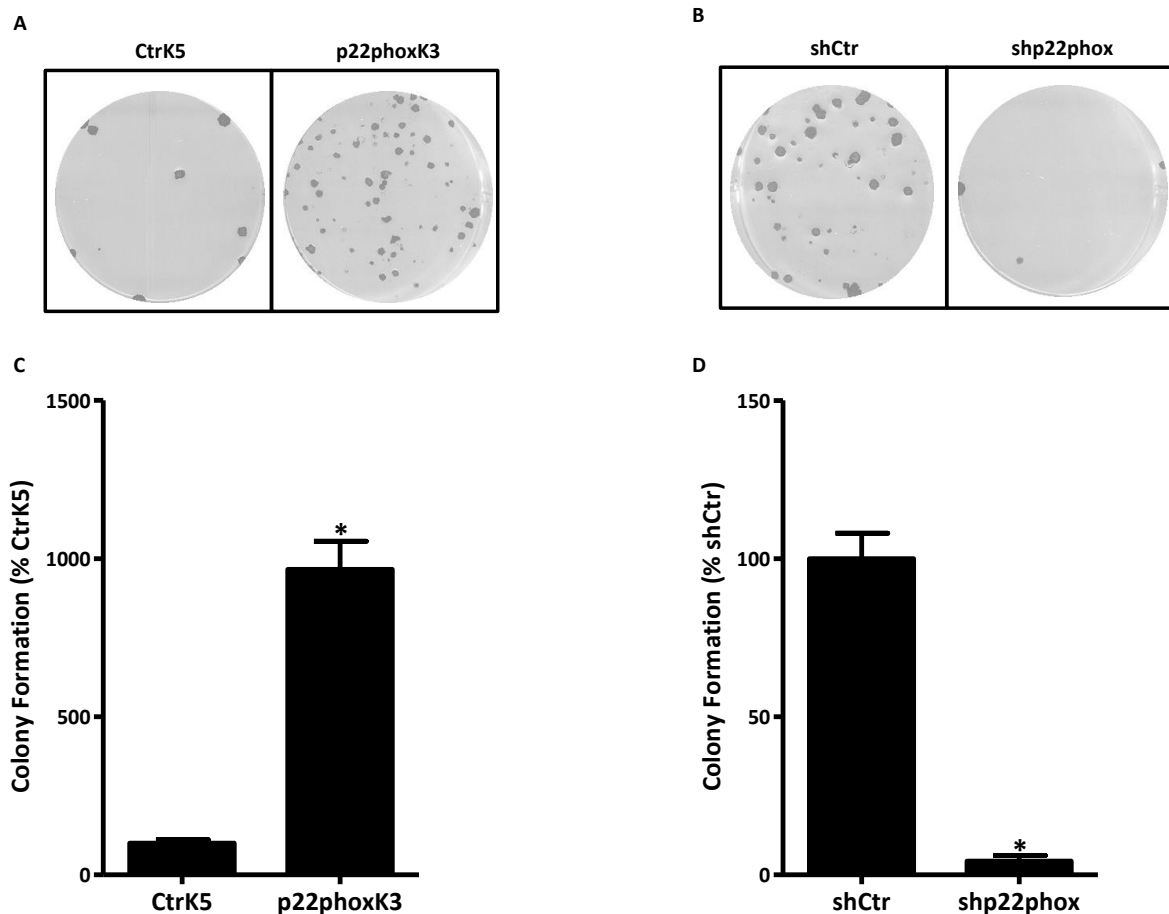


Figure 26: p22phox modulates the ability of HepG2 cells to form colonies. Stably transfected HepG2 cells with (A) empty control vector (CtrK5) or p22phox plasmid (p22phoxK3) and (B) vector encoding for control shRNA (shCtr) or short hairpin RNA against p22phox (shp22phox), were seeded in 6-well plates. Formation of colonies was assessed after 30 days. Colonies were stained with crystal violet (0.5% w/v). Pictures were taken and the number of colonies was counted. Representative images are shown. (C)(D) Data are presented as relative changes to control set to 100% (n=3, *p<0.05: over-expressing p22phox vs. control and knocked-down p22phox vs. control, SEM).

4.1.4 Control of HepG2 tumour growth by p22phox in vivo

4.1.4.1 Silencing of p22phox reduces HepG2 tumour growth in a xenograft mouse model

To study the role of p22phox in tumour progression in an vivo model, a xenograft mouse model was used with HepG2 cells stably transfected with a shRNA against p22phox (shp22phox) or with control shRNA (shCtr). The experiments were performed in collaboration with Dr. Guenther Richter (University Hospital Klinikum rechts der Isar, Technical University of Munich).

Cells ($3,0 \times 10^6$) were injected into the groin of immunodeficient ($Rag2^{-/-}\gamma C^{-/-}$) male mice. Five mice were used per group ("shCtr" and "shp22phox" groups). After 46 days, the mice were

sacrificed and the tumours were isolated and evaluated. Tumours had developed in 10 out of 10 mice. The tumour shapes in both groups were very heterogeneous, but overall the average tumour weight of xenografts from the “shp22phox” group was lower than from the control “shCtr” group (Figure 27). p22phox protein was reduced in the “shp22phox” tumours compared to controls as determined by Western blot analysis (Figure 27). The results obtained from the *in vivo* experiments are in line with the *in vitro* results verifying the important role of p22phox in HepG2 tumour progression.

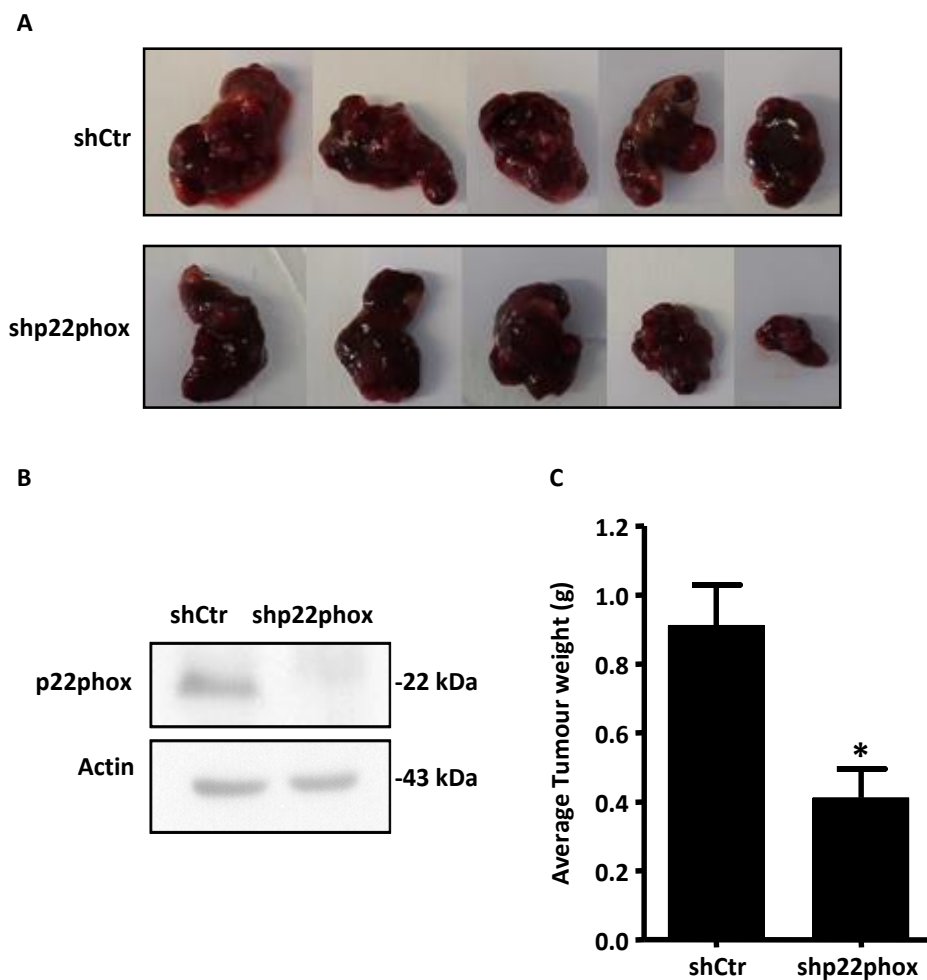


Figure 27: p22phox modulates tumour growth in a xenograft mouse model. Mice were injected with stably transfected HepG2 cells with plasmids encoding for shRNA against p22phox (shp22phox) or control shRNA (shCtr). (A) Tumours were isolated 46 days after injection and pictures of all tumours are shown. (B) Corresponding xenograft tissue protein samples were prepared and submitted to Western blotting using an antibody against p22phox. A representative blot is displayed. Actin was used as loading control. (C) Tumour weights were measured. Data are presented as average tumour weight (g) (n=5, *p-value<0.05: tumour weight of shp22phox tumours vs. tumour weight of shCtr tumours, STD).

4.1.4.2 p22phox modulates the balance between proliferation and apoptosis in HepG2

xenografts

To further analyse differences in proliferative activity between control and shp22phox expressing clones, xenografts were stained for Ki-67 via immunohistochemistry (IHC). Compared to control tumours, staining for Ki-67 was decreased in tumours with reduced levels of p22phox. To test whether apoptosis mediates the reduction in tumour growth, expression of cleaved caspase 3 was examined. Indeed, tumours from shp22phox clones showed increased levels of cleaved caspase 3 compared to controls indicating higher ratios of apoptotic cell death (Figure 28).

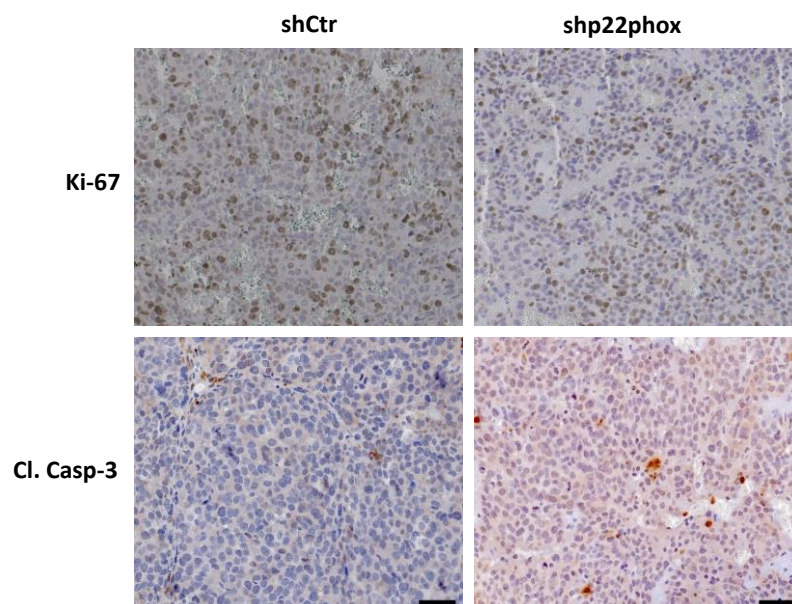


Figure 28: Proliferation and apoptosis are modulated in p22phox depleted HepG2 xenografts. 5 μ m sections of paraffin embedded xenograft tumours derived from p22phox depleted HepG2 cells stably transfected with either shRNA against p22phox (shp22phox) or control shRNA (shCtr) were cut and stained for the proliferation marker Ki-67 or the apoptosis marker cleaved caspase-3 (Cl. Casp-3). Representative images are shown, size bar = 50 μ m for all panel segments.

4.1.5 Proteomic analysis of p22phox over-expressing HepG2 cells

4.1.5.1 Two dimensional gel electrophoresis (2-DE) analysis

In a next step we evaluated whether increased levels of p22phox in HepG2 cells would differentially affect the proteome compared to control cells by employing a suitable gel based proteomic platform.

First, preliminary two-dimensional gel electrophoresis (2-DE) experiments were performed for optimization purposes of the targeted analysis. All experimental parameters such as the concentration of the protein sample, the type of the immobiline pH gradient strips, the gel concentration and the gel staining method were evaluated. After, the 2-DE gels were generated on the highest possible degree of reproducibility giving emphasis on minimizing errors due to inter-gel variability. The gels which did not meet high quality and reproducibility criteria were omitted from the analysis. All suitable 2-DE gels after staining, scanning and digitalisation, were submitted to image software analysis using SameSpots (Non Linear Dynamics, Newcastle upon Tyne, UK). The analysis resulted in the identification of dysregulated protein spots. The theoretical isoelectric point pI and the theoretical molecular weight M_r of all identified spots were estimated.

2-DE protein expression patterns on immobilized pH 4-7 gradient strips (IPGs) were compared between p22phox over-expressing (p22K1 and p22K3) clones and control (CtrK2 and CtrK5) clones. A total of 722 spots were retained as correctly matched and identified across all gels and were subjected to statistical analysis. A number of 16 protein spots exhibited statistically significant differences between the control and p22phox over-expressing cells at a fold change exceeding the level of biological variation found in the control samples and were thus selected as differentially expressed. Of them, 13 had higher abundance in the p22phox over-expressing cells, while 3 were more abundant in the control cells (Figure 29).

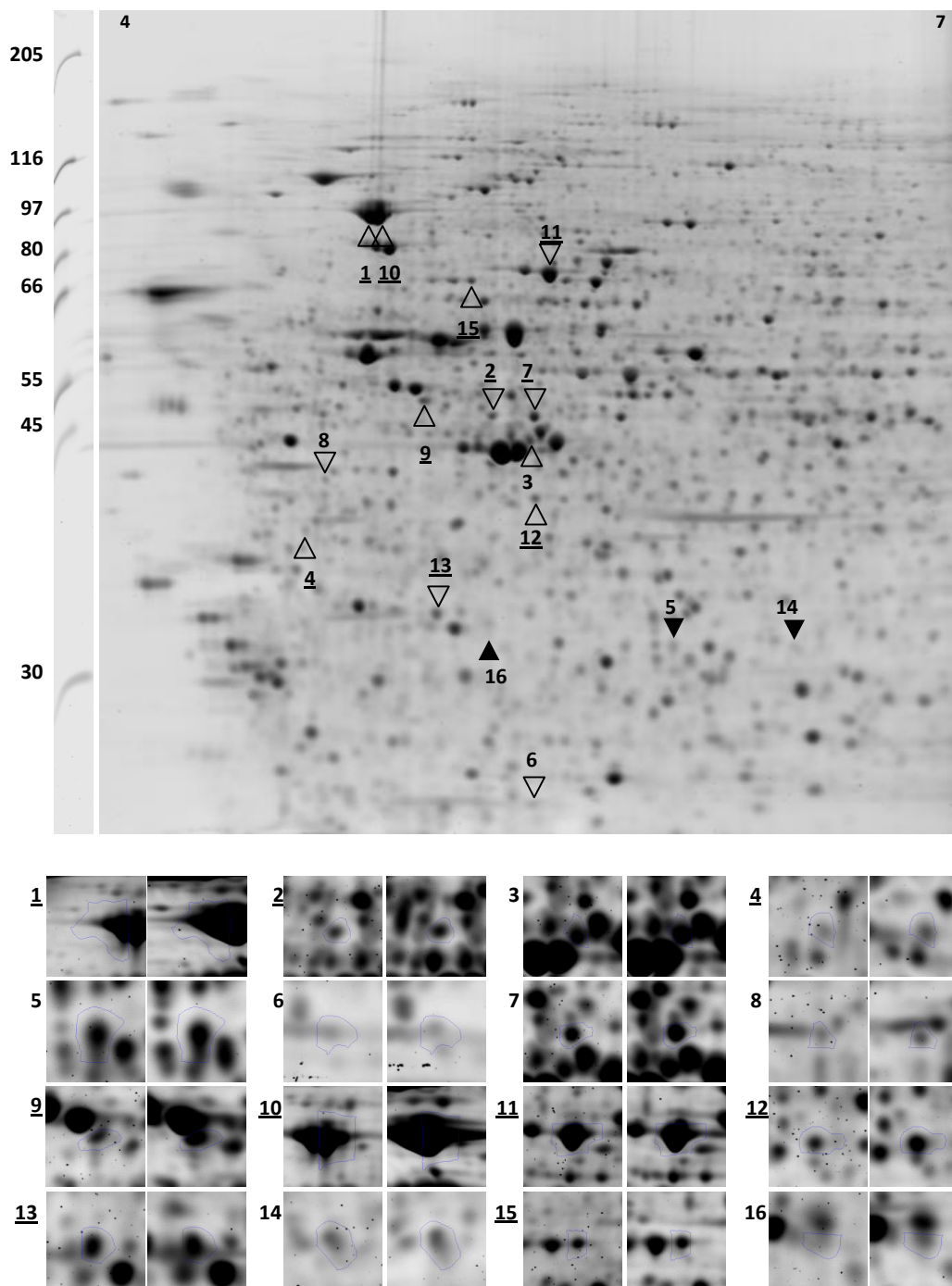


Figure 29: Proteins differentially expressed in control versus p22phox over-expressing HepG2 cells. Up: A representative 2-DE gel image displaying all sixteen dysregulated protein spots. Protein functions which were found as differentially expressed are indicated with numbers and arrows. Underlined numbers correspond to successfully identified proteins as given on Table 40. Empty arrows correspond to up regulation and filled arrows to down regulation of proteins. The gel was prepared using acidic IPG strips (pH area 4-7). Down: Numbered pairs of magnified images of all sixteen dysregulated protein spots which are derived from representative 2-DE gels showing the differential expression patterns between control HepG2 samples (left image of each numbered pair) and p22phox over-expressing HepG2 samples (right image of each numbered pair). Underlined numbers of pairs correspond to successfully identified proteins as given on Table 40.

4.1.5.2 Mass spectrometry (MS) analysis

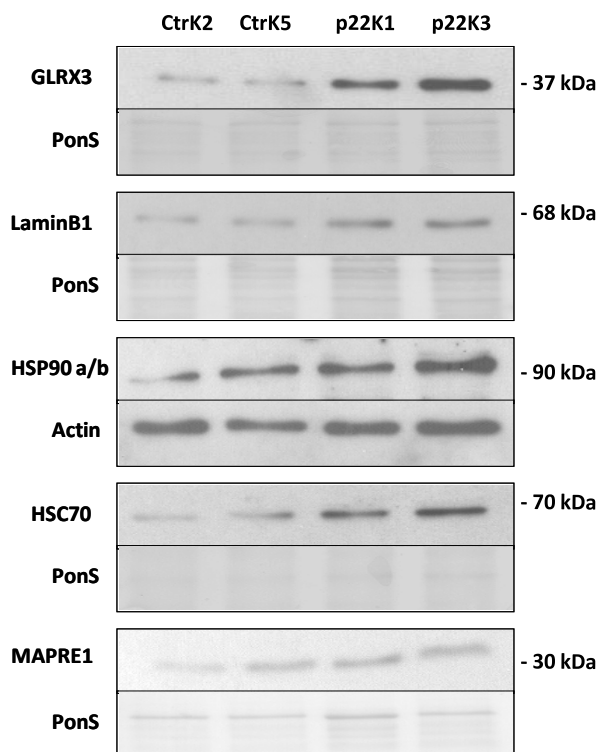
The sixteen protein spots which exhibited statistically significant differences were excised from preparative 2-DE gels prepared using samples of both control and p22phox over-expressing cells and stained with silver. The spots were analyzed subsequently by LTQ Orbitrap XL ETD mass spectrometry (ThermoScientific, Dreieich, Germany) at Fritz Lipmann Institute, Jena, Germany. Single hits were obtained for three spots, while ten spots contained more than two proteins. One other protein consisting of a complex mixture of proteins contained a protein differentially expressed in a neighbouring spot. Altogether MS/MS analysis successfully identified nine protein functions from ten spots, all of them up-regulated in p22phox over-expressing cells (Table 40).

Table 40: Protein functions differentially expressed in p22phox over-expressing HepG2 cells.

Spot	Protein name	p-value	fold regulation	direction
1	Heat shock protein 90-alpha	0.004	1.4	Up
2 (7)	Heterogeneous nuclear ribonucleoprotein F	0.047	1.6	Up
4	Charged multivesicular body protein 4b	0.045	1.7	Up
9	26S protease regulatory subunit 6B	0.030	1.6	Up
10	Heat shock protein 90-beta	0.020	1.4	Up
11	Heat shock cognate 71 kDa protein	0.044	1.4	Up
12	Glutaredoxin 3	0.030	1.8	Up
13	Microtubule-associated protein RP/EB family member1	0.021	1.8	Up
15	Lamin-B1	0.027	1.4	Up

4.1.5.3 Validation of differentially expressed proteins

To validate selected differentially expressed protein spots which were identified by the MS analysis, Western blot analyses were performed (Figure 30). Biological replicates of stably transfected HepG2 control cells (CtrK2 and CtrK5 clones) and p22phox over-expressing cells (p22K1 and p22K3 clones) were used in order to confirm the expression patterns of six protein species (Glutaredoxin-3, Lamin B1, Heat shock protein 90-alpha, Heat shock protein 90-beta, Heat shock cognate 71 kDa protein and Microtubule-associated protein RP/EB family member 1). Densitometric analyses were performed for all protein bands and the values were subsequently normalised to their respective protein concentration (loading controls: actin blots or Ponceau S staining). In all cases, Western blot results were consistent with the proteomic analysis (2-DE/MS) results (Table 40).



3

Figure 30: Validation by Western blot of selected proteins identified as differentially expressed in p22phox over-expressing HepG2 cells. Whole cell protein lysates (50 μ g) from stably transfected HepG2 control (CtrK2 and CtrK5) and p22phox over-expressing (p22K1 and p22K3) cells were immunostained using antibodies against human Glutaredoxin 3 (GLRX3), Lamin B1 (LaminB1), Heat shock protein 90 alpha & beta (HSP90 a/b), Heat shock cognate 71 kDa protein (HSC70), and Microtubule-associated protein RP/EB family member1 (MAPRE1). Ponceau S (PonS) staining or beta-actin (Actin) were used as loading control. The displayed blots are representative for at least three independent experiments.

4.1.5.4 Pathway and network analysis of differentially expressed proteins

The Ingenuity Pathway Analysis (IPA) software (Ingenuity Systems, Redwood City, USA) provides the ability to map differentially expressed proteins to functional networks and canonical pathways. Therefore, regarding the present study, the identified set of differentially expressed proteins which were validated by Western blotting, have been the input for the IPA analysis. Functional networks were constructed based on these selected differentially expressed proteins in combination with other interacting molecules as they were given by the Ingenuity's knowledge database. The network which appeared statistically the most significant, is presented on Figure 31. Moreover, IPA software suggested several diseases/disorders, biological functions, canonical pathways and toxicity for the differentially expressed proteins involved (Tables 41-44).

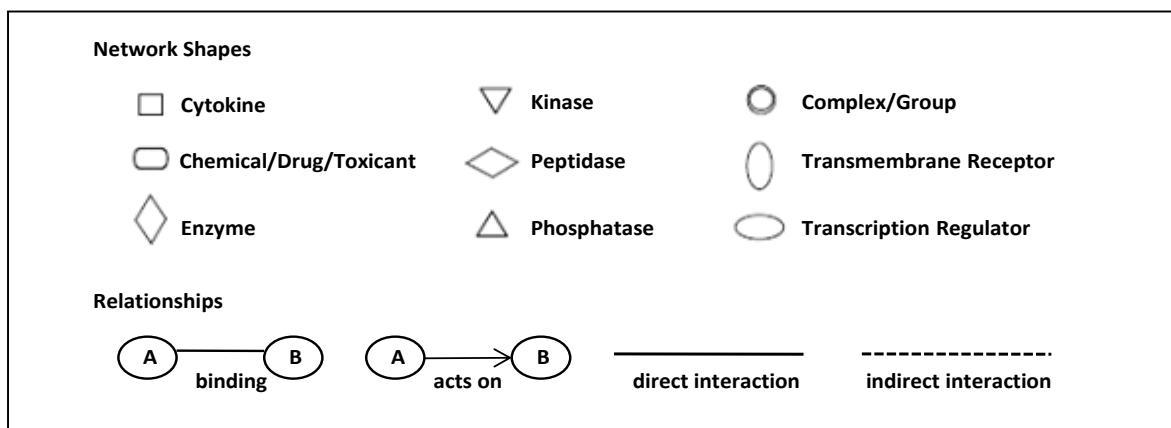
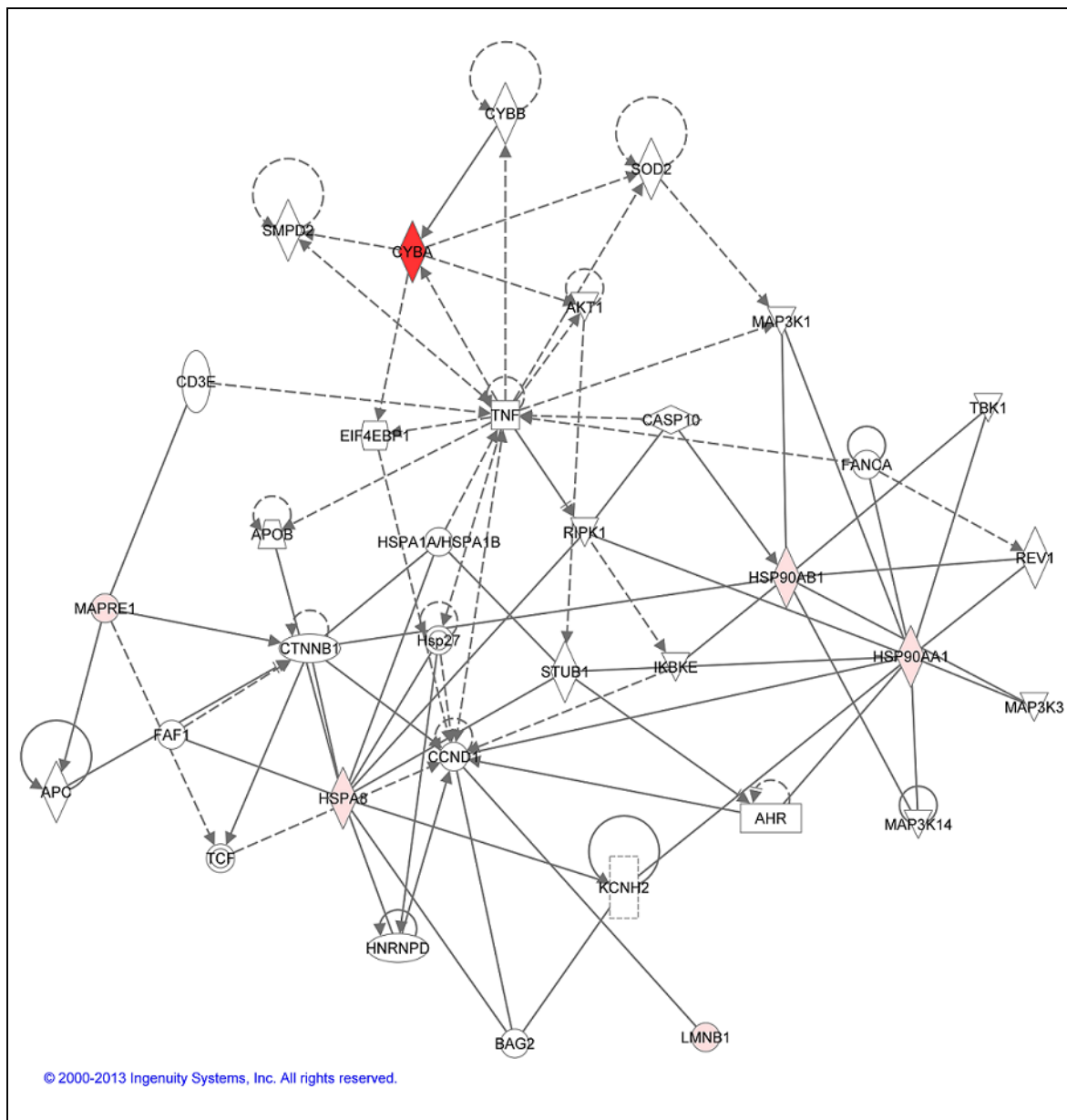


Figure 31: Protein interaction network revealed by IPA software analysis. Shades of red represent up-regulation functions of the identified proteins. A major sub-network within the network is centered on HSP90.

Table 41: Top diseases and disorders given by IPA.

Name	p-Value
Cancer	5,21e-07 – 3,74e-02
Reproductive system disease	5,21e-07 – 3,63e-02
Renal and urological disease	1,04e-06 – 4,00e-05
Gastrointestinal disease	3,53e-05 – 2,98e-02
Hepatic system disease	3,53e-05 – 5,24e-04

Table 42: Top molecular and cellular functions given by IPA.

Name	p-Value
Cell signalling	4,50e-04 – 4,50e-04
Cellular assembly and organization	4,50e-04 – 8,97e-03
Cellular function and maintenance	4,50e-04 – 8,97e-03
Lipid metabolism	4,50e-04 – 2,70e-03
Molecular transport	4,50e-04 – 1,80e-03

Table 43: Top canonical pathways given by IPA.

Name	p-Value
eNOS signalling	1,69e-05
Aldosterone signalling in epithelial cells	3,05e-05
Protein ubiquitination pathway	1,44e-04
Glucocorticoid receptor signalling	1,50e-04
Mitotic roles of polo-like kinase	3,24e-04

Table 44: Top toxicity lists given by IPA.

Name	p-Value
Hypoxia-inducible factor signalling	4,02e-04
Mechanism of gene regulation by peroxisome proliferators via PPAR α	7,44e-04
Aryl hydrocarbon receptor signalling	1,76e-03
PPAR α /RXR α activation	2,38e-03
NRF2-mediated oxidative stress response	3,51e-03

4.1.6 Role of HSP90 in the p22phox proliferative response of HepG2 cells

Based on the proteomics findings and bioinformatics data analysis, demonstrating increased HSP90 levels in p22phox over-expressing HepG2 cells, we analyzed whether HSP90 would be involved in p22phox dependent proliferative activity. HSP90 has been proven to be related to tumour proliferation [142-144].

To this end, we applied an inhibitor of HSP90 (NVP-AYU922, 100 nM) [145, 146] to control and p22phox over-expressing HepG2 cells for 24 hours. Western blot analyses performed with antibodies against HSP90 indicated no change in the protein levels by the inhibitor as expected (Figure 32). However, levels of HSP70 and HSP27 were increased in the HepG2 cells treated with NVP-AYU922 inhibitor of HSP90. It is well recognized that one of the molecular signatures of many HSP90 inhibitors is an up-regulation of the antiapoptotic and cytoprotective HSP70 protein, a consequence that is believed to reduce the overall antitumour efficacy of these compounds [147, 148].

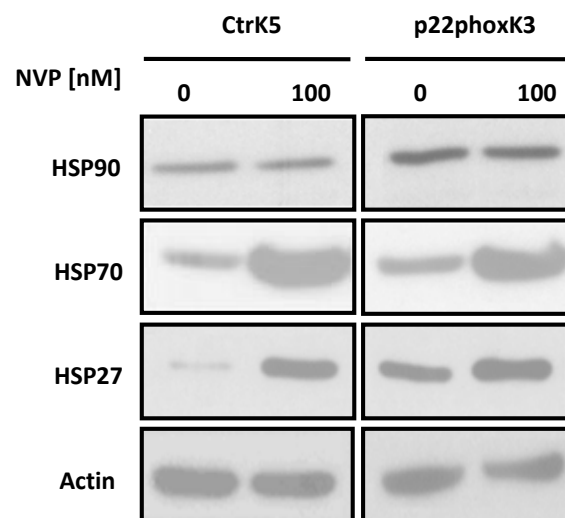


Figure 32: Inhibition of HSP90 affects expression of HSP70 and HSP27 in HepG2 cells. Stably transfected HepG2 cells over-expressing p22phox (p22phoxK3 samples) or empty control vector (CtrK5 samples) were treated with the HSP90 inhibitor NVP-AUY922 (100 nM) for 24 h. Western blot was performed using antibodies against heat shock protein 90 alpha/beta (HSP90), heat shock protein 70 (HSP70) and heat shock protein 27 (HSP27). Actin was used as loading control.

We next evaluated whether inhibition of HSP90 would affect the proliferative activity induced by p22phox. Ki-67 staining revealed that inhibition of HSP90 reduced the number of positively stained cells (Figure 33). In addition, we found that treatment with the HSP90 inhibitor abolished clonogenic activity in control and p22phox over-expressing HepG2 cells (Figure 34).

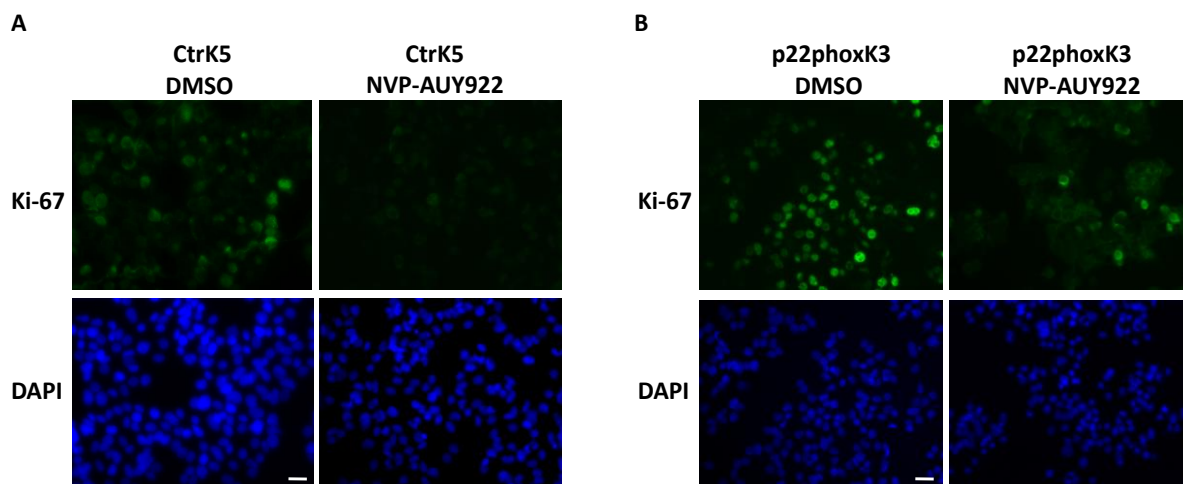


Figure 33: HSP90 inhibition modulates the p22phox mediated expression of proliferation marker Ki-67. Stably transfected HepG2 cells with (A) control levels of p22phox (CtrK5) and (B) enhanced levels of p22phox (p22phoxK3), were treated with HSP90 inhibitor NVP-AUY922 (100 nM). Immunofluorescence (IF) was performed using antibody against Ki-67 (green colour). Nuclei were counterstained with DAPI (blue colour). Fluorescence images were taken at a 20x magnification (size bar 12 μm).

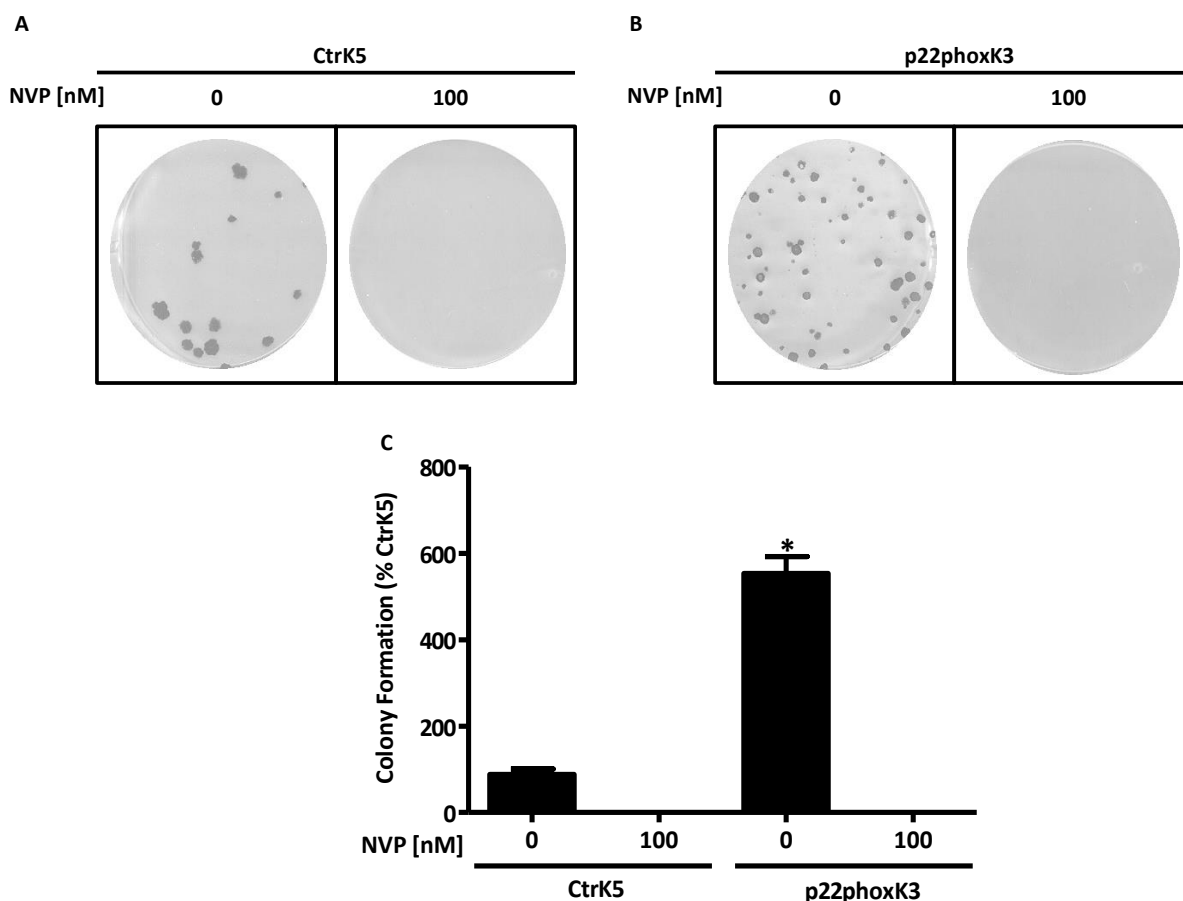


Figure 34: HSP90 inhibition diminishes clonogenic activity in HepG2 cells. (A) HepG2 control cells (CtrK5) and (B) p22phox over-expressing cells (p22phoxK3) were seeded in 6-well plates and treated with the HSP90 inhibitor NVP-AUY922 (100 nM). Formation of colonies was assessed after 30 days. Colonies were stained with crystal violet (0.5% w/v). Pictures were taken and the number of colonies was counted. Representative images are shown. (C) Data are presented as relative change to untreated CtrK5 clone set to 100% (n=3, *p<0.05 over-expressing vs. control p22phox, SEM).

To further validate the importance of HSP90 in the p22phox regulated pathways we determined the levels of proteins known to be involved in the balance between proliferation and apoptosis.

First, we assessed whether p22phox affects phosphorylation of Akt as an indicator of cell survival, proliferation and glucose metabolism. Compared to controls, levels of phosphorylated Akt were enhanced in p22phox over-expressing clones. Application of the HSP90 inhibitor completely abolished this response.

To determine whether inhibition of HSP90 would affect apoptosis as a mechanism explaining decreased proliferative activity we assessed the levels of Cleaved Caspase-3, PARP and p53. While neither control nor p22phox over-expressing cells showed Cleaved Caspase-3 or cleaved PARP, application of HSP90 inhibitor substantially increased the levels of those proteins in both cell lines. Similarly, the levels of p53 were substantially increased in cells treated with the HSP90 inhibitor (Figure 35). Collectively, these data suggest that inhibition of HSP90 promotes apoptosis of control and p22phox over-expressing HepG2 cells.

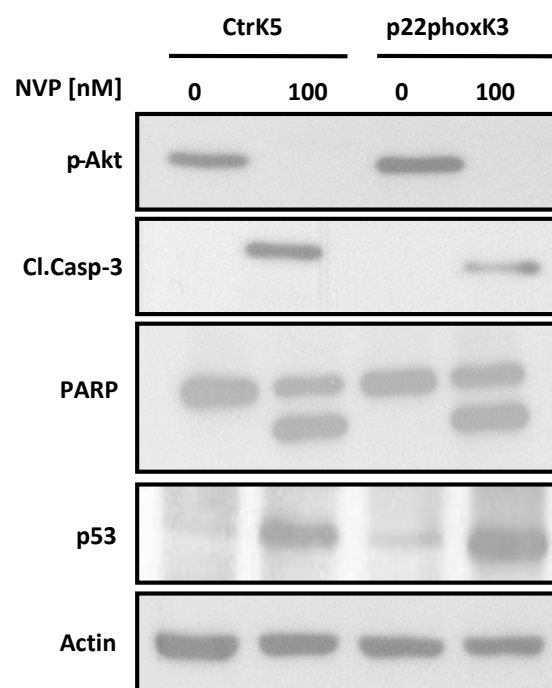


Figure 35: HSP90 inhibition increases apoptosis marker levels in HepG2 cells. HepG2 cells over-expressing p22phox (p22K3 samples) or empty control vector (CtrK5 samples) were treated with the HSP90 inhibitor NVP-AUY922 (100 nM) for 24 h. Cell lysates were immunostained using antibodies against phosphorylated Akt (p-Akt), cleaved Caspase 3 (Cl.Casp-3), PARP and p53. Actin was used as loading control.

4.1.7 Regulation of Cathepsin D by p22phox in HepG2 cells

4.1.7.1 p22phox modulates Cathepsin D expression

Cathepsin D is an aspartic lysosomal endopeptidase present in most mammalian cells. It affects major cellular biological processes such as proliferation, angiogenesis and apoptosis [149]. Increased levels of Cathepsin D have been associated in several human neoplastic tissues [150, 151]. Cathepsin D has also been shown to contribute to breast cancer metastasis, in the malignant progression of melanocytic tumours and hepatic carcinomas [152-156]. Although ROS have been linked to Cathepsin D function [157], the role of NADPH oxidases in the regulation of this protease is not known.

To assess a putative link between p22phox and Cathepsin D, protein expression levels of Cathepsin D were determined in p22phox over-expressing HepG2 cells and p22phox depleted HepG2 cells. Cathepsin D levels were enhanced in p22phox over-expressing HepG2 cells and reduced in p22phox depleted HepG2 cells, respectively (Figure 36).

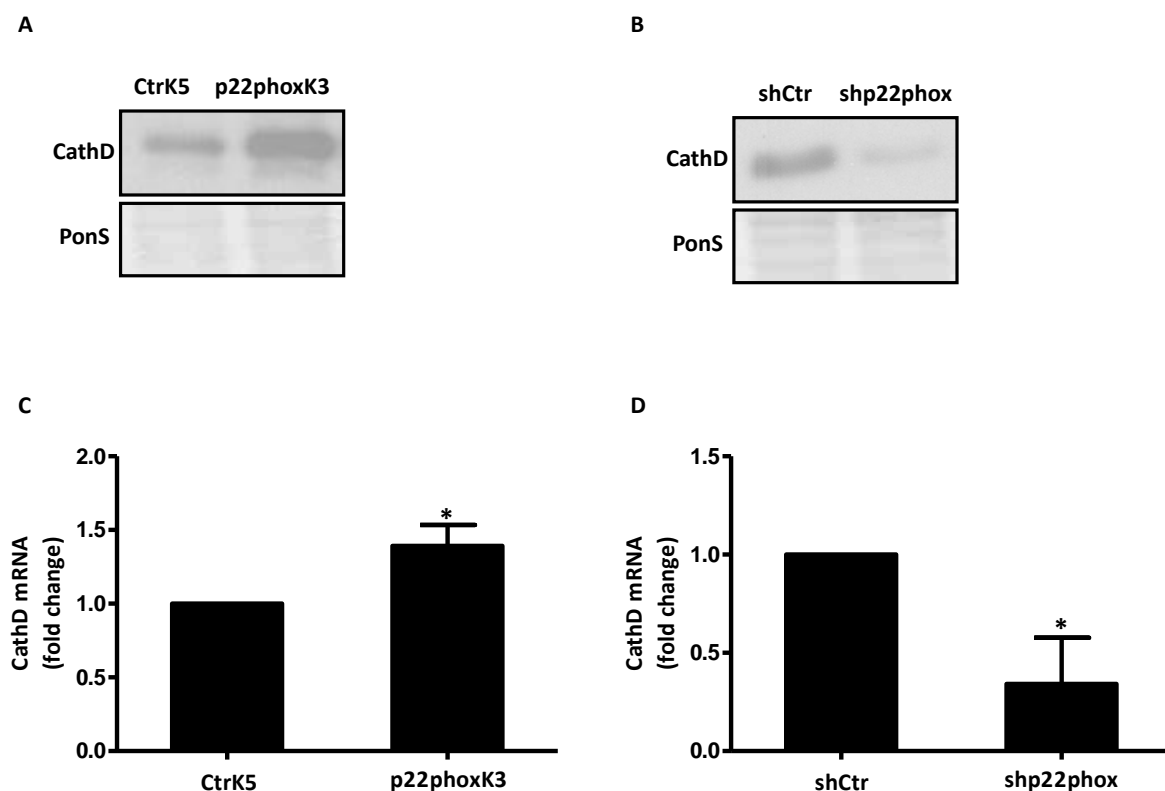


Figure 36: Cathepsin D expression levels in p22phox modified HepG2 cells. Up: Stably transfected HepG2 cells with (A) empty control vector (CtrK5) or p22phox plasmid (p22phoxK3) and (B) vector encoding for control shRNA (shCtr) or short hairpin RNA against p22phox (shp22phox), were analyzed by Western blot using an antibody against Cathepsin D. Actin was used as loading control. The displayed blots are representative for at least three independent experiments. Down: RNA of stably transfected HepG2 cells with (C) empty control vector (CtrK5) or p22phox plasmid (p22phoxK3) and (D) vector encoding for control shRNA (shCtr) or short hairpin RNA against

p22phox (shp22phox), was isolated. After cDNA synthesis, qPCR for Cathepsin D mRNA was performed. Data are presented as relative change to control clones (CtrK5 or shCtr) after normalization to beta actin. (n=3,*p<0.05: p22phoxK3 vs. CtrK5 or shp22phox vs. shCtr, SEM).

To determine whether Cathepsin D is dependent on p22phox at the transcriptional level, mRNA levels of Cathepsin D were assessed on the established cellular model systems of stably transfected HepG2 cells with enhanced and reduced levels of p22phox. Indeed, mRNA levels of Cathepsin D were higher in p22phox over-expressing cells and reduced in p22phox depleted cells compared to controls, respectively (Figure 36). Therefore, these results underline the dependency of Cathepsin D on p22phox at the transcriptional level.

4.1.7.2 The modulation of Cathepsin D by p22phox is ROS dependent

In order to test whether the p22phox modulated Cathepsin D levels are dependent on the ROS, HepG2 wild type cells were treated with hydrogen peroxide (H₂O₂) in the concentrations of 100 μM and 200 μM, thus artificially inducing cells with ROS. After performing Western blot analysis on these samples, we showed that H₂O₂ treatment resulted in the increase of Cathepsin D expression levels proportionally to the concentration applied. Also, a control and a p22phox over-expressing HepG2 clone, were pre-treated with the antioxidant N-acetyl Cysteine (NAC, 5 mM) and Western blot for Cathepsin D was performed for these samples, too. Treatment with NAC reduced the Cathepsin D expression in the p22phox over-expressing clone to the level of the control clone supporting the evidence that Cathepsin D expression is ROS dependent (Figure 37).

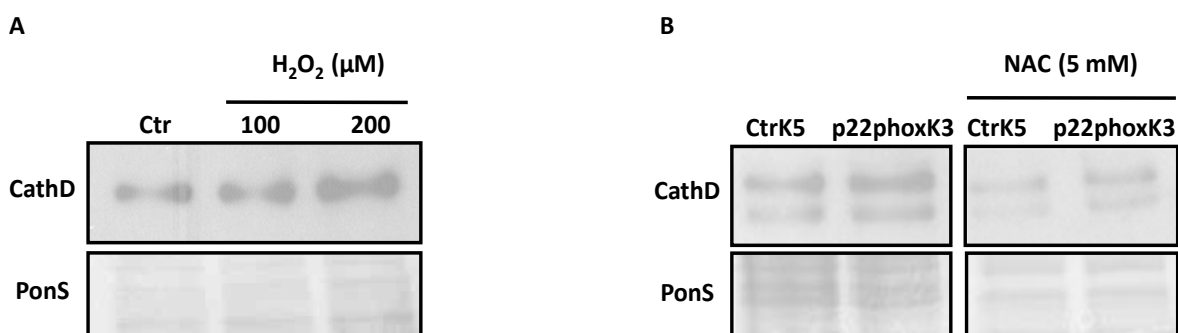


Figure 37: p22phox mediates Cathepsin D expression via ROS. (A) HepG2 cells were treated with hydrogen peroxide (H₂O₂) and Western blot analysis was performed using an antibody against Cathepsin D. Ponceau S (PonS) staining was used as loading control. The displayed blots are representative for at least three independent experiments. (B) HepG2 cells over-expressing p22phox (p22phoxK3) or with empty control vector (CtrK5) were treated with N-acetyl-cysteine (NAC) and Western blot analysis was performed using an antibody against Cathepsin D. Ponceau S (PonS) staining was used as loading control. The displayed blots are representative for at least three independent experiments.

4.1.7.3 p22phox regulates Cathepsin D localization and secretion

In a next step, intracellular localization of Cathepsin D in HepG2 cells was investigated. Results show that in cells over-expressing p22phox, Cathepsin D is highly diffused and secreted compared to the control cells in which Cathepsin D appears to be accumulated more firmly in the lysosomes (Figure 38). Moreover, Western blot analysis confirmed that p22phox modulates secretion of Cathepsin D. The observed secreted protein in the western blot analysis could be identified as Cathepsin D by using specific siRNA against Cathepsin D for silencing its expression (Figure 39).

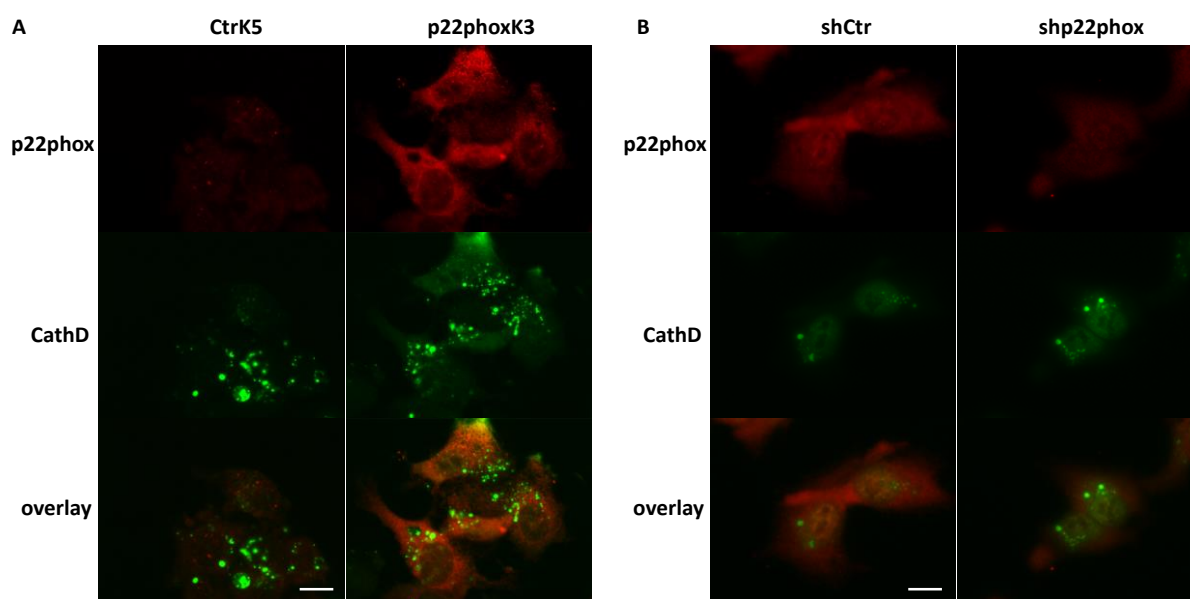


Figure 38: p22phox modulates Cathepsin D localization. Stably transfected HepG2 cells (A) over-expressing p22phox (p22phoxK3) and (B) over-expressing siRNA against p22phox (shp22phox) were immunostained using antibodies against p22phox (red colour) and Cathepsin D (green colour). Overlay pictures of p22phox and Cathepsin D staining are displayed. Fluorescence images were taken at a 60x magnification (size bar = 20 μm).

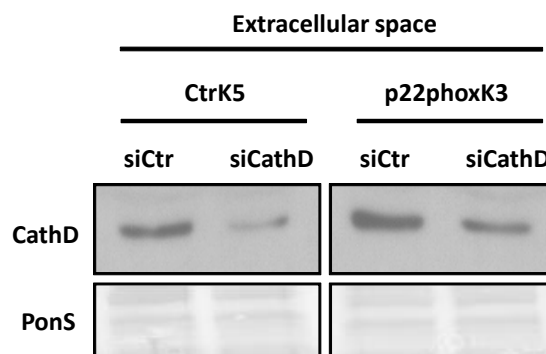


Figure 39: p22phox modulates secretion of Cathepsin D. Stably transfected HepG2 cells over-expressing p22phox (p22phoxK3 samples) or with empty control vector (CtrK5 samples) were transfected with siRNA against Cathepsin D (siCathD) or control siRNA (siCtr). 24 h post-transfection, western blot analysis was performed with supernatants of the samples using an antibody against Cathepsin D (CathD). Ponceau S (PonS) served as loading control.

4.1.7.4 p22phox affects lysosomal structure in HepG2 cells

Cathepsin D is mainly localized in the lysosomes. Therefore we investigated whether p22phox would affect the structure of lysosomes in p22phox over-expressing cells using LysoTracker, a fluorescence dye that accumulates in acidic organelles. HepG2 cells were stained with LysoTracker probe and fluorescence pictures were taken with a fluorescence microscope at two different magnifications displaying a group of cells (20x) and a representative single cell (60x) accordingly. HepG2 cells over-expressing p22phox showed higher affinity to the probe compared to the control cells. On a reverse way, HepG2 clones with silenced p22phox showed weaker lysotracker staining (Figure 40).

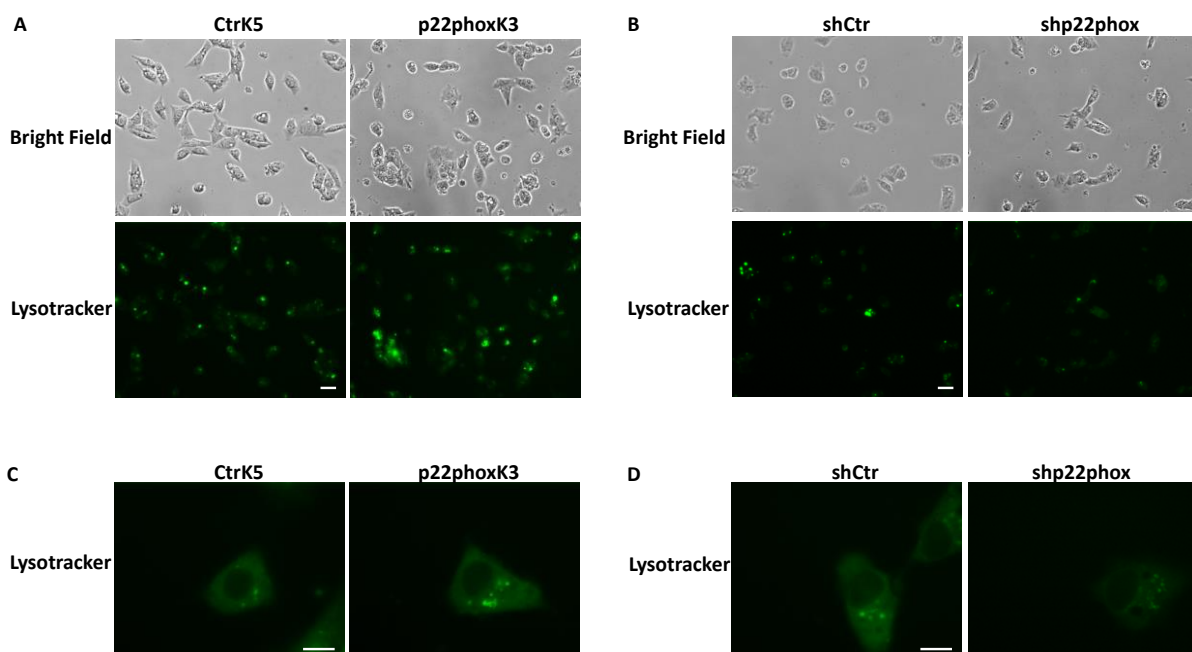


Figure 40: p22phox modulates lysosomal processing of Cathepsin D. Stably transfected HePG2 cells (A) with enhanced p22phox levels (p22phoxK3) and (B) reduced p22phox levels (shp22phox) were stained with the lysotracker fluorescence probe (green). Fluorescence images were taken at a 20x magnification (size bar = 12 μ m). Also, bright field pictures were taken at the same magnification (20x) showing the corresponding number of cells. Parts (C) and (D) of the figure show respectively to (A) and (B), lysotracker fluorescence images which were taken at a 60x magnification of a representative cell (size bar = 20 μ m).

4.1.7.5 Evaluation of Cathepsin D effect on the proliferative activity of HepG2 cells

As it is reported that the pro-proliferative effect of Cathepsin D is mainly mediated by the pathophysiological secretion of Cathepsin D by tumour cells [158, 159], we next investigated the secretion pathway of Cathepsin D. First, HepG2 wild type cells were transiently transfected using siRNA against Cathepsin D. Intracellular expression levels of Cathepsin D were evaluated

by immunoblotting. Also, extracellular levels of Cathepsin D were assessed by Western blotting detecting the secreted form of Cathepsin D in the corresponding media of the cells used to prepare the cell lysates (Figure 41). Silencing of the Cathepsin D protease could be clearly observed in the cell lysate as well as in the supernatant of HepG2 cells. To assess the impact of Cathepsin D on the proliferation of HepG2 cells, control and HepG2 cells with silenced Cathepsin D were seeded into 96-well plates. The proliferative and metabolic activity was evaluated using the BrdU ELISA and Alamar Blue assays. Indeed, reduced levels of Cathepsin D resulted in reduced proliferation of HepG2 cells indicating the firm role of Cathepsin D in cancer cell proliferative activity (Figure 41).

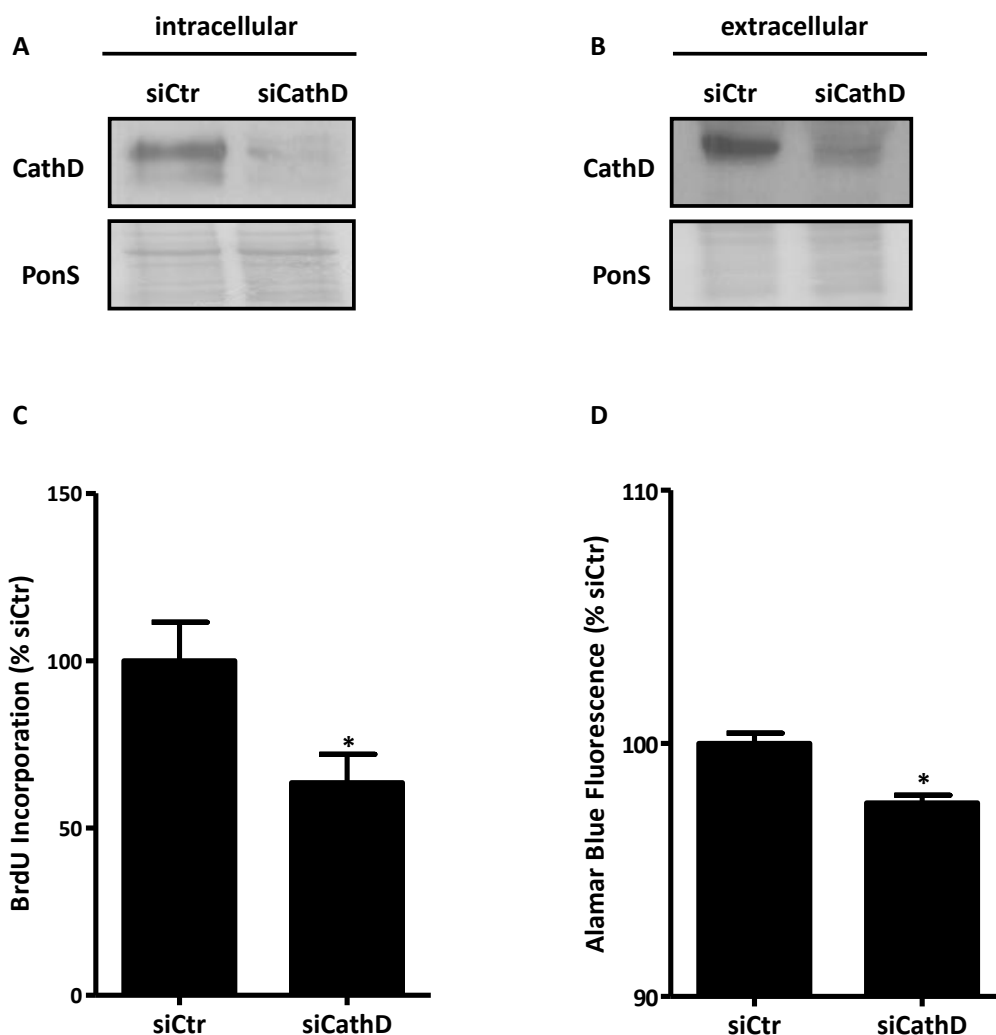


Figure 41: Silencing Cathepsin D reduces HepG2 proliferation. HepG2 cells were transfected with siRNA against Cathepsin D (siCathD) or control siRNA (siCtr). 48 hours post-transfection, Western blot was performed (A) with the cell lysate or (B) the supernatant for Cathepsin D. Ponceau S (PonS) staining served as loading control. Also, the transfected cells were seeded in 96-well plates for (C) BrdU proliferation assay and (D) Alamar Blue metabolic activity assay. Data are presented as relative change to control set to 100% (n=3, *p<0.05: siCathD cells vs. siCtr cells).

Cathepsin D is known to be induced by thrombin [160, 161]. Therefore, HepG2 wild type cells were stimulated with thrombin and Western blot analysis for Cathepsin D was performed. Indeed intra- and extracellular levels of Cathepsin D were increased by thrombin (Figure 42). In addition the proliferative activity of cells was subsequently assessed. Proportional to the Cathepsin D levels, the proliferation of cells demonstrated a mild increase (Figure 42).

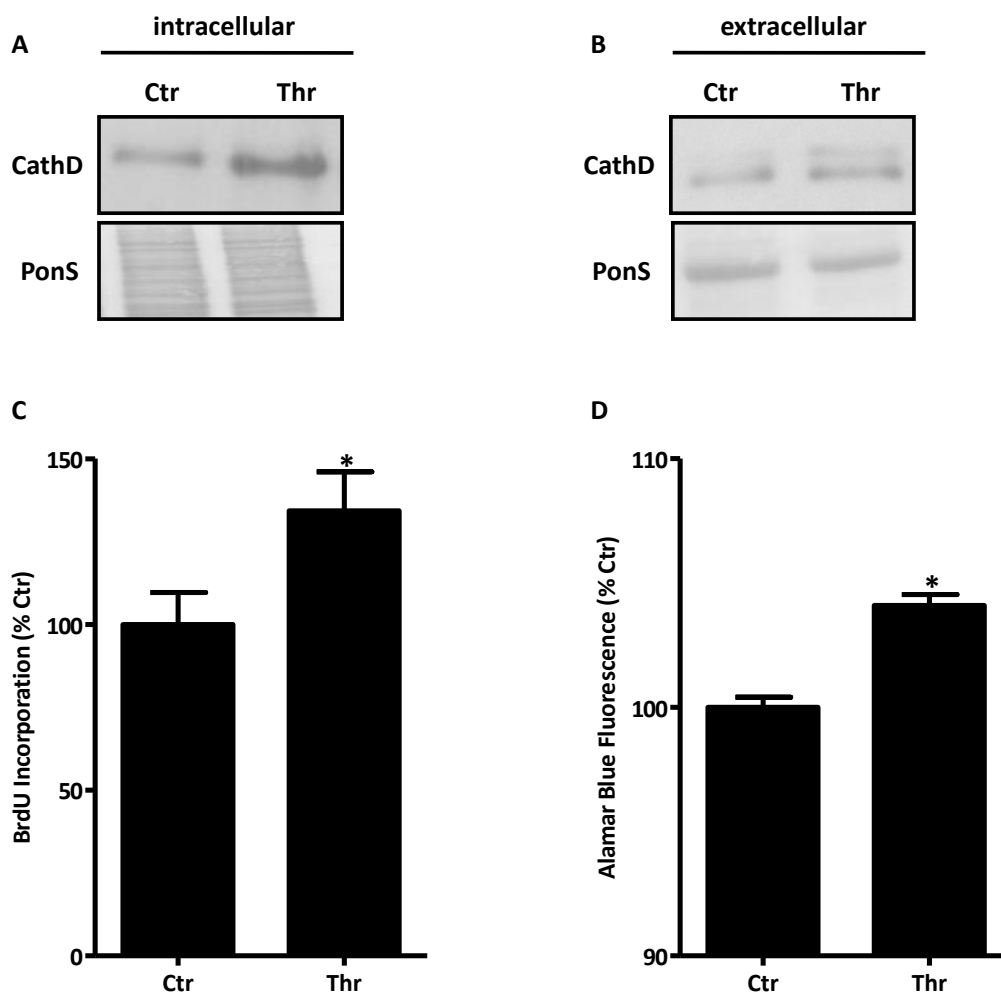


Figure 42: Thrombin induces Cathepsin D expression and proliferation in HepG2 cells. HepG2 cells were treated with thrombin (3 units) for 4h. Western blot was performed with (A) cell lysates or (B) supernatant for Cathepsin D (CathD). Ponceau S (PonS) staining served as loading control. Also, the stimulated cells were seeded in 96-well plates for (C) BrdU proliferation assay and (D) Alamar Blue metabolic activity assay. Data are presented as relative change to control set to 100% (n=3, *p<0.05: Thrombin stimulated cells vs. control cells).

4.1.7.6 p22phox modulates HepG2 proliferation dependent on Cathepsin D

To check whether p22phox mediated tumour progression is Cathepsin D dependent, stably transfected p22phox over-expressing HepG2 cells were further transiently transfected with siRNA against Cathepsin D.

In order to assess the transient transfection efficiency, immunoblotting was used (Figure 43). Indeed, silencing of Cathepsin D was successful in both control and p22phox over-expressing clones, as a reduction of Cathepsin D expression levels could be observed at intracellular level.

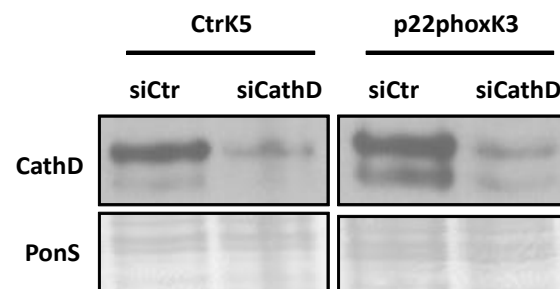


Figure 43: Silencing Cathepsin D in p22phox over-expressing HepG2 cells. Stably transfected HepG2 cells over-expressing p22phox (p22phoxK3 samples) or with empty control vector (CtrK5 samples) were transfected with siRNA against Cathepsin D (siCathD) or control siRNA (siCtr). 24 h post-transfection, western blot analysis was performed with cell lysates for Cathepsin D (CathD). Ponceau S (PonS) served as loading control.

In a next step, the impact of Cathepsin D on proliferation of stably transfected HepG2 cells was investigated by silencing Cathepsin D by specific RNA followed by either Alamar Blue assay or immunofluorescence assay for the proliferation marker Ki-67. siRNA transfection of Cathepsin D reduced metabolic activity in both control and p22phox over-expressing clones, however only in the p22phox over-expressing clone the decrease in metabolic activity was significantly reduced (Figure 44). Similarly, the increased staining for the proliferation marker Ki-67 in p22phox over-expressing HepG2 cells was substantially reduced in the presence of siCathD (Figure 44).

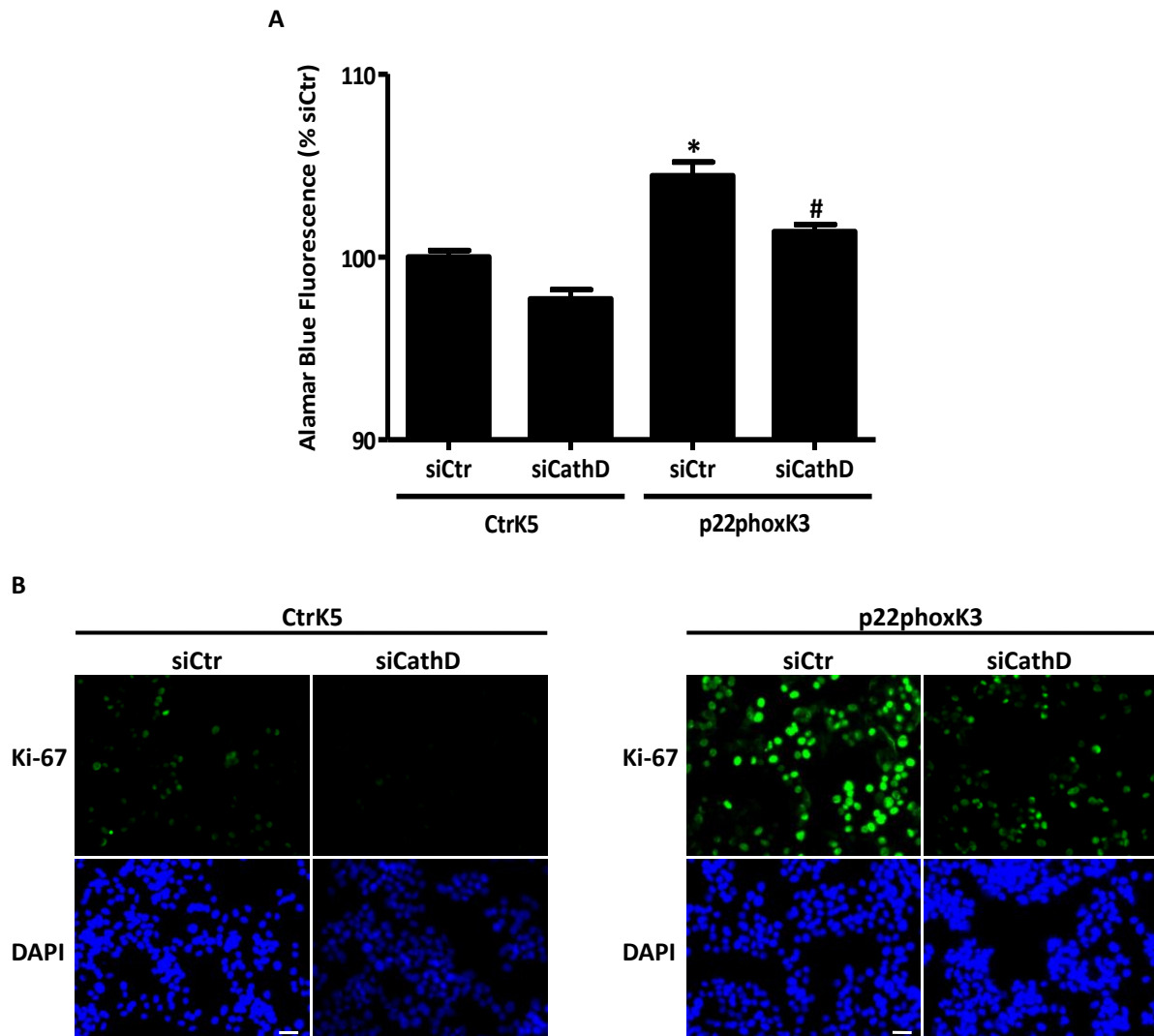


Figure 44: Silencing of Cathepsin D reduces p22phox mediated staining for Ki-67. Stably transfected HepG2 cells over-expressing p22phox (p22phoxK3) or empty control vector (CtrK5) were transfected with siRNA against Cathepsin D (siCathD) or control siRNA (siCtr). (A) 24h post transfection, cells were seeded in 96 wells plates before metabolic activity was determined by Alamar Blue fluorescence. Data are presented as relative changes to CtrK5 clone set to 100% (n=3, *p<0.05: p22phoxK3 vs. CtrK5, #p<0.05: p22phoxK3 siCathD vs. p22phoxK3 siCtr, SEM). (B) 24h post-transfection, cells were seeded into a 8 well μ -slide (60.000 cells per well). Immunofluorescence (IF) was performed using an antibody against proliferation marker Ki-67 (green colour). Nuclei were counterstained with DAPI (blue). Fluorescence images were taken at a 20x magnification (size bar=12 μ m).

In addition, a clonogenic assay (Figure 45) was performed using control and silenced p22phox over-expressing HepG2 samples. Results showed that depletion of Cathepsin D decreases the capacity of cells to form colonies and this effect, similarly to the previous results, was significantly incurred in the p22phox over-expressing clone. Thus, results derived from the Alamar Blue assays, immunofluorescence staining for Ki-67 marker and colony formation assays, underline the modulating role of p22phox in Cathepsin D dependent HepG2 proliferation, metabolic activity and cell survival capacity.

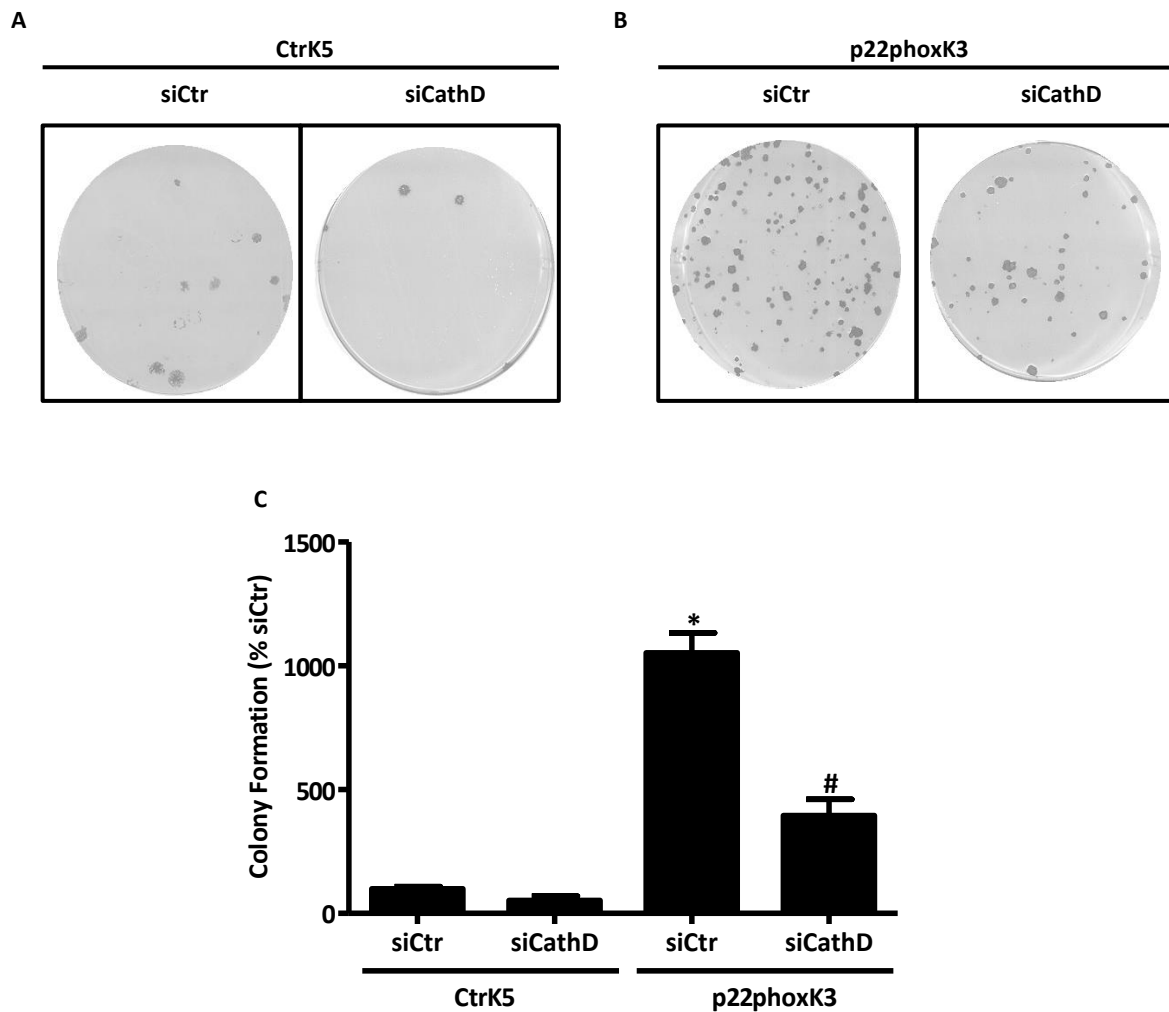


Figure 45: Cathepsin D modulates the ability of p22phox in HepG2 cells to form colonies. Stably transfected HepG2 cells with (A) empty control vector (CtrK5 samples) and (B) over-expressing p22phox (p22phoxK3) were transfected with siRNA against Cathepsin D (siCathD) or control siRNA (siCtr). 24 h post-transfection, cells were seeded in 6-well plates (1500 cells per well). Formation of colonies was assessed after 30 days. Colonies were stained with crystal violet (0.5% w/v). Pictures were taken and the number of colonies was counted. Representative images are shown. (C) Data are presented as relative changes to CtrK5 clone set to 100% (n=3, *p<0.05: p22phoxK3 vs. CtrK5, #p<0.05: p22phoxK3 siCathD vs. p22phoxK3 siCtr, SEM).

Last, stably transfected HepG2 cells over-expressing p22phox were pretreated with pepstatin A, a well known inhibitor of Cathepsin D, and were seeded in 96-well plates in order to assess proliferation using Alamar Blue assay. Indeed, the pre-treatment with pepstatin A reduced proliferation of p22phox to the same level of control cells further indicating that p22phox mediated proliferation is controlled by Cathepsin D (Figure 46).

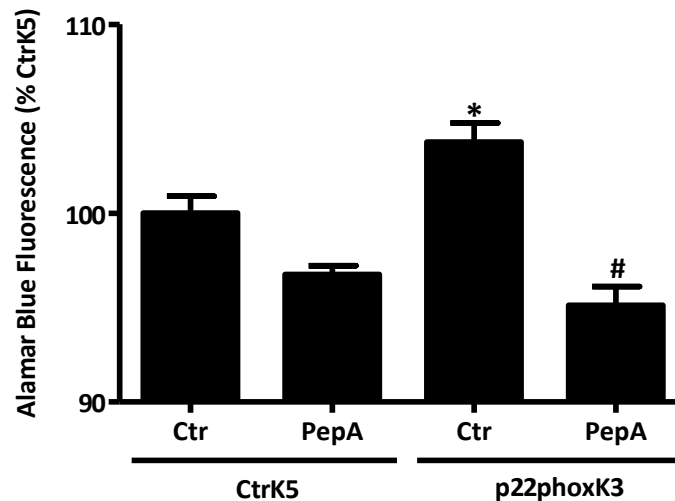


Figure 46: Cathepsin D inhibition with Pepstatin A reduces cellular metabolic activity. Stably transfected HepG2 cells over-expressing p22phox (p22K3 samples) or with empty control vector (CtrK5 samples) were seeded in 96 well plates. After 18h, cells were pre-treated with 50 μ M Pepstatin A (PepA) for 24 h before metabolic activity was determined by Alamar Blue fluorescence. Data are presented as relative changes to untreated CtrK5 clone set to 100% (n=3, *p<0.05: p22phoxK3 vs. CtrK5, #p<0.05: p22phoxK3 PepA treatment vs. p22phoxK3 Ctr, SEM).

4.1.7.7 p22phox regulates Cathepsin D expression in HepG2 xenografts

In order to assess the *in vivo* association of p22phox and Cathepsin D levels, formalin-fixed paraffin embedded tumour tissue sections derived from the xenograft model experiments were stained against Cathepsin D. Indeed, Cathepsin D levels were decreased in xenografts from the p22phox knockdown cells compared to controls, highlighting the regulatory role of p22phox on Cathepsin D expression. In addition, Cathepsin D appeared to be localized intracellularly (Figure 47).

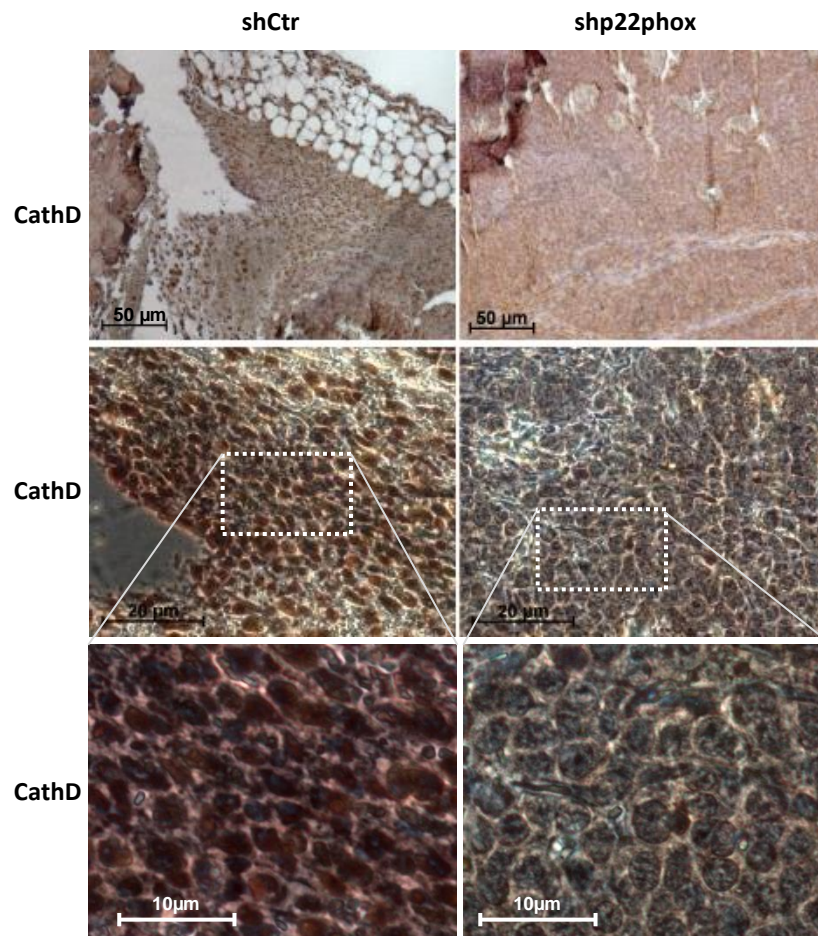


Figure 47: IHC analysis of xenograft mouse sections targeting Cathepsin D. 5 µm sections of paraffin embedded xenograft tumours derived from HepG2 cells stably transfected with either shRNA against p22phox (shp22phox) or control shRNA (shCtr) were cut and stained for Cathepsin D (CathD). Representative images are shown, at 10x (upper row) and 40x (middle row) magnification. The lower row displays respective magnified selected areas of the middle row.

Chapter 5: Discussion

5.1 Discussion

5.1.1 p22phox modulates ROS levels in HepG2 cells

Reactive oxygen species (ROS) derived from NADPH oxidases have been increasingly acknowledged to contribute to various pathways important in tumour pathophysiology [14, 28]. In this project we used hepatoblastoma HepG2 cells expressing enhanced or diminished levels of the NADPH oxidase subunit p22phox.

Our experimental findings indicate that modulating p22phox levels in HepG2 cells by either over-expressing or depleting p22phox results in a significant increase or decrease in p22phox levels. The quantification of mRNA levels showed an approximately 3 fold up regulation and the quantification of protein levels showed an average 4,5 fold up regulation of p22phox in the p22phox over-expressing clones compared to control clones which was associated with a concomitant increase in ROS levels, respectively. Interestingly, ROS generation as determined by DHE fluorescence showed only an average of 1,8 fold up regulation compared to control. This suggests that p22phox alone is not sufficient to regulate ROS generation, but that ROS generation is also dependent of other subunits, such as NOX1, NOX2 and NOX4, which are required for ROS generation and expressed in HepG2 cells. Previously, we have shown in endothelial cells that NOX2 and NOX4 are equally important for basal ROS generation for ROS generation with p22phox [162].

In contrast, regarding the p22phox depleted HepG2 cells, p22phox expression is 2,5 fold down-regulated and this is in line with a 2 fold reduction of ROS generation indicating that basal ROS levels are quite proportional to p22phox levels. Furthermore, these results show that the main portion of basal ROS in HepG2 cells is derived from NADPH oxidases. In addition, we performed immunofluorescence staining of the cells for p22phox showing equal distribution of p22phox protein expression among cells of the same clone. Moreover, intracellular localization resembles the endoplasmic reticulum as it is reported by us and other groups [162, 163]. There was no difference observed in intracellular localization of p22phox among the different clones indicating that the over-expression of p22phox does not affect its intracellular localization and thus, its physiological function.

5.1.2 p22phox modulates proliferation of HepG2 cells

In a next step, we showed that enhanced levels of p22phox in HepG2 cells increase proliferation whereas silenced levels of p22phox decrease proliferation in HepG2 cells. p22phox dependent proliferative activity was mediated by ROS, since cells treated with NAC showed reduction of their proliferative activity. In a similar way, previous studies in our lab on NOX2, NOX4 and p22phox, have shown the mediating role of these proteins in the proliferative activity of endothelial cells and smooth muscle cells [160, 162, 164]. In line with our results, another study demonstrated that over-expression of p22phox mediated the anti-apoptotic effects of growth factors in pancreatic cancer cells, thus contributing to a pro-proliferative effect [165].

We further showed that p22phox modulates metabolic activity by Alamar Blue fluorescence of HepG2 cells. This assay is an estimate of metabolic activity and has been served to indicate viability and proliferation. Thus, in line with results from BrdU assay, there is strong indication that p22phox levels modulate the proliferative activity of HepG2 cells. Moreover, colony formation experiments showed that increase of p22phox in HepG2 cells leads to increased number of colonies compared to control cells and decrease of p22phox in HepG2 cells leads to decreased number of colonies compared to control cells.

In addition, p22phox deficient HepG2 cells showed reduced xenograft growth. Furthermore, experimental data from our lab using p22phox over-expressing HepG2 cells showed an increase in xenograft growth compared to control HepG2 cells adding value on the important modulating role of p22phox in tumour progression in this type of liver cancer. In support, in a pancreatic cancer model system, the knockdown of p22phox led to a significant decrease in cell growth, colony formation capacity and tumour growth in vivo based on a mouse xenograft model, too [165]. Moreover, another published work showed that p22phox mediated ROS contribute to angiogenesis and tumour growth in prostate cancer [55, 165]. Knockdown of p22phox decreased prostate cancer cell proliferation, colony formation capacity, and inhibited tumour angiogenesis and tumour growth in a mouse xenograft model included in the same study [55].

In conclusion, our data indicate that p22phox enhances ROS generation in HepG2 cells which subsequently leads to enhanced proliferation of these cells.

5.1.3 Proteomic analysis of HepG2 cells over-expressing p22phox

In this study, 2DE gel based proteomic analysis revealed a list of differentially expressed proteins due to enhanced levels of p22phox in HepG2 cells.

Glutaredoxin-3 (Glx3, also known as Grx3, PICOT, TXNL2 or Trx-like 2) was identified as up-regulated protein in p22phox over-expressing HepG2 cells. Glutaredoxins (Glx) are [2Fe-2S]-binding protein proteins responsible for specific catalysis of removal of the glutathionyl moiety from protein-mixed disulfides (deglutathionylation). These small redox enzymes of approximately one hundred amino-acid residues use glutathione as a cofactor. In contrast to thioredoxins, which are reduced by thioredoxin reductase, no oxidoreductase exists that specifically reduces glutaredoxins. Instead, glutaredoxins are reduced by the oxidation of glutathione. Oxidized glutathione is then regenerated by glutathione reductase. Together these molecules compose the glutathione system [166]. Glutaredoxin class of enzymes possesses an active centre disulfide bond. It exists in either a reduced or an oxidized form where the two cysteine residues are linked in an intramolecular disulfide bond. Glutaredoxins function as electron carriers in the glutathione-dependent synthesis of deoxyribonucleotides by the enzyme ribonucleotide reductase. Importantly, glutaredoxins act as antioxidants and they have been shown to be critical in maintaining redox homeostasis in living cells [167]. By acting as part of the anti-oxidant program, they are involved in protecting cells from oxidative stress. Our findings that p22phox which enhanced ROS, also enhances an antioxidant protein, suggest the presence of an internal negative feedback loop which might be relevant for fine tuning p22phox dependent ROS levels and to protect the cells from adverse effects of ROS overload.

In fact, glutaredoxins have been shown to control apoptosis and play a role in immune cell response, embryogenesis, and regulation of cardiac hypertrophy [168]. Particularly in the field of oncology, Glx3 has been associated with cancer cell growth and has been shown to be over-expressed in human colon and lung carcinoma [169]. Thus enhanced levels of Glx3 might contribute to the enhanced proliferative response of p22phox over-expressing HepG2 cells. In support, Glx3 was shown to promote breast cancer cell growth by activating NF- κ B signaling [170].

Moreover, the microtubule-associated protein RP/EB family member 1 (MAPRE1) protein, or else known as end-binding protein 1 (EB1), was found also with increased levels in p22phox over-expressing HepG2 cells compared to control cells. MAPRE1 (or EB1) is a 35-kDa, mildly

acidic, leucine zipper protein belonging to microtubules-associated RP/EB1 family [171]. It was first identified by its binding to the APC protein which is often mutated in familial and sporadic forms of colorectal cancer [172]. Also, EB1 has been reported to be over-expressed in esophageal squamous cell carcinoma, gastric adenocarcinoma and hepatocellular carcinoma [173-176]. Depletion of EB1 promoted apoptosis of human non-small-cell lung cancer via ROS and Bax-mediated mitochondrial dysfunction [177]. This phenomenon was potentiated in radiation-treated EB1-knockdown cells and was largely blocked by NAC suggesting the involvement of ROS in the anti-apoptotic function. Thus induction of EB1 by p22phox might contribute to p22phox dependent proliferation by acting as an anti-apoptotic.

The results also showed that p22phox enhanced cells express increased levels of lamin B1 as compared to control cells. Lamin B1 is an intermediate filament protein of the nuclear envelope [178]. It belongs to the B-type lamins which arise from two different genes, *LMNB1* and *LMNB2*. Lamin B1 is required for proper organogenesis and organism survival. Mice that lack a functional *LMNB1* gene, die minutes after birth, and fibroblasts from these mice have misshaped nuclei and undergo premature senescence in culture [179]. Therefore, decreased levels of lamin B1 can serve as a senescence biomarker [180]. Lamin B has been suggested to play a role in cancer development and other diseases with ROS involvement [181, 182].

The proliferation defects induced by silencing Lamin B1 were accompanied by a p53-dependent reduction in mitochondrial reactive oxygen species (ROS), over-expression of lamin B1 on the other hand, increased the proliferation rate and delayed the onset of senescence of WI-38 cells in conjunction with a cell cycle arrest at the G1/S boundary [183]. Up-regulation of lamin B1 by p22phox might be part of a survival strategy and contribute to HepG2 tumour progression by preventing senescence. Maintenance of mitochondrial ROS by lamin B1 might be an interesting strategy in the light of increased ROS levels by p22phox suggesting a link between this enzyme and mitochondria as it has been recently described [183, 184].

Moreover, increase of p22phox protein levels resulted in changes in the abundance of proteins belonging to the family of heat shock proteins (HSPs). We found higher levels of heat shock protein 90 alpha (HSP90-alpha), heat shock protein 90 beta (HSP90-beta) and heat shock cognate protein 71 (named also as HSPA8 or HSC70) in p22phox over-expressing cells compared to control cells.

Heat shock proteins are over-expressed in a wide range of human cancers and are implicated in tumour cell proliferation, differentiation, invasion, metastasis, death, and recognition by

the immune system. HSP90 is key to the stability and function of a host of proteins that are important to the tumour cell, such as BCR-ABL, ERB-B2, epidermal growth factor receptor (EGFR), CRAF, BRAF, AKT, MET, VEGFR, FLT3, androgen and estrogen receptors, hypoxia-inducible factor (HIF)-1a, and telomerase, the list of which is being constantly updated [185]. Apart from its interaction with various client proteins such as HIF1a, which has also been shown to be regulated by p22phox [186], HSP90 has been reported to buffer cellular ROS although its mechanism of action remains poorly understood [187]. These findings again point to a scenario where ROS generating systems such as p22phox coregulate their safeguard helping to control and fine tune cellular ROS levels.

Heat shock cognate protein 70 (HSC70) is a constitutively expressed molecular chaperone which belongs to the heat shock protein 70 (HSP70) family. HSC70 has different properties compared with HSP70 and other heat shock family members [188]. Regarding cancer, the expression of HSC70 is higher in some tumour cell lines compared to normal cell lines [189]. HSC70 functions as a chaperone by trafficking proteins to different cellular compartments and is important in endocytosis [190]. HSC70 is also involved in Akt [191, 192] and NF- κ B signaling [193]. Importantly, HSC70 also regulates cell survival [194] and confers protection from several forms of cellular stresses, such as metabolic stress and oxidative stress [195, 196]. Thus far, the mechanism of regulation of HSC70 remains unclear, but it appears that its expression is regulated by KLF4 [197]. Thus, our findings that p22phox increases HSC70 which regulates cell survival and protects against oxidative stress, suggest that this protein might contribute to the proliferative response induced by p22phox. Again it might also be part of the protective antioxidant system which is concomitantly up-regulated by p22phox.

Interestingly, the present proteomic analysis revealed that p22phox mediated ROS results in differential expression of proteins which most of them are firmly linked to tumour progression and protection against oxidative stress. Regarding IPA analysis, the results supported the correlation of the identified dysregulated proteins to tumour proliferation and development. Cancer was identified as the top disease and cellular signalling as the top molecular function. Moreover, hypoxia-inducible factor (HIF) signalling was given by IPA analysis based on its correlation between HIF and ROS [198, 199] as well as the as one between HIF and cancer [200, 201]. Last, there has been shown also that HPS90 correlates with HIF. In general, IPA analysis underlined the important role of p22phox in regard to tumour progression.

5.1.4 Role of HSP90 in the p22phox regulated proliferation of HepG2 cells

After having shown the importance of the modulating role of p22phox in tumour progression using both *in vitro* and *in vivo* experimental tools, and since 2-DE analysis showed that HSP90 is up-regulated by p22phox, we decided to further investigate that interesting link between p22phox and HSP90 in regard to tumour progression. Our data showed that application of the HSP90 inhibitor (NVP-AUY922) in control and p22phox over-expressing HepG2 cells decreased the expression of p-Akt (Figure 35) as well as the expression of cleaved caspase-3, PARP and p53 levels (Figure 35) which indicate induction of apoptosis. As a result, we could show that inhibition of HSP90 decreased p22phox dependent proliferation in HepG2 cells and abrogated clonogenic activity.

It is known that p-Akt is involved in the balance between proliferation and apoptosis [202, 203] and it has been previously described that p-Akt is linked to tumour progression [204]. In line with this study, it has been shown that HSP90 inhibition results in degradation of p-Akt in multiple myeloma (MM) cells. The HSP90 inhibitor (NVP-AUY922) led to a significant reduction in myeloma cell viability and induced G2 cell cycle arrest, degradation of caspase-8 and caspase-3, and induction of apoptosis. In addition, a very pronounced and ubiquitous effect was the strong upregulation of HSP70, which is a well established cellular response to inhibition of HSP90 [205, 206].

On the other hand, treatment with the HSP90 inhibitor increased the expression of the anti-apoptotic and cytoprotective HSP70 (Figure 32). These findings even though they appear contradictory, are consistent with previously published reports of HSP90 inhibitors [147, 207]. In addition, up-regulation of HSP70 was also seen in myeloma cells treated with the HSP90 inhibitor (NVP-AUY922), which showed signs of apoptosis [205, 206]. This contradiction could be explained by suggesting that the pro-apoptotic effect induced by the cleavage of Casp3, PARP and p53 proteins and other possible signalling pathways involved in HSP90 inhibition, apparently prevails over the anti-apoptotic effect induced by the increase of HSP70. As such, the pro-apoptotic effect of HSP90 inhibition might contribute to the decrease of HepG2 tumour cell proliferation that we observed after the application of the HSP90 inhibitor.

Also, in line with our study again, previous studies have shown that inhibition of HSP90 decreases tumour proliferation [208-211]. Therefore, there are several drug candidates besides NVP-AUY922 that target HSP90 inhibition, some of them in advanced phases of clinical trials. HSP90 inhibitors have been developed to cause the eventual inactivation,

destabilization, and degradation of numerous chaperone-dependent client proteins. These drugs have shown promising anti-tumour activity in preclinical model systems [212]. The fact that HSP90 inhibitors selectively affect tumour cells over normal cells gives promise that there will be a therapeutic window upon their use [213, 214]. Although we do not know exactly which HSP90 client proteins regulated by p22phox were affected in our study, we can speculate that HIF1a, which has been identified as important HSP90 client protein [215] and which has been shown to be up-regulated by p22phox in different cell types [186], might be also the target in our study.

Interestingly, a recent study associated HSP90 and NADPH oxidase ROS production. In more detail, it was shown that pharmacological and genetic inhibition of HSP90 directly reduces NADPH oxidase derived superoxide. The explanation lies on the fact that HSP90 binds to the C-terminus of NOXes 1-3 and 5 which is necessary for superoxide production [216]. Although we did not determine ROS levels in the presence of the HSP90 inhibitor, these data suggest that HSP90 inhibitors might directly affect NADPH oxidase function, and that the subsequent decrease in ROS generation might decrease proliferation and activate an apoptotic program.

Taken together with the results that p22phox increases HSP90 levels, these data indicate that HSP90 is an important molecule linking p22phox to increased proliferation of HepG2 cells.

5.1.5 Role of Cathepsin D in the p22phox regulated proliferation of HepG2 cells

In this study, we were able to provide a novel functional link between p22phox and Cathepsin D. We showed that p22phox modulates Cathepsin D at both mRNA and protein expression level in HepG2 cells. Over-expressing p22phox induced expression of Cathepsin D and demonstrated elevated levels of the secreted form of Cathepsin D.

Our results demonstrated a clear association of Cathepsin D levels with p22phox levels in a ROS dependent way. Staining for Cathepsin D in tissue sections derived from a mouse xenograft model established with p22phox deficient HepG2 cells, showed decreased Cathepsin D levels further validating the *in vitro* results (Figure 47). Moreover, the results showed that silencing p22phox not only decreases Cathepsin D expression, but also influences Cathepsin D localization (Figures 38, 47). Indeed, p22phox over-expression resulted in a higher number of vesicles localized to the membrane indicating a higher secretion of Cathepsin D (Figure 38). We see that in p22phox over-expressing cells there might be an increased number

of vesicular structures containing Cathepsin D. Together with our findings that Cathepsin D levels in the supernatant were increased in p22phox overexpressing cells, these findings suggest that p22phox stimulates the secretion of Cathepsin D.

This goes in line with reports from literature [40] where increased ROS production is associated with increased Cathepsin D expression. Moreover, the staining patterns on both immunofluorescence and immunohistochemistry data (Figures 38, 47) show that upon silencing p22phox, Cathepsin D levels are reduced. The localization can only be clearly evident in the immunofluorescence data (Figure 38) where the few observed vesicles seem to be localized intracellularly. In the immunohistochemistry data (Figure 47) we can only clearly see that Cathepsin D levels are lower in silenced p22phox xenografts and that Cathepsin D is not localized in the nucleus. It is difficult to distinguish cytosol and extracellular space due to the small and densely packed tumour cells.

In addition, by silencing Cathepsin D, we showed that p22phox induced proliferation in HepG2 cells was reduced. Also, another study showed that increased levels of extra-cellular Cathepsin D act as a mitogenic factor promoting tumour proliferation [149], a fact which is in line with our results of increased extracellular Cathepsin D levels modulating proliferation in HepG2 cells. Our results further showed that p22phox is homogeneously distributed inside the cell, indicative of an association with the Endoplasmic Reticulum (ER) (Figure 38). Cathepsin D on the other hand seems to be localized in a punctuate manner inside the cell, highlighting its potential association with lysosomes. These results are in line with the literature in which the localization of Cathepsin D within acidic compartments of lysosomes, pre-lysosomal and endosomal vesicles has been well described [40].

Moreover, a recent study associated thrombin with Cathepsin D in regard to angiogenesis, tumour growth and metastasis in breast cancer cells and five additional types of cancer cells and HUVEC cells. It was shown that over-expressed Cathepsin D enhanced angiogenesis as well as tumour growth and metastasis [161]. In support, we could show that thrombin induced tumour cell proliferation in HepG2 wild type cells. In contrast, silencing Cathepsin D in HepG2 cells and pepstatin A treatment of p22phox over-expressing HepG2 cells led to reduction of tumour cell proliferation. Although we did not examine the levels of p22phox induced by thrombin in HepG2 cells, we have previously shown in our lab that thrombin increases p22phox expression and function in vascular cells [160], concomitant with increased proliferation and angiogenesis [149]. One might thus speculate that thrombin induces

p22phox levels in HepG2 cells subsequently increases Cathepsin D levels and HepG2 proliferation.

It should be noted however that studies dealing with the diagnostic and prognostic value of Cathepsin D in cancer are complicated, by the fact that there are several forms of Cathepsin D in a cell at the same time: pro-Cathepsin D, intermediate enzymatically active Cathepsin D and mature heavy and light chain Cathepsin D. Also, since different methodologies have been used for pro-Cathepsin D/Cathepsin D quantification, and Cathepsin D has been assessed in both intra-cellular and extra-cellular compartments, conflicting results were made available in the literature [151].

A study of interest associated Cathepsin D and ROS by showing that Cathepsin D induces ROS mediated apoptosis via cleavage of thioredoxin, a protein similar to glutaredoxin-3 found in our proteomic analysis. In contrast to our results, here a pro-apoptotic action of Cathepsin D was observed, however, only intracellular Cathepsin D levels were investigated and not extracellular Cathepsin D levels which exhibit proliferative action [159]. In addition, the differences could be further explained by the used model system. In contrast to our study, endothelial cells and not cancer cells were used. These findings clearly indicate that the function of Cathepsin D is strongly dependent of the cellular environment and whether intra- or extra-cellular Cathepsin D is investigated, as it was previously pointed out.

Regarding future perspectives based on the findings of the present study, we recommend additional studies on different tumour cell lines. In a large number of clinical studies, the association of Cathepsin D with tumour size, tumour grade, tumour aggressiveness, incidence of metastasis, prognosis, and a degree of chemoresistance in variety of solid tumours including neuroblastoma, glioma, melanoma, endometrial and ovarian tumours, colorectal carcinoma, head and neck tumours, thyroid tumours, pancreatic tumours, lung carcinoma, liver tumours, bladder carcinoma, prostate tumours and gastric carcinoma has been reported [153, 217-221]. In particular, regarding the association of Cathepsin D in liver cancer, increased Cathepsin D activity levels have been observed in human hepatoma tissues as compared to its normal counterparts [153]. Other experimental data indicated that Cathepsin D, in concert with other proteolytic enzymes, could be involved in the process of tissue remodeling which occurs during the evolution of cirrhosis [151]. Notably, the majority of dedicated clinical studies for Cathepsin D demonstrated the important role of this protease as a tumour biomarker with poor prognostic value in the case of breast cancer [222]. Cathepsin D is

overexpressed and secreted at high levels by human epithelial breast cancer cells and stimulates cancer cell proliferation, fibroblast outgrowth, angiogenesis and metastasis [154, 219, 220, 223]. Therefore, based on our results by investigating the role of Cathepsin D in a liver cancer cell line, it would be of great interest to carry out further research using different cancer cell lines such as MCF-7 breast cancer cells.

Moreover, it has been reported that expression levels of p22phox and endogenous ROS are upregulated in prostate carcinoma. Elevated p22phox expression promotes prostate cancer cell proliferation, tumour growth and tumour angiogenesis through Akt/ERK/HIF/VEGF signaling pathways [55]. These results, which are supported by the present findings, implicate that the modulation of action of p22phox may act as a potential new therapeutic strategy for treatment of different types of cancer in the future. The identification of the ROS-driven phenotype by p22phox in tumour pathology could entail valuable clinical applications.

Taken together, based on the interesting cross-talk between p22phox and Cathepsin D which was identified in liver cancer cells, we could suggest further studies aiming to demonstrate the value of these two proteins as potential cancer biomarkers and targets for therapeutic interventions. So far, a large number of molecular markers has been identified and evaluated in a variety of different cancers. Often, the same markers have been used for more than one type of cancers indicating the current lack of specificity of these markers. Although some markers have shown promising clinical diagnostic and prognostic value of disease progression, very few have been fully validated for assessing clinical patients' outcome in large and well characterized populations. Such an example is serum PSA for monitoring men with prostate cancer [224]. Therefore, not a single marker but rather a combination of different markers will be more effective in cancer diagnosis or prognosis. To this end, in order to enable a potential use of p22phox and Cathepsin D as clinical biomarkers, first a detailed planning of clinical studies would be required. For achieving clinical use of cancer candidate-markers, it is a prerequisite apart from a tumour mechanistic relevance incidence, to analyze and demonstrate their value according to particular types of tumour. A clinically useful molecular marker should have high sensitivity and specificity [224]. Thus, evaluation of the clinical role of p22phox and Cathepsin D cross-talk in samples from breast cancer patients, could provide us with insightful data leading to the development of a strong evidence-based panel of markers. Consequently, this could be a more adequate strategy to monitor breast cancer patients.

In conclusion, to best of our knowledge, there are no available data in the literature up to present date showing a direct correlation between p22phox and Cathepsin D. Therefore, the study identified a novel and important functional link in cellular signaling. Without doubt, further investigation should be promoted to enhance understanding in the mechanistic pathways underlying p22phox mediated ROS signaling in tumour progression via Cathepsin D.

5.1.6 Limitations of the study

The present study has revealed very interesting results as described previously. Nevertheless, there have been some limitations worth outlining them, too.

First of all, a limitation that has to be pointed out is that HepG2 cells have been used exclusively in this study. To extend the pathophysiological relevance of these observations, thus, further research is suggested upon our findings using different types of cancer cells.

Moreover, the availability of a limited number of clones in the established cellular model systems of HepG2 cells consisted a limitation to the study [225]. Particularly, in the case of stably transfected HepG2 cells with reduced levels of p22phox, it was made difficult to implement a statistically strong design for a proteomic analysis as it has been the case for the p22phox over-expressing HepG2 cells. Additionally, in the case of the stably transfected HepG2 cells with enhanced levels of p22phox, even though there have been available two control and two p22phox over-expressing clones, we observed that the clones were growing irregularly, thus making it difficult to achieve always the sufficient number of cells for experiments. As a result, only two representative clones (one control and one p22phox over-expressing clone) have been incorporated in all corresponding experiments of the study. One could speculate that the limited number of p22phox deficient clones is a result of the reduced ROS generation. Clones with much stronger reduction in p22phox levels and thus, reduced ROS levels, would have not survived the selection process - only clones with a moderate reduction of p22phox levels and thus, remaining basal levels of ROS, sufficient to allow proliferation might have survived. In general, conducting research with genetically modified cells especially with integrated transgenic DNA is challenging as one can never exclude side effects due to the integrating site of the transgenic DNA [226]. To exclude these effects, other model systems may be used to verify our findings including transgenic animals and transient transfection as a method for over-expressing or silencing the target gene.

Regarding the gel based proteomic analysis of the study, due to technical challenges known to be involved in the reproducibility of 2-DE gels in the basic area of pH [227], we selected to perform the 2-DE analysis and validate corresponding results using only immobilized pH gradient (IPG) strips at the acidic area of pH.

Last, in the present study, we decided to investigate the role of the protease Cathepsin D in the p22phox mediated tumour progression. The results revealed the identification of an interesting functional link. However, taking into account the complexity of the Cathepsin D, further investigation is recommended. It has been reported that different studies focused on Cathepsin D so far, entail inconsistencies due to the limitations of identifying all existing different isoforms of the protease detected in both intracellular and extracellular environment of diverse tumour cells [159]. Also, analysis of the Cathepsin D secretion levels are challenging in the used model system of our study, as the over-expression of p22phox is permanent in the stably transfected HepG2 cells. An inducible p22phox over-expressing system would be of interest to further investigate the link between p22phox and Cathepsin D.

In conclusion, despite the limitations of this study, the provided data show novel interesting insights in the intracellular pathways regulated by p22phox derived ROS.

Chapter 6: Summary

6.1 Summary

The overall aim of the present thesis has been to enhance the understanding of the functional role of the NADPH oxidase subunit p22phox mediated reactive oxygen species (ROS) in tumour progression by employing a combination of proteomics, *in silico*, *in vitro* and *in vivo* tools. Liver cancer was selected as the model system to investigate tumour progression, particularly genetically modified hepatoblastoma (HepG2) cells. Therefore, the primary objective was to assess cellular model systems available in our laboratory. Clones of stably transfected HepG2 cells with enhanced and reduced levels of p22phox were validated in regard to protein expression, gene regulation and ROS production.

In a next step, we employed a gel based proteomic platform (2-DE) as a protein expression profiling method which allowed us to screen and identify differentially expressed proteins at a global cellular level, due to enhanced levels of p22phox. Subsequently, we assessed the relevance of the identified protein species to tumour progression and correlated them with existing literature data. Bioinformatics tools were used in order to facilitate this last objective. After a successful proteomic analysis and *in silico* pathway analysis, the association of p22phox to cancer signaling pathways and other protein species of interest such as the heat shock protein 90 (HSP90) became clear. In order to test the validity of the findings, we employed an array of *in vitro* assays evaluating the role of p22phox in tumour cell proliferation and survival ability. Particular focus was given on HSP90 functional correlation to p22phox and the results indeed revealed that HSP90 inhibition in p22phox over-expressing HepG2 cells reduces tumour proliferation via apoptosis.

In addition, the study's findings were further validated by showing not only *in vitro*, but also *in vivo* that p22phox protein modulates tumour progression. In a mouse xenograft model, depletion of p22phox in HepG2 cells resulted in diminished tumour growth. Finally, incorporation of Cathepsin D, an important tumour biomarker, in the experimental set-ups showed that a potential signaling pathway in regard to tumour progression is due to the interaction of p22phox mediated ROS and Cathepsin D.

In conclusion, the findings of the present study come to underline the biologically significant role of the NADPH oxidase p22phox protein in tumour progression via ROS signaling both *in vitro* and *in vivo*. We suggest that inhibition of p22phox could be a potential new therapeutic strategy for cancer treatments in the future.

Appendix 1: Acknowledgements

Acknowledgements

The present doctoral dissertation was carried out at the German Heart Center Munich in the framework of the Ph.D. program: “Medical Life Science and Technology”, Faculty of Medicine, Technical University of Munich (TUM).

Initially, I would like to express my acknowledgements and deep appreciation to the research and academic hosts of my thesis:

My Ph.D. advisor, Prof. Agnes Görlach, gave me the opportunity to carry out my thesis as a member of her team that focuses on biomedical research in the fields of cardiology and oncology. She provided me with valuable guidance throughout my thesis project and promoted my exposure to additional expert labs of molecular medicine and proteomics. Without doubt, she helped me substantially to broaden my scientific scope and competences. Her limitless energy and enthusiasm for the research lines that she follows, worked as an example for conducting my research, too.

My two Ph.D. committee mentors, Prof. Gabriele Multhoff and Prof. Manfred Schmitt, both experts in cancer research based at the TUM University Hospital “Klinikum rechts der Isar”, shared generously their long lasting experience in a very friendly and efficient way. Their counselling contributed to the directions I chose to follow during my thesis and their suggestions and support verified my confidence to pursue my ideas and plans.

All the colleagues at the German Heart Center, particularly the present and past members of my department, helped me to fulfil the aims of my thesis and converted my working space into a welcoming, pleasant and creative environment. Especially, I would like to express my thankfulness for two close colleagues of mine: Dr. Andreas Petry stood by me in an invaluable manner throughout the whole duration of my thesis. I have always relied on his help, guidance, support and availability as well as I have incredibly enjoyed our long “troubleshooting” dialogues. Also, it was a pleasure and honour to work with Dr. Zuwen Zhang. Apart from receiving Zuwen’s help and guidance in my thesis, I have shared with him several times my problems, thoughts and plans for issues which exceeded the limits of our working relationship and I have always received his genuine interest and support. Thus, I identify him now apart from a great colleague, as a precious friend, too.

The head of the coordination office of the Ph.D. program “Medical Life Science and Technology”, Dr. Katrin Offe, has helped me with unparalleled motivation via her position and responsibilities to accomplish my thesis in the framework of the Ph.D. program. Furthermore, during her lectures and our discussions, I have learnt a lot based on the uniquely balanced combination of scientific experience and sense of professionalism that was transmitted to me by her.

Additionally, I would like to express the following acknowledgements and thoughts:

Taking profit of the privileges that the European Union offers to its citizens, I got the chance besides the country of my origin, to live either for studies or work in seven additional Member States. I feel now blessed for the experience I acquired but mostly for all the remarkable friends and colleagues I gained from each country during this route. Their help, trust, advice and support follow always my thoughts having undoubtedly a major impact towards the conclusion of my thesis ...and not only: these are also a great asset into my overall evolution as a scientist, human being, citizen and professional.

My family, by providing me always with unconditional love and support, helps me beyond any expectation in every single step I do. I learn through their example and they are for me a “constant” in a world full of variables. I am grateful to have them by my side.

Finally, I would like to state my enthusiasm coming with the conclusion of my Ph.D. thesis. This is due to the fact that on the one hand, I judge my Ph.D. as a landmark in my scientific maturation and overall career progression. On the other hand, the years of the dissertation have been for me a very meaningful “journey of knowledge” which, despite all difficulties, based on motivation and persistence, was claimed and fulfilled in the way that I was dreaming.

I sincerely hope for the utility of this work,

Ioannis Vouldis

Appendix 2: Index of figures and tables

Index of figures

Figure 1: Presentation of the hallmarks of cancer	6
Figure 2: Cascade of reactions involving ROS generation	9
Figure 3: Locations of NOX proteins in the human body	11
Figure 4: Subunit composition of the seven mammalian NADPH oxidase isoforms	12
Figure 5: Schematic overview of the structure and activation of the phagocytic NADPH oxidase	14
Figure 6: Integration of NOX oxidase-derived ROS with the hallmarks of cancer	16
Figure 7: A hypothesis for the function of NOX-derived ROS in the progression of carcinogenesis	17
Figure 8: Proteomic technology applied to cancer-patient management	20
Figure 9: Applications of proteomic technologies	21
Figure 10: Principle of the DHE assay for the measurement of ROS	33
Figure 11: Principle of the Alamar Blue metabolic activity assay	35
Figure 12: Schematic overview of the immunofluorescence assay and fluorescence microscope	37
Figure 13: Schematic overview of the polymerase chain reaction (PCR)	40
Figure 14: Diagram depicting major experimental stages in a xenograft mouse model	43
Figure 15: Schematic overview of the western blot analysis	46
Figure 16: Schematic overview of the proteomic analysis employed in the present study	48
Figure 17: Schematic overview of the 2-DE image analysis	55
Figure 18: Western blot analysis of p22phox modified HepG2 cells	61
Figure 19: Quantitative PCR analysis of p22phox modified HepG2 cells	62
Figure 20: Immunofluorescence analysis of p22phox modified HepG2 cells	62
Figure 21: p22phox modulates ROS generation in HepG2 cells	63
Figure 22: p22phox modulates proliferation of HepG2 cells	64
Figure 23: Expression of proliferation marker Ki-67 in p22phox modified HepG2 cells	65
Figure 24: p22phox modulates the metabolic activity of HepG2 cells	65
Figure 25: p22phox mediated metabolic activity is ROS dependent	66
Figure 26: p22phox modulates the ability of HepG2 cells to form colonies	67
Figure 27: p22phox modulates tumour growth in a xenograft mouse model	68
Figure 28: Proliferation and apoptosis are modulated in p22phox depleted HepG2 xenografts	69
Figure 29: Proteins differentially expressed in control versus p22phox over-expressing HepG2 cells	71
Figure 30: Validation by Western blot of selected proteins identified as differentially expressed in p22phox over-expressing HepG2 cells	73
Figure 31: Protein interaction network revealed by IPA software analysis	74
Figure 32: Inhibition of HSP90 affects expression of HSP70 and HSP27 in HepG2 cells	76
Figure 33: HSP90 inhibition modulates the p22phox mediated expression of proliferation marker Ki-67	77
Figure 34: HSP90 inhibition diminishes clonogenic activity in HepG2 cells	77
Figure 35: HSP90 inhibition increases apoptosis marker levels in HepG2 cells	78

Figure 36: Cathepsin D expression levels in p22phox modified HepG2 cells	79
Figure 37: p22phox mediates Cathepsin D expression via ROS	80
Figure 38: p22phox modulates Cathepsin D localization	81
Figure 39: p22phox modulates secretion of Cathepsin D	81
Figure 40: p22phox modulates lysosomal processing of Cathepsin D	82
Figure 41: Silencing Cathepsin D reduces HepG2 proliferation	83
Figure 42: Thrombin induces Cathepsin D expression and proliferation in HepG2 cells	84
Figure 43: Silencing Cathepsin D in p22phox over-expressing HepG2 cells	85
Figure 44: Silencing of Cathepsin D reduces p22phox mediated staining for Ki-67	86
Figure 45: Cathepsin D modulates the ability of p22phox in HepG2 cells to form colonies	87
Figure 46: Cathepsin D inhibition with Pepstatin A reduces cellular metabolic activity	88
Figure 47: IHC analysis of xenograft mouse sections targeting Cathepsin D	89

Index of tables

Table 1: Selected ROS mediated diseases	10
Table 2: Tissue expression of the NOX proteins	11
Table 3: Mammalian cell lines	26
Table 4: Cell culture media and reagents	26
Table 5: siRNA targets	26
Table 6: Primers used in qPCR	26
Table 7: Kits	26
Table 8: Primary antibodies used in IF/IHC	27
Table 9: Secondary antibodies used in IF/IHC	27
Table 10: Staining probes used in fluorescence microscopy	27
Table 11: Equipment used in cellular and molecular biology methods	27
Table 12: Reagents used in cellular and molecular biology methods	27
Table 13: Primary antibodies used in Western blot analysis	28
Table 14: Secondary antibodies used in Western blot analysis	28
Table 15: Equipment used in 2-DE and Western blot analyses	28
Table 16: Chemical solvents and reagents	28
Table 17: Reagents used in in 2-DE and Western blot analyses	29
Table 18: General equipment and device	29
Table 19: Animals used in the xenograft model	30
Table 20: Software	30
Table 21: Databases	30
Table 22: Composition of RT-PCR master mix solutions	41
Table 23: Composition of laemmlie lysis buffer	44

Table 24: Preparation of stacking and running gels used in Western blot method	46
Table 25: Composition of running and transfer buffers	47
Table 26: Composition of TBS-T buffer	47
Table 27: Composition of enhanced chemi-luminescent (ECL) reagents type 1 and 2	47
Table 28: Composition of the tris-sucrose wash buffer	49
Table 29: Composition of the lysis buffer used in 2-DE	49
Table 30: Composition of the rehydration buffer solution	50
Table 31: IEF running conditions	51
Table 32: Composition of the equilibration buffer	51
Table 33: Composition of the 2-DE gels	52
Table 34: Composition of the 2-DE anode and cathode buffers	53
Table 35: SDS-PAGE running conditions	53
Table 36: Protocol used in the RuBPS staining of 2-DE gels	54
Table 37: Protocol used in the silver staining of 2-DE gels	54
Table 38: Protocol used in the de-staining and dehydration of excised protein spots	57
Table 39: Protocol used in the reduction and alkylation of excised protein spots	57
Table 40: Protein functions differentially expressed in p22phox over-expressing HepG2 cells	72
Table 41: Top diseases and disorders given by IPA	75
Table 42: Top molecular and cellular functions given by IPA	75
Table 43: Top canonical pathways given by IPA	75
Table 44: Top toxicity lists given by IPA	75

Appendix 3: References

References

1. Boyle, P., Levin, B., *World Cancer Report 2008*. 2008, IARC.
2. Fritz A, et al., *International Classification of Diseases for Oncology*. third edition ed. 2000: World Health Organization.
3. Birch, J.M. and H.B. Marsden, *A classification scheme for childhood cancer*. *Int J Cancer*, 1987. **40**(5): p. 620-4.
4. Golub, T.R., et al., *Molecular classification of cancer: class discovery and class prediction by gene expression monitoring*. *Science*, 1999. **286**(5439): p. 531-7.
5. Tomatis, L. and A. Aitton, *Cancer, causes, occurrence, and control*. 1990, International Agency for Research on Cancer (Lyon and New York). p. xvi, 352.
6. Turner, N., A. Tutt, and A. Ashworth, *Hallmarks of 'BRCAness' in sporadic cancers*. *Nat Rev Cancer*, 2004. **4**(10): p. 814-9.
7. Liu, B., et al., *Mismatch repair gene defects in sporadic colorectal cancers with microsatellite instability*. *Nat Genet*, 1995. **9**(1): p. 48-55.
8. Weinberg, R.A., *How cancer arises*. *Sci Am*, 1996. **275**(3): p. 62-70.
9. *NCI Dictionary of Cancer Terms*. Available from: <http://www.cancer.gov/dictionary>.
10. *Glossary of Cancer Research Terms*. Available from: <http://www.aacr.org/>.
11. Hanahan, D. and R.A. Weinberg, *The hallmarks of cancer*. *Cell*, 2000. **100**(1): p. 57-70.
12. Hanahan, D. and R.A. Weinberg, *Hallmarks of cancer: the next generation*. *Cell*, 2011. **144**(5): p. 646-74.
13. Negrini, S., V.G. Gorgoulis, and T.D. Halazonetis, *Genomic instability--an evolving hallmark of cancer*. *Nat Rev Mol Cell Biol*, 2010. **11**(3): p. 220-8.
14. Brieger, K., et al., *Reactive oxygen species: from health to disease*. *Swiss Med Wkly*, 2012. **142**: p. w13659.
15. Fruehauf, J.P. and F.L. Meyskens, Jr., *Reactive oxygen species: a breath of life or death?* *Clin Cancer Res*, 2007. **13**(3): p. 789-94.
16. Nathan, C. and A. Cunningham-Bussel, *Beyond oxidative stress: an immunologist's guide to reactive oxygen species*. *Nat Rev Immunol*, 2013. **13**(5): p. 349-61.
17. Paravicini, T.M. and R.M. Touyz, *NADPH oxidases, reactive oxygen species, and hypertension: clinical implications and therapeutic possibilities*. *Diabetes Care*, 2008. **31 Suppl 2**: p. S170-80.
18. Kolarova, H., et al., *The expression of NADPH oxidases and production of reactive oxygen species by human lung adenocarcinoma epithelial cell line A549*. *Folia Biol (Praha)*, 2010. **56**(5): p. 211-7.
19. Seno, T., et al., *Involvement of NADH/NADPH oxidase in human platelet ROS production*. *Thromb Res*, 2001. **103**(5): p. 399-409.
20. Jiang, F., Y. Zhang, and G.J. Dusting, *NADPH oxidase-mediated redox signaling: roles in cellular stress response, stress tolerance, and tissue repair*. *Pharmacol Rev*, 2011. **63**(1): p. 218-42.
21. Bae, Y.S., et al., *Regulation of reactive oxygen species generation in cell signaling*. *Mol Cells*, 2011. **32**(6): p. 491-509.
22. Lambeth, J.D., *NOX enzymes and the biology of reactive oxygen*. *Nat Rev Immunol*, 2004. **4**(3): p. 181-9.
23. Dickinson, B.C. and C.J. Chang, *Chemistry and biology of reactive oxygen species in signaling or stress responses*. *Nat Chem Biol*, 2011. **7**(8): p. 504-11.
24. Rahman, K., *Studies on free radicals, antioxidants, and co-factors*. *Clin Interv Aging*, 2007. **2**(2): p. 219-36.
25. Datta, K., S. Sinha, and P. Chattopadhyay, *Reactive oxygen species in health and disease*. *Natl Med J India*, 2000. **13**(6): p. 304-10.
26. Waris, G. and H. Ahsan, *Reactive oxygen species: role in the development of cancer and various chronic conditions*. *J Carcinog*, 2006. **5**: p. 14.
27. Chopra, A., et al., *Apoptotic protein expression, glycogen content, DNA ploidy and cell proliferation in hepatoblastoma subtyping and their role in prognostication*. *Pediatric Surgery International*, 2010. **26**(12): p. 1173-1178.
28. Bedard, K. and K.-H. Krause, *The NOX family of ROS-generating NADPH oxidases: Physiology and pathophysiology*. *Physiological Reviews*, 2007. **87**(1): p. 245-313.
29. Babior, B.M., *NADPH oxidase*. *Curr Opin Immunol*, 2004. **16**(1): p. 42-7.
30. Babior, B.M., J.D. Lambeth, and W. Nauseef, *The neutrophil NADPH oxidase*. *Arch Biochem Biophys*, 2002. **397**(2): p. 342-4.

31. Brown, D.I. and K.K. Griendling, *Nox proteins in signal transduction*. Free Radic Biol Med, 2009. **47**(9): p. 1239-53.
32. Quinn, M.T., M.C. Ammons, and F.R. Deleo, *The expanding role of NADPH oxidases in health and disease: no longer just agents of death and destruction*. Clin Sci (Lond), 2006. **111**(1): p. 1-20.
33. Drummond, G.R., et al., *Combating oxidative stress in vascular disease: NADPH oxidases as therapeutic targets*. Nat Rev Drug Discov, 2011. **10**(6): p. 453-71.
34. Rivera, J., et al., *Nox isoforms in vascular pathophysiology: insights from transgenic and knockout mouse models*. Redox Rep, 2010. **15**(2): p. 50-63.
35. Nauseef, W.M., *Assembly of the phagocyte NADPH oxidase*. Histochem Cell Biol, 2004. **122**(4): p. 277-91.
36. Geiszt, M. and T.L. Leto, *The Nox family of NAD(P)H oxidases: host defense and beyond*. J Biol Chem, 2004. **279**(50): p. 51715-8.
37. El-Benna, J., et al., *Phagocyte NADPH oxidase: a multicomponent enzyme essential for host defenses*. Arch Immunol Ther Exp (Warsz), 2005. **53**(3): p. 199-206.
38. Dinauer, M.C., *Regulation of neutrophil function by Rac GTPases*. Curr Opin Hematol, 2003. **10**(1): p. 8-15.
39. Price, M.O., et al., *Rac activation induces NADPH oxidase activity in transgenic COSphox cells, and the level of superoxide production is exchange factor-dependent*. J Biol Chem, 2002. **277**(21): p. 19220-8.
40. Rada, B. and T.L. Leto, *Oxidative innate immune defenses by Nox/Duox family NADPH oxidases*. Contrib Microbiol, 2008. **15**: p. 164-87.
41. Parkos, C.A., et al., *Primary structure and unique expression of the 22-kilodalton light chain of human neutrophil cytochrome b*. Proc Natl Acad Sci U S A, 1988. **85**(10): p. 3319-23.
42. Quinn, M.T., et al., *Reconstitution of defective respiratory burst activity with partially purified human neutrophil cytochrome B in two genetic forms of chronic granulomatous disease: possible role of Rap1A*. Blood, 1992. **79**(9): p. 2438-45.
43. Zalba, G., et al., *NADPH oxidase-mediated oxidative stress: genetic studies of the p22(phox) gene in hypertension*. Antioxid Redox Signal, 2005. **7**(9-10): p. 1327-36.
44. Cai, H., K.K. Griendling, and D.G. Harrison, *The vascular NAD(P)H oxidases as therapeutic targets in cardiovascular diseases*. Trends Pharmacol Sci, 2003. **24**(9): p. 471-8.
45. Brennan, L.A., et al., *Increased superoxide generation is associated with pulmonary hypertension in fetal lambs: a role for NADPH oxidase*. Circ Res, 2003. **92**(6): p. 683-91.
46. Guzik, T.J., et al., *Systemic regulation of vascular NAD(P)H oxidase activity and nox isoform expression in human arteries and veins*. Arterioscler Thromb Vasc Biol, 2004. **24**(9): p. 1614-20.
47. Miller, F.J., Jr., et al., *Superoxide production in vascular smooth muscle contributes to oxidative stress and impaired relaxation in atherosclerosis*. Circ Res, 1998. **82**(12): p. 1298-305.
48. Heymes, C., et al., *Increased myocardial NADPH oxidase activity in human heart failure*. J Am Coll Cardiol, 2003. **41**(12): p. 2164-71.
49. Liou, G.Y. and P. Storz, *Reactive oxygen species in cancer*. Free Radic Res, 2010. **44**(5): p. 479-96.
50. Newburger, P.E., et al., *Development of the superoxide-generating system during differentiation of the HL-60 human promyelocytic leukemia cell line*. J Biol Chem, 1984. **259**(6): p. 3771-6.
51. Gorch, A., et al., *Photometric characteristics of haem proteins in erythropoietin-producing hepatoma cells (HepG2)*. Biochem J, 1993. **290** (Pt 3): p. 771-6.
52. Li, Y. and M.A. Trush, *Diphenyleneiodonium, an NAD(P)H oxidase inhibitor, also potently inhibits mitochondrial reactive oxygen species production*. Biochem Biophys Res Commun, 1998. **253**(2): p. 295-9.
53. Brar, S.S., et al., *An NAD(P)H oxidase regulates growth and transcription in melanoma cells*. American Journal of Physiology-Cell Physiology, 2002. **282**(6): p. C1212-C1224.
54. Block, K. and Y. Gorin, *Aiding and abetting roles of NOX oxidases in cellular transformation*. Nat Rev Cancer, 2012. **12**(9): p. 627-37.
55. Li, Q., et al., *NADPH oxidase subunit p22(phox)-mediated reactive oxygen species contribute to angiogenesis and tumor growth through AKT and ERK1/2 signaling pathways in prostate cancer*. Biochim Biophys Acta, 2013. **1833**(12): p. 3375-85.
56. Lassegue, B., A. San Martin, and K.K. Griendling, *Biochemistry, physiology, and pathophysiology of NADPH oxidases in the cardiovascular system*. Circ Res, 2012. **110**(10): p. 1364-90.
57. Hayaishi-Okano, R., et al., *Association of NAD(P)H oxidase p22 phox gene variation with advanced carotid atherosclerosis in Japanese type 2 diabetes*. Diabetes Care, 2003. **26**(2): p. 458-63.
58. Oberley, L.W., T.D. Oberley, and G.R. Buettner, *Cell division in normal and transformed cells: the possible role of superoxide and hydrogen peroxide*. Med Hypotheses, 1981. **7**(1): p. 21-42.

59. Pham-Huy, L.A., H. He, and C. Pham-Huy, *Free radicals, antioxidants in disease and health*. Int J Biomed Sci, 2008. **4**(2): p. 89-96.
60. Hussain, S.P., L.J. Hofseth, and C.C. Harris, *Radical causes of cancer*. Nat Rev Cancer, 2003. **3**(4): p. 276-85.
61. Gupta, S.C., et al., *Upsides and downsides of reactive oxygen species for cancer: the roles of reactive oxygen species in tumorigenesis, prevention, and therapy*. Antioxid Redox Signal, 2012. **16**(11): p. 1295-322.
62. Huber, L.A., *Is proteomics heading in the wrong direction?* Nat Rev Mol Cell Biol, 2003. **4**(1): p. 74-80.
63. Cox, J. and M. Mann, *Is proteomics the new genomics?* Cell, 2007. **130**(3): p. 395-8.
64. Farrah, T., et al., *The state of the human proteome in 2012 as viewed through PeptideAtlas*. J Proteome Res, 2013. **12**(1): p. 162-71.
65. Tyers, M. and M. Mann, *From genomics to proteomics*. Nature, 2003. **422**(6928): p. 193-7.
66. Liotta, L.A., E.C. Kohn, and E.F. Petricoin, *Clinical proteomics: personalized molecular medicine*. JAMA, 2001. **286**(18): p. 2211-4.
67. Ardekani, A.M., L.A. Liotta, and E.F. Petricoin, 3rd, *Clinical potential of proteomics in the diagnosis of ovarian cancer*. Expert Rev Mol Diagn, 2002. **2**(4): p. 312-20.
68. Calvo, K.R., L.A. Liotta, and E.F. Petricoin, *Clinical proteomics: from biomarker discovery and cell signaling profiles to individualized personal therapy*. Biosci Rep, 2005. **25**(1-2): p. 107-25.
69. Krieg, R.C., et al., *Clinical proteomics for cancer biomarker discovery and therapeutic targeting*. Technol Cancer Res Treat, 2002. **1**(4): p. 263-72.
70. Meani, F., et al., *Clinical application of proteomics in ovarian cancer prevention and treatment*. Mol Diagn Ther, 2009. **13**(5): p. 297-311.
71. Petricoin, E.F., et al., *Clinical proteomics: translating benchside promise into bedside reality*. Nat Rev Drug Discov, 2002. **1**(9): p. 683-95.
72. Mallick, P. and B. Kuster, *Proteomics: a pragmatic perspective*. Nat Biotechnol, 2010. **28**(7): p. 695-709.
73. Schirle, M., M. Bantscheff, and B. Kuster, *Mass spectrometry-based proteomics in preclinical drug discovery*. Chem Biol, 2012. **19**(1): p. 72-84.
74. Gorg, A., *Two-dimensional electrophoresis with immobilized pH gradients: current state*. Biochem Soc Trans, 1993. **21**(1): p. 130-2.
75. Gorg, A., et al., *Two-dimensional polyacrylamide gel electrophoresis with immobilized pH gradients in the first dimension (IPG-Dalt): the state of the art and the controversy of vertical versus horizontal systems*. Electrophoresis, 1995. **16**(7): p. 1079-86.
76. Gorg, A., et al., *Two-dimensional electrophoresis of proteins in an immobilized pH 4-12 gradient*. Electrophoresis, 1998. **19**(8-9): p. 1516-9.
77. Gorg, A., et al., *The current state of two-dimensional electrophoresis with immobilized pH gradients*. Electrophoresis, 2000. **21**(6): p. 1037-53.
78. Bjellqvist, B., et al., *Isoelectric focusing in immobilized pH gradients: principle, methodology and some applications*. J Biochem Biophys Methods, 1982. **6**(4): p. 317-39.
79. Westermeier, R., et al., *High-resolution two-dimensional electrophoresis with isoelectric focusing in immobilized pH gradients*. J Biochem Biophys Methods, 1983. **8**(4): p. 321-30.
80. Raymond, S. and B. Aurell, *Two-Dimensional Gel Electrophoresis*. Science, 1962. **138**(3537): p. 152-3.
81. O'Farrell, P.H., *High resolution two-dimensional electrophoresis of proteins*. J Biol Chem, 1975. **250**(10): p. 4007-21.
82. Rabilloud, T., *Two-dimensional gel electrophoresis in proteomics: old, old fashioned, but it still climbs up the mountains*. Proteomics, 2002. **2**(1): p. 3-10.
83. Lopez-Terrada, D., et al., *Hep G2 is a hepatoblastoma-derived cell line*. Hum Pathol, 2009. **40**(10): p. 1512-5.
84. Alberts B, et al., in *Molecular Biology of the Cell*. 2002, Garland Science: New York.
85. Hu, W.S., et al., *Effect of glucose on the cultivation of mammalian cells*. Dev Biol Stand, 1987. **66**: p. 279-90.
86. Giard, D.J., et al., *In vitro cultivation of human tumors: establishment of cell lines derived from a series of solid tumors*. J Natl Cancer Inst, 1973. **51**(5): p. 1417-23.
87. Burki, H.J., et al., *Inactivation of mammalian cells after disintegration of 3H or 125I in cell DNA at -196 degrees C*. Int J Radiat Biol Relat Stud Phys Chem Med, 1973. **24**(4): p. 363-75.
88. Groskreutz, D.a.S., E.T., *Reporter systems*, in *Methods in Molecular Biology*, R.Tuan, Editor. 1997, Humana Press: NJ. p. 63.
89. Gorman, C.M., D.P. Lane, and P.W. Rigby, *High efficiency gene transfer into mammalian cells*. Philos Trans R Soc Lond B Biol Sci, 1984. **307**(1132): p. 343-6.

90. Brummelkamp, T.R., R. Bernards, and R. Agami, *A system for stable expression of short interfering RNAs in mammalian cells*. *Science*, 2002. **296**(5567): p. 550-3.
91. Paddison, P.J., et al., *Short hairpin RNAs (shRNAs) induce sequence-specific silencing in mammalian cells*. *Genes Dev*, 2002. **16**(8): p. 948-58.
92. Paddison, P.J., A.A. Caudy, and G.J. Hannon, *Stable suppression of gene expression by RNAi in mammalian cells*. *Proc Natl Acad Sci U S A*, 2002. **99**(3): p. 1443-8.
93. Paddison, P.J., et al., *Short hairpin activated gene silencing in mammalian cells*. *Methods Mol Biol*, 2004. **265**: p. 85-100.
94. Sorescu, D., et al., *Superoxide production and expression of nox family proteins in human atherosclerosis*. *Circulation*, 2002. **105**(12): p. 1429-35.
95. Lim, S.D., et al., *Increased Nox1 and hydrogen peroxide in prostate cancer*. *Prostate*, 2005. **62**(2): p. 200-7.
96. Hawker, J.R., Jr., *Chemiluminescence-based BrdU ELISA to measure DNA synthesis*. *J Immunol Methods*, 2003. **274**(1-2): p. 77-82.
97. Vega-Avila, E. and M.K. Pugsley, *An overview of colorimetric assay methods used to assess survival or proliferation of mammalian cells*. *Proc West Pharmacol Soc*, 2011. **54**: p. 10-4.
98. Maghni, K., O.M. Nicolescu, and J.G. Martin, *Suitability of cell metabolic colorimetric assays for assessment of CD4+ T cell proliferation: comparison to 5-bromo-2-deoxyuridine (BrdU) ELISA*. *J Immunol Methods*, 1999. **223**(2): p. 185-94.
99. Abe, T., S. Takahashi, and Y. Fukuuchi, *Reduction of Alamar Blue, a novel redox indicator, is dependent on both the glycolytic and oxidative metabolism of glucose in rat cultured neurons*. *Neurosci Lett*, 2002. **326**(3): p. 179-82.
100. Rampersad, S.N., *Multiple applications of Alamar Blue as an indicator of metabolic function and cellular health in cell viability bioassays*. *Sensors (Basel)*, 2012. **12**(9): p. 12347-60.
101. Franken, N.A., et al., *Clonogenic assay of cells in vitro*. *Nat Protoc*, 2006. **1**(5): p. 2315-9.
102. Alberts, D.S., et al., *In-vitro clonogenic assay for predicting response of ovarian cancer to chemotherapy*. *Lancet*, 1980. **2**(8190): p. 340-2.
103. Odell, I.D. and D. Cook, *Immunofluorescence techniques*. *J Invest Dermatol*, 2013. **133**(1): p. e4.
104. Franke, W.W., et al., *Different intermediate-sized filaments distinguished by immunofluorescence microscopy*. *Proc Natl Acad Sci U S A*, 1978. **75**(10): p. 5034-8.
105. Bignami, A., et al., *Localization of the glial fibrillary acidic protein in astrocytes by immunofluorescence*. *Brain Res*, 1972. **43**(2): p. 429-35.
106. Kurki, P., K. Ogata, and E.M. Tan, *Monoclonal antibodies to proliferating cell nuclear antigen (PCNA)/cyclin as probes for proliferating cells by immunofluorescence microscopy and flow cytometry*. *J Immunol Methods*, 1988. **109**(1): p. 49-59.
107. Coons, A.H., *The development of immunohistochemistry*. *Ann N Y Acad Sci*, 1971. **177**: p. 5-9.
108. Scott, R.J., et al., *A comparison of immunohistochemical markers of cell proliferation with experimentally determined growth fraction*. *J Pathol*, 1991. **165**(2): p. 173-8.
109. Myers, T.W. and D.H. Gelfand, *Reverse transcription and DNA amplification by a *Thermus thermophilus* DNA polymerase*. *Biochemistry*, 1991. **30**(31): p. 7661-6.
110. Dieffenbach, C.W. and G.S. Dveksler, *Setting up a PCR laboratory*. *PCR Methods Appl*, 1993. **3**(2): p. S2-7.
111. Dieffenbach, C.W., T.M. Lowe, and G.S. Dveksler, *General concepts for PCR primer design*. *PCR Methods Appl*, 1993. **3**(3): p. S30-7.
112. Attatipaholkun, W.H., et al., *A novel method for the preparation of large cDNA fragments from dengue-3 RNA genome by long RT-PCR amplification*. *Southeast Asian J Trop Med Public Health*, 2000. **31 Suppl 1**: p. 126-33.
113. Ribaud, R., et al., *Preparation of RNA from tissues and cells*. *Curr Protoc Neurosci*, 2001. **Appendix 1**: p. Appendix 11.
114. Chomczynski, P. and N. Sacchi, *Single-step method of RNA isolation by acid guanidinium thiocyanate-phenol-chloroform extraction*. *Anal Biochem*, 1987. **162**(1): p. 156-9.
115. Pfaffl, M.W., *A new mathematical model for relative quantification in real-time RT-PCR*. *Nucleic Acids Res*, 2001. **29**(9): p. e45.
116. Pfaffl, M.W., G.W. Horgan, and L. Dempfle, *Relative expression software tool (REST) for group-wise comparison and statistical analysis of relative expression results in real-time PCR*. *Nucleic Acids Res*, 2002. **30**(9): p. e36.
117. Heid, C.A., et al., *Real time quantitative PCR*. *Genome Res*, 1996. **6**(10): p. 986-94.

118. Gibson, U.E., C.A. Heid, and P.M. Williams, *A novel method for real time quantitative RT-PCR*. *Genome Res*, 1996. **6**(10): p. 995-1001.
119. Sanger, F., S. Nicklen, and A.R. Coulson, *DNA sequencing with chain-terminating inhibitors*. 1977. *Biotechnology*, 1992. **24**: p. 104-8.
120. Morton, C.L. and P.J. Houghton, *Establishment of human tumor xenografts in immunodeficient mice*. *Nat Protoc*, 2007. **2**(2): p. 247-50.
121. Sausville, E.A. and A.M. Burger, *Contributions of human tumor xenografts to anticancer drug development*. *Cancer Res*, 2006. **66**(7): p. 3351-4, discussion 3354.
122. Richter, G.H., et al., *EZH2 is a mediator of EWS/FLI1 driven tumor growth and metastasis blocking endothelial and neuro-ectodermal differentiation*. *Proc Natl Acad Sci U S A*, 2009. **106**(13): p. 5324-9.
123. Giavalisco, P., et al., *Extraction of proteins from plant tissues for two-dimensional electrophoresis analysis*. *Electrophoresis*, 2003. **24**(1-2): p. 207-16.
124. Stadlmayr, G., et al., *Genome-scale analysis of library sorting (GALibSo): Isolation of secretion enhancing factors for recombinant protein production in Pichia pastoris*. *Biotechnol Bioeng*, 2010. **105**(3): p. 543-55.
125. Adolphs, K.W., et al., *Isolation of a protein scaffold from mitotic HeLa cell chromosomes*. *Proc Natl Acad Sci U S A*, 1977. **74**(11): p. 4937-41.
126. Bradford, M.M., *A rapid and sensitive method for the quantitation of microgram quantities of protein utilizing the principle of protein-dye binding*. *Anal Biochem*, 1976. **72**: p. 248-54.
127. Congdon, R.W., G.W. Muth, and A.G. Splittgerber, *The binding interaction of Coomassie blue with proteins*. *Anal Biochem*, 1993. **213**(2): p. 407-13.
128. Kurien, B.T. and R.H. Scofield, *Western blotting*. *Methods*, 2006. **38**(4): p. 283-93.
129. Han, X., A. Aslanian, and J.R. Yates, 3rd, *Mass spectrometry for proteomics*. *Curr Opin Chem Biol*, 2008. **12**(5): p. 483-90.
130. Lamanda, A., et al., *Improved Ruthenium II tris (bathophenanthroline disulfonate) staining and destaining protocol for a better signal-to-background ratio and improved baseline resolution*. *Proteomics*, 2004. **4**(3): p. 599-608.
131. Heukeshoven, J. and R. Dernick, *Improved silver staining procedure for fast staining in PhastSystem Development Unit. I. Staining of sodium dodecyl sulfate gels*. *Electrophoresis*, 1988. **9**(1): p. 28-32.
132. R-Development-Core-Team, *R: A language and environment for statistical computing*, R Foundation for Statistical Computing. 2006. Vienna, Austria, <http://www.R-project.org>.
133. Sarkar, D., *Lattice: Multivariate Data Visualization with R*. R package version 0.20-0, 2008.
134. Magdeldin, S., et al., *Basics and recent advances of two dimensional- polyacrylamide gel electrophoresis*. *Clin Proteomics*, 2014. **11**(1): p. 16.
135. Valcu, C.M., et al., *Comparative proteomic analysis of responses to pathogen infection and wounding in Fagus sylvatica*. *J Proteome Res*, 2009. **8**(8): p. 4077-91.
136. Benjamini, Y. and Y. Hochberg, *Controlling the false discovery rate: a practical and powerful approach to multiple testing*. *Journal of the Royal Statistical Society*, 1995. **57**(1): p. 289-300.
137. Shevchenko, A., C.-M. Valcu, and M. Junqueira, *Tools for exploring the proteomosphere*. *Journal of Proteomics*, 2009. **72**(2): p. 137-144.
138. Valcu, C.-M. and M. Valcu, *Reproducibility of two-dimensional gel electrophoresis at different replication levels*. *Journal of Proteome Research*, 2007. **6**(12): p. 4677-4683.
139. Meitzler, J.L., et al., *NADPH Oxidases: A Perspective on Reactive Oxygen Species Production in Tumor Biology*. *Antioxid Redox Signal*, 2013.
140. Coso, S., et al., *NADPH oxidases as regulators of tumor angiogenesis: current and emerging concepts*. *Antioxid Redox Signal*, 2012. **16**(11): p. 1229-47.
141. Clerkin, J.S., et al., *Mechanisms of ROS modulated cell survival during carcinogenesis*. *Cancer Lett*, 2008. **266**(1): p. 30-6.
142. Goetz, M.P., et al., *The Hsp90 chaperone complex as a novel target for cancer therapy*. *Ann Oncol*, 2003. **14**(8): p. 1169-76.
143. Trepel, J., et al., *Targeting the dynamic HSP90 complex in cancer*. *Nat Rev Cancer*, 2010. **10**(8): p. 537-49.
144. Miyata, Y., H. Nakamoto, and L. Neckers, *The therapeutic target Hsp90 and cancer hallmarks*. *Curr Pharm Des*, 2013. **19**(3): p. 347-65.
145. Garon, E.B., et al., *The HSP90 inhibitor NVP-AUY922 potently inhibits non-small cell lung cancer growth*. *Mol Cancer Ther*, 2013. **12**(6): p. 890-900.
146. Jensen, M.R., et al., *NVP-AUY922: a small molecule HSP90 inhibitor with potent antitumor activity in preclinical breast cancer models*. *Breast Cancer Res*, 2008. **10**(2): p. R33.

147. Schilling, D., et al., *Radiosensitization of normoxic and hypoxic h1339 lung tumor cells by heat shock protein 90 inhibition is independent of hypoxia inducible factor-1alpha*. PLoS One, 2012. **7**(2): p. e31110.
148. Gaspar, N., et al., *Mechanistic evaluation of the novel HSP90 inhibitor NVP-AUY922 in adult and pediatric glioblastoma*. Mol Cancer Ther, 2010. **9**(5): p. 1219-33.
149. Berchem, G., et al., *Cathepsin-D affects multiple tumor progression steps in vivo: proliferation, angiogenesis and apoptosis*. Oncogene, 2002. **21**(38): p. 5951-5.
150. Reid, W.A., M.J. Valler, and J. Kay, *Immunolocalization of cathepsin D in normal and neoplastic human tissues*. J Clin Pathol, 1986. **39**(12): p. 1323-30.
151. Benes, P., V. Vetvicka, and M. Fusek, *Cathepsin D--many functions of one aspartic protease*. Crit Rev Oncol Hematol, 2008. **68**(1): p. 12-28.
152. Brouillet, J.P., et al., *Increased plasma cathepsin D concentration in hepatic carcinoma and cirrhosis but not in breast cancer*. Clin Biochem, 1991. **24**(6): p. 491-6.
153. Leto, G., et al., *Cathepsin D expression levels in nongynecological solid tumors: clinical and therapeutic implications*. Clin Exp Metastasis, 2004. **21**(2): p. 91-106.
154. Rochefort, H., F. Capony, and M. Garcia, *Cathepsin D: a protease involved in breast cancer metastasis*. Cancer Metastasis Rev, 1990. **9**(4): p. 321-31.
155. Tandon, A.K., et al., *Cathepsin D and prognosis in breast cancer*. N Engl J Med, 1990. **322**(5): p. 297-302.
156. Zhu, L., et al., *Overexpression of cathepsin D in malignant melanoma*. Fukuoka Igaku Zasshi, 2013. **104**(10): p. 370-5.
157. Haendeler, J., et al., *Cathepsin D and H2O2 stimulate degradation of thioredoxin-1: implication for endothelial cell apoptosis*. J Biol Chem, 2005. **280**(52): p. 42945-51.
158. Vetvicka, V., et al., *Procathepsin D and cancer: From molecular biology to clinical applications*. World J Clin Oncol, 2010. **1**(1): p. 35-40.
159. Fusek, M. and V. Vetvicka, *Dual role of cathepsin D: ligand and protease*. Biomed Pap Med Fac Univ Palacky Olomouc Czech Repub, 2005. **149**(1): p. 43-50.
160. Djordjevic, T., et al., *The expression of the NADPH oxidase subunit p22phox is regulated by a redox-sensitive pathway in endothelial cells*. Free Radic Biol Med, 2005. **38**(5): p. 616-30.
161. Hu, L., et al., *Thrombin up-regulates cathepsin D which enhances angiogenesis, growth, and metastasis*. Cancer Res, 2008. **68**(12): p. 4666-73.
162. Petry, A., et al., *NOX2 and NOX4 mediate proliferative response in endothelial cells*. Antioxidants & Redox Signaling, 2006. **8**(9-10): p. 1473-1484.
163. Van Buul, J.D., et al., *Expression and localization of NOX2 and NOX4 in primary human endothelial cells*. Antioxid Redox Signal, 2005. **7**(3-4): p. 308-17.
164. Briones, A.M., et al., *Differential regulation of Nox1, Nox2 and Nox4 in vascular smooth muscle cells from WKY and SHR*. J Am Soc Hypertens, 2011. **5**(3): p. 137-53.
165. Edderkaoui, M., et al., *NADPH oxidase activation in pancreatic cancer cells is mediated through Akt-dependent up-regulation of p22phox*. J Biol Chem, 2013. **288**(51): p. 36259.
166. Fernandes, A.P. and A. Holmgren, *Glutaredoxins: glutathione-dependent redox enzymes with functions far beyond a simple thioredoxin backup system*. Antioxid Redox Signal, 2004. **6**(1): p. 63-74.
167. Kalinina, E.V., N.N. Chernov, and A.N. Saprin, *Involvement of thio-, peroxi-, and glutaredoxins in cellular redox-dependent processes*. Biochemistry (Mosc), 2008. **73**(13): p. 1493-510.
168. Li, H., et al., *Human glutaredoxin 3 forms [2Fe-2S]-bridged complexes with human BolA2*. Biochemistry, 2012. **51**(8): p. 1687-96.
169. Cha, M.K. and I.H. Kim, *Preferential overexpression of glutaredoxin3 in human colon and lung carcinoma*. Cancer Epidemiol, 2009. **33**(3-4): p. 281-7.
170. Qu, Y., et al., *Thioredoxin-like 2 regulates human cancer cell growth and metastasis via redox homeostasis and NF-kappaB signaling*. J Clin Invest, 2011. **121**(1): p. 212-25.
171. Liu, M., et al., *EB1 acts as an oncogene via activating beta-catenin/TCF pathway to promote cellular growth and inhibit apoptosis*. Mol Carcinog, 2009. **48**(3): p. 212-9.
172. Ladd, J.J., et al., *Increased plasma levels of the APC-interacting protein MAPRE1, LRG1, and IGFBP2 preceding a diagnosis of colorectal cancer in women*. Cancer Prev Res (Phila), 2012. **5**(4): p. 655-64.
173. Zhou, J., et al., *[Gene expression profiles in squamous esophageal cancer tissues and adjacent almost normal tissues]*. Zhonghua Yi Xue Yi Chuan Xue Za Zhi, 1999. **16**(5): p. 303-6.
174. Nishigaki, R., et al., *Proteomic identification of differentially-expressed genes in human gastric carcinomas*. Proteomics, 2005. **5**(12): p. 3205-13.

175. Fujii, K., et al., *Proteomic study of human hepatocellular carcinoma using two-dimensional difference gel electrophoresis with saturation cysteine dye*. *Proteomics*, 2005. **5**(5): p. 1411-22.
176. El-Rifai, W., et al., *Expression profiling of gastric adenocarcinoma using cDNA array*. *Int J Cancer*, 2001. **92**(6): p. 832-8.
177. Kim, M.J., et al., *Depletion of end-binding protein 1 (EB1) promotes apoptosis of human non-small-cell lung cancer cells via reactive oxygen species and Bax-mediated mitochondrial dysfunction*. *Cancer Lett*, 2013. **339**(1): p. 15-24.
178. Sun, S., et al., *Circulating Lamin B1 (LMNB1) biomarker detects early stages of liver cancer in patients*. *J Proteome Res*, 2010. **9**(1): p. 70-8.
179. Vergnes, L., et al., *Lamin B1 is required for mouse development and nuclear integrity*. *Proc Natl Acad Sci U S A*, 2004. **101**(28): p. 10428-33.
180. Freund, A., et al., *Lamin B1 loss is a senescence-associated biomarker*. *Mol Biol Cell*, 2012. **23**(11): p. 2066-75.
181. Dreesen, O., et al., *The contrasting roles of lamin B1 in cellular aging and human disease*. *Nucleus*, 2013. **4**(4): p. 283-90.
182. Dreesen, O., et al., *Lamin B1 fluctuations have differential effects on cellular proliferation and senescence*. *J Cell Biol*, 2013. **200**(5): p. 605-17.
183. Shimi, T., et al., *The role of nuclear lamin B1 in cell proliferation and senescence*. *Genes Dev*, 2011. **25**(24): p. 2579-93.
184. Dikalov, S., *Cross talk between mitochondria and NADPH oxidases*. *Free Radic Biol Med*, 2011. **51**(7): p. 1289-301.
185. Banerji, U., *Heat shock protein 90 as a drug target: some like it hot*. *Clin Cancer Res*, 2009. **15**(1): p. 9-14.
186. Gorchach, A., et al., *Thrombin activates the hypoxia-inducible factor-1 signaling pathway in vascular smooth muscle cells: Role of the p22(phox)-containing NADPH oxidase*. *Circ Res*, 2001. **89**(1): p. 47-54.
187. Beck, R., et al., *Hsp90 is cleaved by reactive oxygen species at a highly conserved N-terminal amino acid motif*. *PLoS One*, 2012. **7**(7): p. e40795.
188. Liu, T., C.K. Daniels, and S. Cao, *Comprehensive review on the HSC70 functions, interactions with related molecules and involvement in clinical diseases and therapeutic potential*. *Pharmacol Ther*, 2012. **136**(3): p. 354-74.
189. Maeda, A., et al., *Aberrant expression of photoreceptor-specific calcium-binding protein (recoverin) in cancer cell lines*. *Cancer Res*, 2000. **60**(7): p. 1914-20.
190. de Waegh, S. and S.T. Brady, *Axonal transport of a clathrin uncoating ATPase (HSC70): a role for HSC70 in the modulation of coated vesicle assembly in vivo*. *J Neurosci Res*, 1989. **23**(4): p. 433-40.
191. Shiota, M., et al., *Heat shock cognate protein 70 is essential for Akt signaling in endothelial function*. *Arterioscler Thromb Vasc Biol*, 2010. **30**(3): p. 491-7.
192. Chen, K., et al., *A critical role of heat shock cognate protein 70 in Apoptin-induced phosphorylation of Akt*. *Biochem Biophys Res Commun*, 2011. **409**(2): p. 200-4.
193. Lim, J.W., K.H. Kim, and H. Kim, *NF-kappaB p65 regulates nuclear translocation of Ku70 via degradation of heat shock cognate protein 70 in pancreatic acinar AR42J cells*. *Int J Biochem Cell Biol*, 2008. **40**(10): p. 2065-77.
194. Powers, M.V., P.A. Clarke, and P. Workman, *Dual targeting of HSC70 and HSP72 inhibits HSP90 function and induces tumor-specific apoptosis*. *Cancer Cell*, 2008. **14**(3): p. 250-62.
195. Chong, K.Y., et al., *Stable overexpression of the constitutive form of heat shock protein 70 confers oxidative protection*. *J Mol Cell Cardiol*, 1998. **30**(3): p. 599-608.
196. Dastoor, Z. and J. Dreyer, *Nuclear translocation and aggregate formation of heat shock cognate protein 70 (Hsc70) in oxidative stress and apoptosis*. *J Cell Sci*, 2000. **113 (Pt 16)**: p. 2845-54.
197. Liu, Y., et al., *Upregulation of the constitutively expressed HSC70 by KLF4*. *Cell Stress Chaperones*, 2008. **13**(3): p. 337-45.
198. Gorchach, A. and T. Kietzmann, *Superoxide and derived reactive oxygen species in the regulation of hypoxia-inducible factors*. *Methods Enzymol*, 2007. **435**: p. 421-46.
199. Kietzmann, T. and A. Gorchach, *Reactive oxygen species in the control of hypoxia-inducible factor-mediated gene expression*. *Semin Cell Dev Biol*, 2005. **16**(4-5): p. 474-86.
200. Semenza, G.L., *Targeting HIF-1 for cancer therapy*. *Nat Rev Cancer*, 2003. **3**(10): p. 721-32.
201. Semenza, G.L., *HIF-1: upstream and downstream of cancer metabolism*. *Curr Opin Genet Dev*, 2010. **20**(1): p. 51-6.

202. Kuo, Y.C., et al., *Regulation of phosphorylation of Thr-308 of Akt, cell proliferation, and survival by the B55alpha regulatory subunit targeting of the protein phosphatase 2A holoenzyme to Akt*. J Biol Chem, 2008. **283**(4): p. 1882-92.
203. Itoh, N., et al., *Phosphorylation of Akt/PKB is required for suppression of cancer cell apoptosis and tumor progression in human colorectal carcinoma*. Cancer, 2002. **94**(12): p. 3127-34.
204. Hammarsten, P., et al., *Phospho-Akt immunoreactivity in prostate cancer: relationship to disease severity and outcome, Ki67 and phosphorylated EGFR expression*. PLoS One, 2012. **7**(10): p. e47994.
205. Usmani, S.Z., R. Bona, and Z. Li, *17 AAG for HSP90 inhibition in cancer--from bench to bedside*. Curr Mol Med, 2009. **9**(5): p. 654-64.
206. Solit, D.B. and G. Chiosis, *Development and application of Hsp90 inhibitors*. Drug Discov Today, 2008. **13**(1-2): p. 38-43.
207. Zalba, G., et al., *NADPH oxidase-dependent superoxide production is associated with carotid intima-media thickness in subjects free of clinical atherosclerotic disease*. Arterioscler Thromb Vasc Biol, 2005. **25**(7): p. 1452-7.
208. Yao, J.Q., et al., *Hsp90 inhibitor 17-allylamino-17-demethoxygeldanamycin inhibits the proliferation of ARPE-19 cells*. J Biomed Sci, 2010. **17**: p. 30.
209. Niikura, Y., et al., *17-AAG, an Hsp90 inhibitor, causes kinetochore defects: a novel mechanism by which 17-AAG inhibits cell proliferation*. Oncogene, 2006. **25**(30): p. 4133-46.
210. Terry, J., et al., *Hsp90 inhibitor 17-allylamino-17-demethoxygeldanamycin prevents synovial sarcoma proliferation via apoptosis in in vitro models*. Clin Cancer Res, 2005. **11**(15): p. 5631-8.
211. Zsebek, B., et al., *Hsp90 inhibitor 17-AAG reduces ErbB2 levels and inhibits proliferation of the trastuzumab resistant breast tumor cell line JIMT-1*. Immunol Lett, 2006. **104**(1-2): p. 146-55.
212. Neckers, L., *Hsp90 inhibitors as novel cancer chemotherapeutic agents*. Trends Mol Med, 2002. **8**(4 Suppl): p. S55-61.
213. Porter, J.R., C.C. Fritz, and K.M. Depew, *Discovery and development of Hsp90 inhibitors: a promising pathway for cancer therapy*. Curr Opin Chem Biol, 2010. **14**(3): p. 412-20.
214. Workman, P., et al., *Drugging the cancer chaperone HSP90: combinatorial therapeutic exploitation of oncogene addiction and tumor stress*. Ann N Y Acad Sci, 2007. **1113**: p. 202-16.
215. Powers, M.V. and P. Workman, *Targeting of multiple signalling pathways by heat shock protein 90 molecular chaperone inhibitors*. Endocr Relat Cancer, 2006. **13 Suppl 1**: p. S125-35.
216. Chen, F., et al., *Hsp90 regulates NADPH oxidase activity and is necessary for superoxide but not hydrogen peroxide production*. Antioxid Redox Signal, 2011. **14**(11): p. 2107-19.
217. Ioachin, E., *Immunohistochemical tumour markers in endometrial carcinoma*. Eur J Gynaecol Oncol, 2005. **26**(4): p. 363-71.
218. Cunat, S., P. Hoffmann, and P. Pujol, *Estrogens and epithelial ovarian cancer*. Gynecol Oncol, 2004. **94**(1): p. 25-32.
219. Mimae, T., et al., *Cathepsin D as a potential prognostic marker for lung adenocarcinoma*. Pathol Res Pract, 2012. **208**(9): p. 534-40.
220. Huang, X.F., et al., *Expressions of chromogranin A and cathepsin D in human primary hepatocellular carcinoma*. World J Gastroenterol, 2000. **6**(5): p. 693-698.
221. Jagodic, M., et al., *Prognostic and predictive value of cathepsins D and L in operable breast cancer patients*. Neoplasma, 2005. **52**(1): p. 1-9.
222. Markicevic, M., et al., *Cathepsin D as an indicator of clinical outcome in early breast carcinoma during the first 3 years of follow-up*. Biomark Med, 2013. **7**(5): p. 747-58.
223. Garcia, M., et al., *Overexpression of transfected cathepsin D in transformed cells increases their malignant phenotype and metastatic potency*. Oncogene, 1990. **5**(12): p. 1809-14.
224. Voorzanger-Rousselot, N. and P. Garnero, *Biochemical markers in oncology. Part I: molecular basis. Part II: clinical uses*. Cancer Treat Rev, 2007. **33**(3): p. 230-83.
225. Chich, J.F., et al., *Statistics for proteomics: experimental design and 2-DE differential analysis*. J Chromatogr B Analyt Technol Biomed Life Sci, 2007. **849**(1-2): p. 261-72.
226. Doerfler, W., et al., *Integration of foreign DNA and its consequences in mammalian systems*. Trends Biotechnol, 1997. **15**(8): p. 297-301.
227. Depagne, J. and F. Chevalier, *Technical updates to basic proteins focalization using IPG strips*. Proteome Sci, 2012. **10**(1): p. 54.